REFERENCE ONLY

UNIVERSITY OF LONDON THESIS

Degree MD Year 2006 Name of Author WHITEHOUSE T

~~Intra-Renal Haemodynamics and~~

~~Tissue Oxygenation~~

VALIDATION OF A MODEL MEASURING
RAT INTRA-RENAL BLOOD FLOW AND
TISSUE OXYGEN.

Submitted for MD Thesis of University College London,

September 2005

Tony Whitehouse

Research Fellow,

Bloomsbury Institute of Intensive Care Medicine,

Wolfson Institute of Biomedical Research,

University College London,

Gower Street,

London WC1E 6BT, United Kingdom.

ProQuest LLC
789 East Eisenhower Parkway
P.O. Box 1346
Ann Arbor, MI 48106-1346

I declare that the work described in this MD thesis is original and is my own.

Tony Whitehouse

London, September 2005

Abstract

Acute renal failure (ARF) is a common condition on the intensive care unit (ICU) and may affect up to 40% of patients (de Mendonca, A. *et al.*, 2000), (Korkeila, M. *et al.*, 2000). Pathophysiological mechanisms remain unclear. Patients who die from sepsis have kidneys that look histologically normal (Hotchkiss, R.S. *et al.*, 1999), while the renal prognosis in survivors is good with <2% requiring long-term renal replacement therapy (Noble, J.S. *et al.*, 2001). This has led some authors to suggest that acute renal failure is a physiological process designed to shut down vital processes and protect the kidney from irreversible damage during a severe insult (Singer, M. *et al.*, 2004). As ninety percent of oxygen consumption is utilised by the mitochondrion (Babcock, G.T. and Wikstrom, M., 1992), metabolic control may be regulated by mitochondrial activity (Beltran, B. *et al.*, 2000). This may be an important mechanism underlying renal failure but is difficult to assess in the intact animal.

Investigation of *in vivo* cell respiration within different regions of the kidney has not been previously reported. Tissue oxygen tension (PtO_2) represents the balance between local oxygen delivery and consumption. Although many groups have measured tissue oxygen tensions in various organs, these have rarely been matched to local flow. Comparison of tissue oxygen to local flow may allow local oxygen consumption to be extrapolated. For example, a rise in PtO_2 without a corresponding increase in flow suggests a reduction in local consumption.

This thesis is based on the development of an anaesthetised Wistar rat model to demonstrate changes in intra-renal regional tissue oxygen tension (using ruthenium fluorescence) and flow (using Doppler microvascular flowmetry) during a variety of physical and pharmacological manipulations. Cardiorespiratory insults comprised an aortic clamp, haemorrhage, hypoxia-reoxygenation and endotoxin. Pharmacological challenges of a loop diuretic (furosemide) and ACE inhibitor (enalaprilat) were also used to alter intra-renal PtO_2 and microvascular flow. Changes in the PtO_2:flow ratio were demonstrated in the cortex, corticomedullary junction and medulla during the various insults. These were suggestive of decreased oxygen consumption in the cortex during hypoxaemia, haemorrhage-resuscitation and enalaprilat; in the corticomedullary junction on resuscitation from haemorrhage; and in the medulla following furosemide.

I have thus generated a robust and reproducible *in vivo* model that can assess intrarenal regional perfusion, tissue oxygenation and, by extrapolation, oxygen consumption during various (patho)physiological and pharmacological manoeuvres.

Acknowledgements

Although individuals receive the accolade of a post-graduate degree, they are rarely completed in absolute isolation. This thesis is, of course, no exception. Indeed, I feel that I have had to depend on more people than would normally be expected. Although some are mentioned first and others later, I should like to thank them all equally and just as gratefully.

Mervyn Singer has been manic, guiding and supportive throughout the 5-year gestation of this part-time thesis. His supervision has facilitated rather than led, enabled rather than pushed and his energetic chutzpah has caused me to continue when it appeared that the experiments might come to nothing.

I should be derelict in my duty should I fail to mention Monty Mythen and Peter Wilson who also partly bankrolled my research time. Monty, in particular, has shown me an entrepreneurial approach to academia that I hope will serve me well over time.

Few of the experiments detailed herein would have been possible without the assistance of Ray Stidwill and Val Taylor: They almost gave up trying to teach me how to do it – I think they were just glad that I was going to stick to Intensive Care and not go into Surgery!

Finally I thank Jo. She knows why.

Abbreviations

[...]	Concentration of ... (Substance)
µm	Micrometre
AI	Autoregulatory Index
ARF	Acute Renal Failure
BPU	Perfusion Units
CRI	Cell Respiration Index
DO_2	Oxygen Delivery
FiO_2	Fraction of Inspired Oxygen
GFR	Glomerular Filtration Rate
Hb	Haemoglobin
ICU	Intensive Care Unit
iU	International Units
kPa	Kilopascals
l	Litre
LDF	Laser Doppler Flow/Flux
LPS	Lipopolysaccharide
mm	Millimetre
mmol	Millimoles
NS	Not Significant
P:F ratio	Ratio of Tissue Oxygen to Tissue Flow
PO_2	Partial Pressure of Oxygen
PaO_2	Arterial Partial Pressure of Oxygen

PtO_2	Tissue Oxygen
ROS	Reactive Oxygen Species
RRT	Renal Replacement Therapy
SpO_2	Oxygen Saturation of Haemoglobin
VO_2	Oxygen Content

Throughout this thesis oxygen partial pressures are reported in kPa. When other authors have reported in non-SI units, the conversion factor of 1 kPa being equivalent to 7.5 torr (or mmHg) is applied:

Contents

Index of Tables

Index of Figures

1 Background

1.1 Renal failure in the intensive care unit

"Mortality is proportional to the number of failing organs" has been the mantra chanted in intensive care units (ICU) for many years. Renal failure is the commonest, yet remains one of the least investigated, organ failure in the critically ill. It is caused, most often, through sepsis (de Mendonca, A. *et al.*, 2000). Other than offering the patient the best intensive care management possible, with appropriate maintenance of blood pressure and flow through judicious use of fluids and vasoactive drug support (Marik, P.E., 2004), there is no specific treatment available to reverse renal dysfunction (O'Leary, M.J. and Bihari, D.J., 2001), (Galley, H.F., 2000a). The introduction of biocompatible membranes has made renal replacement therapy (RRT) an easy, relatively safe and routine procedure on most ICUs. Except in cases of deliberate treatment withdrawal, death from acute renal failure (ARF) is now very rare. ARF is thus often regarded as a relatively minor, easily supported distraction, compared with the weightier cardiorespiratory problems that preoccupy the intensivist.

ARF induced by sepsis remains an enigma. Unexplained features include the mechanism of failure; the excess mortality in patients who develop renal failure despite adequate RRT (de Mendonca, A. *et al.*, 2000), (Sweet, S.J. *et al.*, 1981); the absence of significant renal histological change (Hotchkiss, R.S. *et al.*, 1999) despite anuria and biochemical derangement; the very high incidence of

recovery, even following absolute and prolonged renal failure (Noble, J.S. *et al.*, 2001); and the lag-time for recovery of renal function which may take up to several months.

ARF frequently persists despite early resolution of systemic inflammation and restoration of a normal circulatory profile, only to recover some weeks or months later. Impressively, severe renal failure is usually reversible to such a degree that most patients become independent of RRT. An audit of Scottish ICUs showed that 98.4% of such patients with normal renal function prior to their ICU stay, were independent of RRT by hospital discharge (Noble, J.S. *et al.*, 2001). This is fortunate as, depending on the patient mix and the definition of ARF, the rate of ARF associated with sepsis varies between 9-40% of ICU admissions (Rangel-Frausto, M.S. *et al.*, 1995), (Levy, E.M. *et al.*, 1996), a workload that would overwhelm chronic dialysis units if life-long RRT were required.

Renal failure developing in the ICU is associated with a poor prognosis (de Mendonca, A. *et al.*, 2000). Combined renal and respiratory failure carries a considerably worse prognosis than respiratory failure alone (Sweet, S.J. *et al.*, 1981). Increasing the frequency of intermittent renal replacement from alternate day to daily treatment may improve outcome (Schiffl, H. *et al.*, 2002), (Kellum, J.A. *et al.*, 2002), although Guerin and co-workers (Guerin, C. *et al.*, 2002) found that the mode of RRT (continuous compared with intermittent) did not alter prognosis. In the absence of disease-modifying therapies, it is impossible to measure the specific impact on mortality through preventing ARF. Argument

exists as to whether ARF is a marker of the severity of disease or whether it contributes to mortality *per se*.

"Renal salvage" with furosemide, whilst having some theoretical benefits on reducing tubular cell energy consumption (Brezis, M. and Rosen, S., 1995) and flushing tubular debris out of collecting ducts, has never been shown convincingly to improve either renal function or patient survival. Similarly, the use of dopamine to increase renal flow is not advantageous (Breen, D. and Bihari, D., 1998),(Galley, H.F., 2000b), (Bellomo, R. *et al.*, 2000), and may even be detrimental (Jones, D. and Bellomo, R., 2005), (Holmes, C.L. and Walley, K.R., 2003), (Task Force of the American College of Critical Care Medicine, Society of Critical Care Medicine, (Task Force of the American College of Critical Care Medicine, S.o.C.C.M., 1999) updated (Hollenberg, S.M. *et al.*, 2004)).

In short, ARF in the ICU is a very common condition, usually brought about by the response to sepsis or other inflammatory insults that is easily supported with haemofiltration but which has no specific cure. However, the need for long-term treatment is reduced as the vast majority of renal failure in the critically ill ICU patient reverses spontaneously – a phenomenon whose mechanism remains elusive and whose investigation is difficult.

1.2 Bridging clinical and cell studies

Full recovery of renal function following absolute anuria and metabolic derangement has led authors to consider that '*acute renal failure*' is, in fact, '*acute renal success*' – an elaborate protective mechanism by which the kidney allows itself to hibernate (or aestivate) during acute physiological disturbance. One possible mechanism is through control of oxygen metabolism.

Although cell studies have revealed control mechanisms adjusting renal cell respiration, there are no studies demonstrating this phenomenon *in vivo*. Tissue oxygen (PtO_2) is the balance between local oxygen delivery and consumption. Many groups have published results demonstrating changes in renal PtO_2 (See Section 2.4). However, in the face of unmeasured local flow, it is impossible to distinguish whether these were due to changes in regional flow or to alterations in local oxygen consumption.

Similarly, studies have shown that deep-sea diving animals such as turtles and seals have the ability to alter oxygen consumption in different organs during prolonged breath-holding dives (Hochachka, P.W., 1980), (Guppy, M. *et al.*, 1986) but the mechanisms through which this is achieved are unknown.

Key to the investigation of oxygen control mechanisms and its impact on ARF is a stable, reproducible and validated laboratory animal model. Such a model would allow implementation and assessment of new therapies. Paired intrarenal flow and PtO_2 measurements have only been previously reported in the rat renal

medulla (Liss, P., 1997). None has attempted to extrapolate changes in regional oxygen consumption.

1.3 Project aims

The thesis aims to assess the feasibility of measuring flow and tissue oxygen tension simultaneously in different regions of the kidney, thus allowing a relative assessment of local oxygen consumption during various physiological, pathological, and pharmacological manipulations. Through these it is expected that clinically relevant mechanisms could be studied with the long-term aim of elucidating the renal response in sepsis and other inflammatory insults. I therefore decided to investigate tissue oxygen supply and demand in an anesthetized, fluid-resuscitated Wistar rat model undergoing challenges with drugs (furosemide and enalaprilat), physical manoeuvres (aortic clamping, hyperoxia, hypoxia) and pathophysiological manipulation (sepsis exsanguination/resuscitation).

Experiments outlined in this thesis used a new ruthenium fluorescence-based technology (OxyLite™, Oxford Optronix, Oxford) to contemporaneously measure renal PtO_2 alongside microvascular flow measured by laser Doppler flowmetry (LDF) (OxyFlo™, Oxford Optronix, Oxford) simultaneously from three regions within the rat kidney. By comparing changes in both flow and PtO_2, a regional cell respiration index (CRI) was calculated and changes in cell respiration extrapolated. This is the first time such results have been

demonstrated *in vivo*. Measurement of the decay in PtO_2 following termination of the experiment allowed calculation of the rate of oxygen consumption by the surrounding tissue and confirmation of the probe findings. It also allowed tentative translation of the CRI into quantifiable values.

Measurements were made from three different depths (0.5, 1.5 and 3.5 mm), chosen to correspond anatomically to cortex, cortico-medullary junction (CMJ) and outer medulla on post-mortem examination (studies performed with Dr Marco Novelli, Reader in Histopathology, UCL). Correct placement of the probes was confirmed visually at the end of each experiment.

A series of experiments were performed to assess the effects of various cardiorespiratory insults (aortic clamp, haemorrhage, hypoxia-reoxygenation, endotoxin) and pharmacological challenges (loop diuretic, ACE inhibitor) on intra-renal tissue oxygen and microvascular flow measurements. An aortic clamp was also used to physically reduce renal artery flow and monitor subsequent intra-renal flow changes. The drugs were chosen as a means of manipulating intra-renal flow and regional oxygen consumption separately so that the response from the three regions could be recorded.

The manipulations produced markedly varying effects in each of the different regions of the kidney. Interestingly, regional renal responses are markedly heterogeneous to the different insults.

2 Introduction

2.1 Functions of the kidney

The main function of the kidney is to maintain homeostasis for solutes and water. In health, the total body concentrations of sodium, potassium, calcium *et cetera* stay within tightly controlled limits despite variations in dietary intake or endogenous production. Components that are renally regulated are:

1) Electrolytes
    a. Sodium, the major extracellular cation
    b. Potassium, the major intracellular cation
    c. Chloride, the major extracellular anion
2) Total body water (and therefore osmolality)
3) pH
    a. Through the active excretion of hydrogen ions
    b. By regulating the concentration of HCO_3^-
4) Minerals
    a. Calcium
    b. Phosphate
    c. Magnesium
5) Excretion of endogenously produced waste materials
    a. Urea – product of protein catabolism
    b. Creatinine – produced by skeletal muscle

c. Uric acid – produced from the metabolism of nucleic acids

The kidney also performs a number of endocrine functions:

1) It is the sole source of erythropoietin, released in response to hypoxia and necessary for mobilizing iron in bone marrow to produce haemoglobin for red blood cell production
2) It is the only significant site of production of 1-α-hydroxylase, the final enzyme necessary to produce the active component of the vitamin D pathway, $1,25\text{-}(OH)_2D_3$
3) It is the only source of renin

The kidney is a critical organ in the maintenance of normal blood pressure for a number of reasons:

1) It regulates water and sodium, and thus controls blood volume
2) It controls the renin-angiotensin-aldosterone axis
3) It produces vasodilatory substances

Other functions of the kidney include:

1) Catabolism of small peptide hormones such as insulin
2) Production of glucose via gluconeogenesis during fasting
3) Elimination of many drugs.

2.2 *Anatomy and physiology*

The kidney is a particularly interesting organ in which to study regional changes in flow and oxygenation. Differences in PtO_2 and flow exist at all levels of the kidney. Transverse sectioning of a kidney reveals bands containing cells of different type and function (Figure 2-1). There is general agreement that regional PtO_2 and flow differ in each band, yet there is wide discrepancy in the PtO_2 results reported (Table 2-1). The medulla is traditionally considered to have a high energy requirement coupled with a precarious blood flow. A view now reflected in many physiological textbooks (Guyton, A.C. and Hall, J.E., 1998) is that this anatomical arrangement causes the medulla to live 'at the edge of anoxia' (Heyman, S.N. *et al.*, 1997) and makes this region particularly vulnerable to cardio-respiratory insults. It is therefore a potential cause of hypovolaemic renal failure (Brezis, M. and Rosen, S., 1995), (Heyman, S.N. *et al.*, 1997), endotoxin-induced renal failure (Heyman, S.N. *et al.*, 2000b) and contrast-induced renal failure (Liss, P. *et al.*, 1998). However, variable findings in medullary and cortical PtO_2 values found by other groups using a variety of animal models have cast doubt on this conventional view (Nelimarkka, O., 1984), (Liss, P. *et al.*, 1997a), (Brezis, M. *et al.*, 1994b), (Gunther, H. *et al.*, 1974), (James, P.E. *et al.*, 1996), (Leichtweiss, H.P. *et al.*, 1969).

Not all authors agree that the medulla is the site of ARF. Studies of spontaneously hypertensive rats have suggested that the site most vulnerable to pathological damage are the juxtamedullary nephrons at the corticomedullary junction (Adler, S. and Huang, H., 2002), (Roald, A.B. *et al.*, 2002). This

theory also has many advocates as there are many anatomical and physiological reasons to expect this region to be vulnerable to insults. This is reviewed more thoroughly in the following sections, but briefly:

1) Juxtamedullary nephrons loop into the medulla and play an important role in conserving sodium and concentrating urine. They therefore have the ability to affect renal function.
2) Efferent arterioles draining the juxtamedullary nephron become the *vasa recta*, the sole blood supply to the medulla.
3) Juxtamedullary nephrons maintain a higher filtration rate and always function at full capacity (Lote, C.J., 2000).

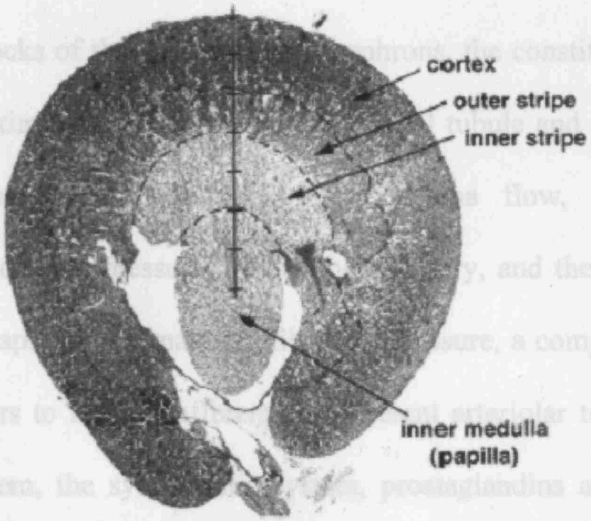

Figure 2-1: Kidney stripe measurements (adapted from (Liss, P. et al., 1997a))

Although comprising only 0.5 per cent of total body weight, the kidneys in health receive 25 per cent of total cardiac output. This is the greatest blood flow per unit weight of tissue found in the body and ensures adequate clearance. In this process, the entire circulating volume is filtered and reabsorbed twice an hour. Daily urinary production is the overspill of the excess between filtration and subsequent reabsorption of approximately 180 litres of plasma per day.

The building blocks of the kidney are the nephrons, the constituent parts being glomerulus, proximal tubule, loop of Henlé, distal tubule and collecting ducts. Glomerular filtration depends upon renal plasma flow, the balance of hydrostatic and oncotic pressures across the capillary, and the permeability of the Bowman's capsule. To maintain filtration pressure, a complex interplay of mediators appears to balance afferent and efferent arteriolar tone. The renin-angiotensin system, the sympathetic system, prostaglandins and NO have all been implicated.

Human kidneys have two populations of nephrons, superficial and juxtamedullary. Delivery of sodium chloride (NaCl) to the thick ascending limb of the loop of Henlé and the distal convoluted tubule of the nephron is determined by glomerular filtration rate (GFR) and proximal tubular function. Although most sodium (60%) is reabsorbed in the proximal tubule, absorption of sodium in the thick ascending limb of the loop of Henlé and urea delivery from the medullary collecting duct ensures the generation of a graduated medullary interstitial hypertonicity. The formation of this gradient allows fine-

tuning of blood osmolarity by the absorption of water in the collecting ducts under the control of vasopressin (anti-diuretic hormone, ADH). At the same time, the complex arrangement of blood vessels ensures a high flow to the glomeruli (predominantly in the cortex) to ensure clearance, and a much lower flow to the medulla to favour reabsorption. The arrangement of nephrons and capillaries that gives the kidney its ability to concentrate urine also makes it vulnerable to hypoxia at times of stress. At its weakest point - the corticomedullary junction - lie the Na/K-ATP pumps responsible for sodium reabsorption and maintenance of the osmotic gradient. (Reviewed in (Guyton, A.C. and Hall, J.E., 1998))

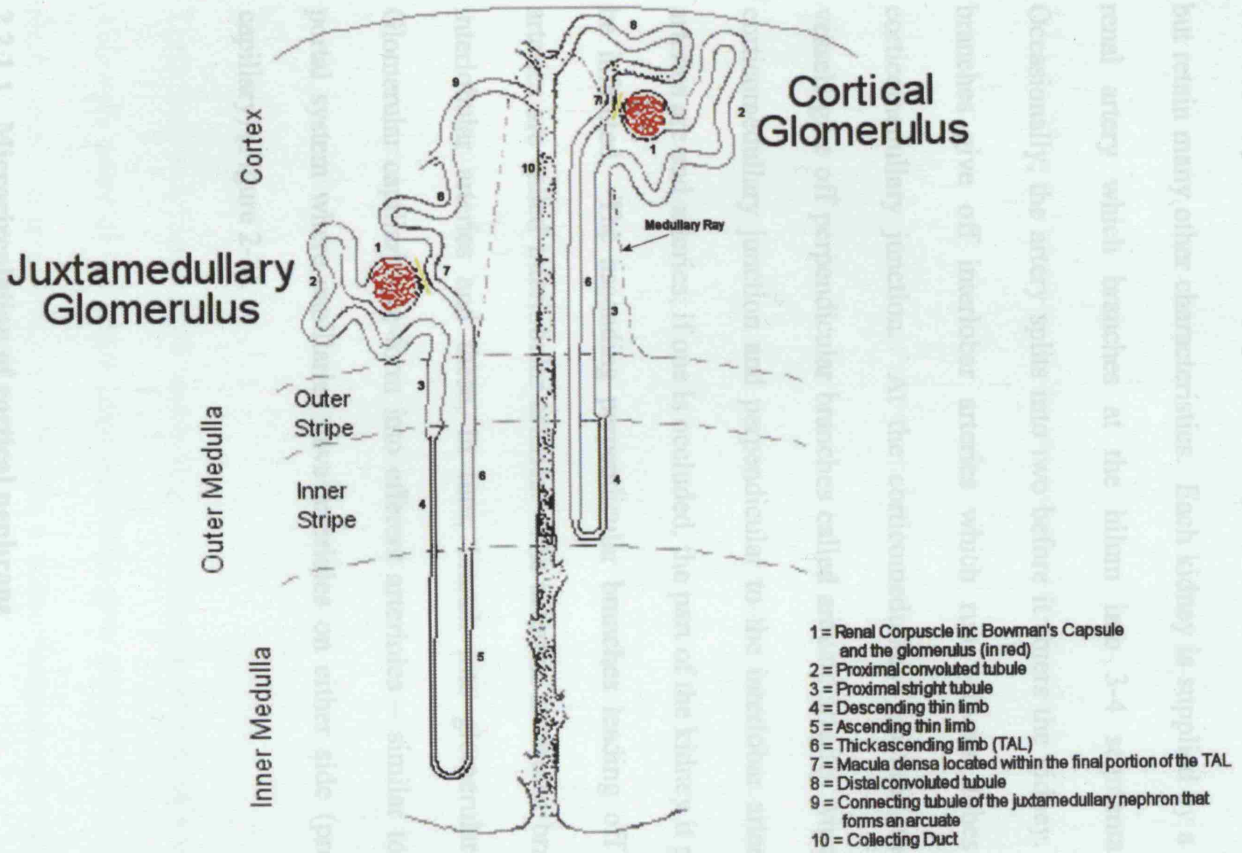

Figure 2-2: Illustrative differences between cortical and juxtamedullary nephrons

2.2.1 Renal blood supply

The anatomy of a rat kidney differs slightly from humans as they are unilobar but retain many other characteristics. Each kidney is supplied by a single main renal artery which branches at the hilum into 3-4 segmental branches. Occasionally, the artery splits into two before it enters the kidney. Segmental branches give off interlobar arteries which run between lobes up to the corticomedullary junction. At the corticomedullary junction, the interlobar vessels give off perpendicular branches called arcuate arteries which run along corticomedullary junction and perpendicular to the interlobar artery. Arcuate arteries are end-arteries; if one is occluded, the part of the kidney it perfuses will be infarcted. The ascending perpendicular branches leading off the arcuate arteries are called interlobular arteries. The afferent arterioles branch off the interlobular arteries and these, in turn, branch into glomerular capillaries. Glomerular capillaries re-form into efferent arterioles – similar to the hepatic portal system where capillaries have arterioles on either side (pre- and post-capillary) (Figure 2-3).

2.2.1.1 Microcirculation of cortical nephrons

Compared with other regions in the kidney, the afferent blood supply of the cortex is relatively simple and arises directly via the renal artery. The afferent

arterioles become the glomerulus which then reforms into an efferent arteriole. The efferent arteriole then breaks down into the peritubular capillary network which reabsorbs 98-99% of glomerular filtrate. Venules from the peritubular capillary network eventually pass to the renal vein.

2.2.1.2 Microcirculation of the juxtamedullary nephrons

The afferent arteriole forms the glomerulus, which then converges to form the efferent arteriole. In contrast to the cortical arterioles, the efferent arteriole becomes the descending vasa recta. The vasa recta are important in two respects:

1) they are the sole blood supply to the medulla (which is therefore supplied by "second-hand" blood – blood that has already flowed through a capillary system and had oxygen extracted from it)
2) they form a countercurrent exchange system

There is free diffusion from descending to ascending vasa recta and *vice versa*. Although many of the physiology textbooks give attention to solutes and the ability to concentrate urine, there is also a countercurrent exchange of oxygen. As a result, oxygen tension may decrease the deeper the vessels penetrate the medulla. It is therefore proposed that the medulla is at increased risk from hypoxic injury during prolonged shock or hypoxemia (Heyman, S.N. *et al.*, 1997), (Heyman, S.N. *et al.*, 1995).

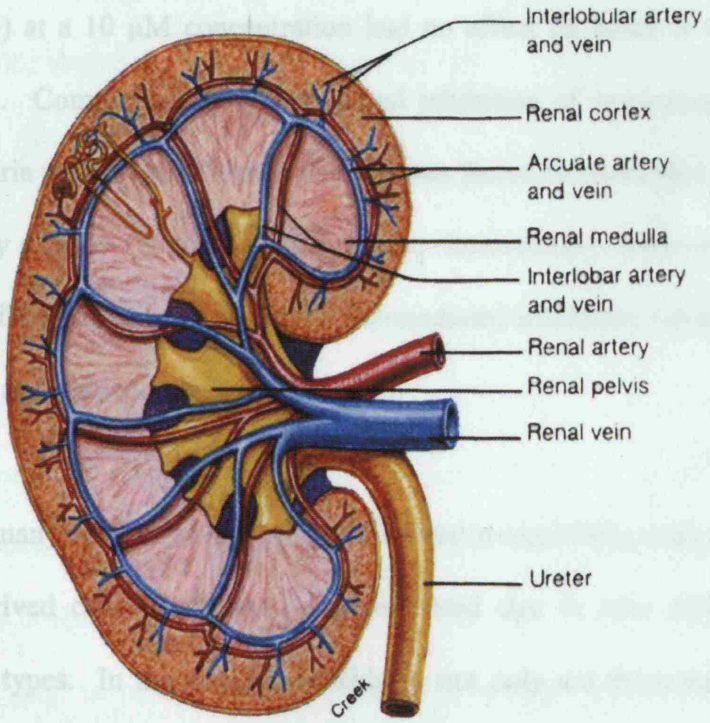

Source: Fox, S.I., Human Physiology, 6th ed., pg. 529.

Figure 2-3: Renal blood supply

2.2.2 Control of cellular consumption by Nitric Oxide (NO)

Isolated renal tubules reduce their oxygen consumption when exposed to NO (Koivisto, A. *et al.*, 1999). The effect of NO is cGMP independent as the selective guanylyl cyclase inhibitor 1H-[1,2,4]oxadiazolo[4,3-a]quinoxalin-1-one (ODQ) at a 10 μM concentration had no effect on basal or NO-inhibited respiration. Comparison of NO-mediated inhibition of respiration in isolated mitochondria was virtually identical and it was therefore concluded that NO was most likely directly acting on mitochondria. Interestingly, however, this group found no differences in sensitivity to NO-mediated inhibition between the outer medullary and cortical tubules.

Although many authors have attributed changes in renal PtO_2 to direct effects on renally-derived cells, it should be remembered that *in vivo* systems contain many cell types. In the case of the kidney, not only are these renally-derived cells but also vascular endothelial, immune-derived and structural cells. For example, Adler (Adler, S. *et al.*, 2001) used mice deficient in endothelial nitric oxide synthase (eNOS) and found that basal oxygen consumption was higher in the knockout mice than in heterozygous controls – as might be expected if NO alters mitochondrial function. When NO production was stimulated using the ACE inhibitor, ramiprilat and bradykinin, the eNOS deficient mice did not decrease their oxygen consumption as much as their heterozygous controls. They concluded that NO production by eNOS is responsible for regulation of renal oxygen consumption in the mouse kidney.

Similarly, Tsai et al (Tsai, A.G. *et al.*, 1998) have shown large oxygen gradients across rat mesentery vasculature either, they propose, as a means of protecting the cells beyond from high oxygen concentrations, for NO production, or as a sump to regulate a constant supply of oxygen to the tissue beyond the supplying vasculature. In considering results obtained for this thesis, it is important to bear in mind that regional PtO_2 changes may be due to changes in the oxygen consumption rates of any of the surrounding cells.

2.3 Control of cellular respiration

The high rate of recovery from absolute anuria and renal failure has brought about proposals that organ failure seen in ICU may be deliberate and preserving rather than co-incidental and damaging. There are physiological systems in nature designed to reduce organ consumption during normal use rather than simply during pathological stress. In order for diving animals to remain underwater for long periods of time, control mechanisms exist that are designed to shut down the kidney and other oxygen-hungry organs (Hochachka, P.W., 1980), (Guppy, M. *et al.*, 1986).

A marine mammal's response to 'exercise' during diving is counter-intuitive when compared with other mammals. When terrestrial mammals exercise, they increase ventilation, cardiac output and induce peripheral vasodilation to skeletal muscle in order to increase perfusion and allow heat dissipation through

the skin (Wagner, P.D., 1991). In contrast, marine mammals are apnoeic, bradycardic and peripherally vasoconstricted (collectively known as the 'dive response'). As cardiac output decreases, reflex peripheral vasoconstriction maintains central arterial blood pressure by reducing flow to all organs and tissues except the brain. All organs and tissues, including the heart, kidneys, and splanchnic organs, experience a reduction in oxygen delivery (Davis, R.W. and Kanatous, S.B., 1999), (Butler, P.J. and Jones, D.R., 1997). By the end of an aerobic dive, the arterial oxygen partial pressure in Weddell seals may be as low as 3.2 kPa (Davis, R.W. and Kanatous, S.B., 1999), which is equivalent to the degree of hypoxaemia experienced by human climbers on the top of Mt Everest (approximately 8850 m). However, these animals do not undergo any adverse effects upon re-oxygenation.

Many of the mechanisms that animals use to reduce renal oxygen demands appear to be invoked during severe pathophysiological septic stress in the human. The mechanisms for these effects have yet to be fully elucidated. Nitric oxide (NO) may be an important mediator through which cells control their oxygen consumption (Beltran, B. *et al.*, 2000). The high rate of recovery from renal failure during sepsis, a condition associated with production of excess amounts of ROS and NO and their by-products (Brealey, D. *et al.*, 2002), has brought about the theory that control of oxygen utilisation lies at the heart of ARF.

The mitochondria represent an important target in sepsis but understanding of the pathophysiology (or, perhaps more correctly, physiology) underlying sepsis-

induced ARF remains scanty. In health, mitochondria have a double membrane forming a sac within a sac. The smooth outer membrane holds numerous transport proteins, while the inner membrane is folded into cristae. Cristae are the sites of ATP synthesis containing the electron transport chain (Complexes I to IV). NADH is converted to NAD^+ and the electrons (donated to Complex I and passed through Complexes II and III) are combined with atmospheric oxygen (provided to Complex IV) to pump hydrogen ions (protons, H^+) from the mitochondrial matrix across the inner membrane into the inter-membrane space. Complex V is a uses the potential difference of the proton gradient to convert ADP to ATP.

It is postulated that there is a final common pathway underlying organ failure that stems directly from the mitochondrion. Mitochondrial respiration is under the physiological control of NO (Beltran, B. *et al.*, 2000) at the site of complex IV in the respiratory chain (Brown, G.C., 2001). Nanomolar concentrations of NO immediately, specifically and reversibly inhibit cytochrome oxidase in competition with oxygen in isolated cytochrome oxidase (Brudvig, G.W. *et al.*, 1980), mitochondria (Beltran, B. *et al.*, 2000), nerve terminals (McNaught, K.S. and Brown, G.C., 1998), cultured cells (hepatocytes (Richter, C. *et al.*, 1994) and astrocytes (Brown, G.C. *et al.*, 1995)), kidney tubules (Koivisto, A. *et al.*, 1999) and tissue slices (Adler, S. *et al.*, 2001). Higher concentrations of NO and its derivatives (peroxynitrite, nitrogen dioxide or nitrosothiols) can cause longer-lasting or even irreversible inhibition of the respiratory chain (Sharpe, M.A. and Cooper, C.E., 1998) and, eventually, cell death. In sepsis, NO is over-produced in quantities that may significantly inhibit oxidative

phosphorylation and thus the amount of ATP production available to the cell (Beltran, B. *et al.*, 2000). Decreases in ATP concentrations, causing a lack of available energy stores to drive the kidney's excretory, secretory and absorptive functions, may prompt cellular shutdown. This could represent a state of 'hibernation' from which the kidney awakens upon recovery. Through this mechanism renal cells may avoid cell death (necrotic and/or apoptotic) from occurring to an extent sufficient to compromise eventual recovery. Mitochondrial dysfunction as an hypothesis has been supported by findings in both septic patients (Brealey, D. *et al.*, 2002) and septic animal models (Brealey, D. *et al.*, 2004).

NO plays an important role in kidney fluid and solute transport (Ortiz, P.A. and Garvin, J.L., 2002). In the proximal tubule, NO has been reported to stimulate net fluid and HCO_3^- flux (Ortiz, P.A. and Garvin, J.L., 2002), whereas only inhibitory effects of NO have been found on the Na^+/H^+ exchanger (Roczniak, A. and Burns, K.D., 1996). In the medullary thick ascending limb of the loop of Henlé (mTAL), NO inhibits net Cl^- and HCO_3^- absorption (Ortiz, P.A. and Garvin, J.L., 2000). These effects are partly mediated by a direct inhibitory action of NO on the Na^+-K^+-$2Cl^-$ co-transporter (Garvin, J.L. and Hong, N.J., 1999) and the Na^+/H^+ exchanger (Ortiz, P.A. *et al.*, 2001).

NO is an important modulator of glomerular and renal haemodynamics. Intrarenal NO is responsible for up to one third of normal renal blood flow and helps to maintain the low renal vascular resistance under normal conditions (Majid, D.S. and Navar, L.G., 2001). Nitric oxide synthase inhibition does not

alter glomerular flow but does decrease total renal flow (Ichihara, A. and Navar, L.G., 1999). NO plays an important role in regulating perfusion of the renal medulla. Local infusion of NOS inhibitors into animals reduces medullary blood flow (Zou, A.P. and Cowley, A.W., Jr., 2003) and leads to hypertension. Spontaneously hypertensive rats have an altered response to NO (Adler, S. and Huang, H., 2002).

It is clear that evolutionary pathways have developed to control cellular respiration under extreme physiology. The term *"Acute Renal Success"* was first coined by Thurau and Boylan in 1976 (Thurau, K. and Boylan, J.W., 1976) with respect to the role of the juxtaglomerular apparatus and the *macula densa* in urinary concentrating ability. The phrase should perhaps come back into vogue as nature has planned that once the organism recovers, renal function may then resume.

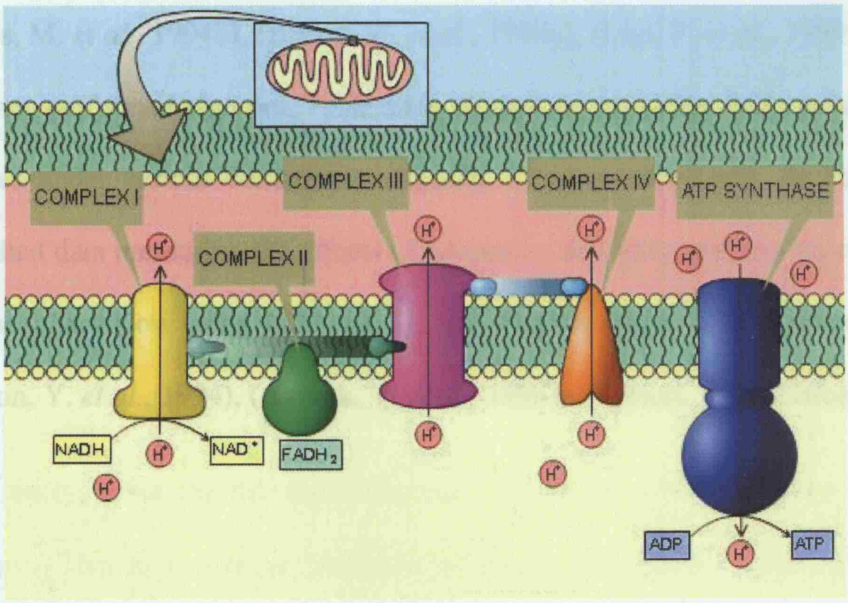

Figure 2-4: The electron transport chain

2.4 Previous work by other groups

Although two groups – one led by Brezis and colleagues, the other by Liss *et al* – have published widely on renal tissue oxygen, neither has fully linked their techniques with tissue flow. Each group has published occasional papers using laser Doppler flow (LDF) to measure changes in cortical and medullary flow (Brezis, M. *et al.*, 1994b), (Brezis, M. *et al.*, 1994a), (Liss, P. *et al.*, 1999a), but have not performed rigorous, systematic studies investigating intra-renal flow changes under various conditions. Agmon, in conjunction with Brezis, also published data measuring the effects of adenosine and indomethacin on cortical and medullary flow using LDF, but did not measure changes in regional PtO_2 (Agmon, Y. *et al.*, 1994), (Agmon, Y. *et al.*, 1993), (Agmon, Y. and Brezis, M., 1993).

2.4.1 Tissue oxygen

2.4.1.1 Measurement tools

Tissue oxygen tension, which represents the balance between local tissue oxygen supply and demand, can be measured by a variety of techniques. The classic tool is the Clark electrode. The Clark cell was first described in 1956

(Clark, L.C.J. and Lyons, C., 1962) and is an ampherometric cell polarised to 800 mV. At this voltage, silver is reduced to silver chloride and water is oxidised (with oxygen) to hydroxide ions. The rate of reaction depends on the availability of oxygen and the net 'movement' of electrons allows a current to be measured. Assuming abundant salt substrate, the rate of reaction is proportional to the concentration of oxygen.

There are problems associated with Clark cells. The major problem in physiological systems is that the probe consumes oxygen as part of the reaction (Takahashi, G.H. and Goldstick, T.K., 1966). The rate of consumption is itself dependent on the concentration of oxygen and, therefore, is not constant and difficult to quantify. It may be significant at the low concentrations of oxygen found in physiological systems such as the renal medulla.

Additionally, silver chloride coats the anode over time and reduces the rate of reaction. This is known as 'isolation of the anode'. Electrolytes must be replaced as chloride ions are depleted and the pH of the system is made more alkali with the production of OH^- ions.

Anode (Ag) reaction

$$2Ag^{+} + 2\,Cl^{-} \leftrightarrow 2AgCl + 2e^{-}$$

Cathode reaction (using platinum, gold, palladium catalyst)

$$2e^{-} + \tfrac{1}{2}O_2 + H_2O \leftrightarrow 2OH^{-}$$

Net result:

$$2Ag^{+} + 2e^{-} + \tfrac{1}{2}O_2 + H_2O + 2\,Cl^{-} \leftrightarrow 2AgCl + 2OH^{-} + 2e^{-}$$

Figure 2-5: Chemical reaction for the Clark electrode

Clark (Clark, L.C.J. and Lyons, C., 1962) adapted a platinum electrode first described by Blinks and Skow in 1938 during studies into photosynthesis (Blinks, L.R. and Skow, R.K., 1938). He constructed an electrode which contained both the anode and cathode bathed in an electrolyte behind an electrically-insulated but gas-permeable polyethylene membrane. This proved to be more accurate and more compact than previous versions and provided a more stable environment for the electron reaction (reviewed in (Severinghaus, J.W. and Astrup, P.B., 1986)). It also allowed improved definition of the diffusion conditions. Miniaturisation to a diameter of 1 μm was shown to have a number of further advantages (Fatt, I., 1964). 95% of the drop in diffusion gradient in the medium around the tip of the probe was reported to be within 6 diameters of the electrode (Takahashi, G.H. and Goldstick, T.K., 1966). Thus the electrodes used by many other renal tissue oxygen models detected a 6 μm layer of oxygen to within 5% accuracy. This is highly specific and reinforces the findings of Baumgartl (Baumgartl, H. *et al.*, 2002). To put this in context, a single glomerulus is 150-200 μm in diameter and a single red blood cell within a large vessel is 12 μm. The necessary blind placement of the probe means that the results could be from within any of those structures. Indeed, in his 1994 paper, Brezis (Brezis, M. *et al.*, 1994a) admits that *"the probe was moved until a good signal was obtained"*. It may be that a poor signal was obtained either when the tip of the probe was inserted into one of these structures or that a poor reading was a true reflection of the renal tissue oxygen.

An alternative technique to measure tissue oxygen tension is the use of ruthenium fluorescence. The theory and technology behind the OxyLite device used in my studies is described in the Methods chapter. A ruthenium crystal sited at the tip of the probe fluoresces when excited by a blue LED light. The probe then measures the decay of the fluorescence returned down a single glass fibre. The half-life of the decay is related inversely to the local oxygen tension as fluorescence is quenched in the presence of oxygen. This is predicted by the Stern-Volmer equation (see later).

The ruthenium fluorescence technique has advantages over conventional polagraphic Clark electrodes in two important ways. Firstly, there is no oxygen consumption. As discussed above, oxygen is continually consumed at the reaction site of the Clark electrode in an unpredictable fashion depending upon anode isolation and the concentration of oxygen itself. The rate of oxygen consumption is especially important at lower oxygen concentrations. Secondly, fluorescence techniques are more accurate at lower values of PtO_2. Because decay of the signal is prolonged at lower oxygen concentrations, the half-life is more accurately measured. As oxygen concentrations in the medulla are low, the ruthenium fluorescence provides a very suitable alternative to the Clark electrode for its measurement.

The volume sampled around the OxyLite™ ruthenium fluorescence probe used in my experiments is believed to be 0.35 mm^3 for oxygen (Jakobsson, A. and Nilsson, G.E., 1993). This volume offers a true reflection of the local tissue oxygen and combines signals from all cell types within the volume of sampling.

It will also include a component from post-capillary blood and will therefore be able to give useful information when oxygen extraction is high. This is in contrast to the Clark electrode where volumes are perhaps too low for the smaller probes; these may potentially not detect changes in venous blood oxygen saturations if sampling occurs close to an arterial vessel.

2.4.1.2 Tissue oxygen studies

On the face of it, revisiting renal tissue oxygenation is to repeat work carried out in the 1980's. Brezis and co-workers published widely on an isolated perfused kidney model (Brezis, M. *et al.*, 1984c), (Brezis, M. *et al.*, 1984b), (Brezis, M. *et al.*, 1985), (Rosen, S. *et al.*, 1992) but progressed to an anaesthetised rat model (Brezis, M. *et al.*, 1994b), (Brezis, M. *et al.*, 1994a). With Epstein's group, they produced work suggesting that the medulla was working 'on the edge of anoxia' (Heyman, S.N. *et al.*, 1997), and therefore the site for acute renal failure either through vascular or tubular mechanisms.

Liss and colleagues also produced a similar *in vivo* model but obtained considerably different baseline results for tissue oxygen tension in the cortex (5.60 kPa compared with 8.13 kPa). He reported very similar responses in both cortex and medulla to hypotension (Liss, P. *et al.*, 1997a), when compared to those reported by Brezis (Brezis, M. *et al.*, 1994b). This group then diversified to concentrate on possible mechanisms for radiocontrast-induced renal failure

(Liss, P., 1997), (Liss, P. *et al.*, 1997a), (Liss, P. *et al.*, 1999a), (Liss, P. *et al.*, 1999b), (Liss, P. *et al.*, 1996), (Liss, P. *et al.*, 1997b).

There are two other reports measuring renal PtO_2 in animal models. Nelimarkka (Nelimarkka, O. *et al.*, 1982) reported PtO_2 changes using a Clark electrode in dogs during exsanguination. James (James, P.E. *et al.*, 1995) used Electron Paramagnetic Resonance (EPR) to report on renal PtO_2 in the mouse. The findings in baseline renal PtO_2 values are summarised in Table 2-1. Variations in experimental technique are summarised in Table 2-3.

Although renal tissue oxygenation has been the subject of many published papers, few have matched tissue oxygen tension to local flow. Indeed, some have failed to monitor basic cardiovascular parameters such as blood pressure while the degree of fluid resuscitation has also been variable. The PtO_2 represents the balance between local oxygen delivery and consumption. Our group and others have previously demonstrated progressive decreases in PtO_2 in various tissues during escalating hypoxaemia (Stidwill, R.P. *et al.*, 1998) or haemorrhage (Singer, M. *et al.*, 1996), (Kwan, M.R. and Hunt, T.K., 1973), (Soller, B.R. *et al.*, 2001), which recovers upon reoxygenation or resuscitation. By contrast, an increase in PtO_2 was recorded in various organ beds during resuscitated sepsis (King, C.J. *et al.*, 1999), (Rosser, D.M. *et al.*, 1996), (Boekstegers, P. *et al.*, 1994) suggesting adequate supply but decreased cellular utilization of oxygen. However, in all of these examples, changes in local blood flow were not measured.

Cortex, kPa (Mean ± SEM)	Medulla, kPa (Mean ± SEM)	Reference
8.13 ± 0.93	2.13 ± 0.53	(Brezis, M. *et al.*, 1994b)
5.60 ± 0.53	4.53 ± 0.80	(Liss, P. *et al.*, 1997a)
5.1	1.27	(Gunther, H. *et al.*, 1974)
4.6	3.3	(Nelimarkka, O., 1984)
6.3	4.8	(Aperia, A.C., 1969)
Not Measured	1.3	(Leichtweiss, H.P. *et al.*, 1969)
3.0 ± 0.17	2.02 ± 0.17	(James, P.E. *et al.*, 1996)
1.6 ± 0.2	1.2±0.3	Thesis

Table 2-1: Renal tissue oxygen values by various groups

Baumgartl and Lubbers (Baumgartl, H. *et al.*, 2002), (Lubbers, D.W. and Baumgartl, H., 1997) produced interesting results using a Clark electrode in canine kidneys by withdrawing it through the renal parenchyma at 10 μm steps to analyse the tissue oxygen within. They produced histograms of the frequencies of results obtained. This 'profiling' of renal tissue (which they also repeated in brain) revealed wide differences in PtO_2 between steps. They reported that most of the steps between measurements were ±10 torr (1.33 kPa). A frequency histogram of the step amplitudes showed a symmetric form: all readings were between -35 and +49 torr (-4.67 and +6.53 kPa) with 90% between -12 and +11 torr (-1.66 and +1.46 kPa) of the previous reading. They noted at distances larger than 100 μm that the amplitude histograms disintegrated. They concluded that their technique could measure the state of oxygen supply of local structures and that the various histogram frequencies could offer a reflection of the *microcirculatory unit* of capillary oxygen supply.

Baumgartl and Lubbers highlighted large variations in PtO_2 within adjacent 10 μm samples. It may be that very small diameter Clark electrodes reflect the PtO_2 in such a specific area of renal tissue that they do not necessarily represent the region as a whole. This may also explain the variation in results obtained and will be expanded in the Discussion chapter.

2.4.2 Renal flow studies

Microvascular flow may be measured in four ways:

1) Laser Doppler flowmetry
2) Microspheres (either fluorescent or radioactive)
3) Intra-vital microscopy.
4) Orthogonal polarisation

Orthogonal polarisation is a new method for visualising the microvasculature (Michel, F. *et al.*, 2004). It produces an image by using scattered polarized light, creating a 'virtual' light source within the observed tissue. This makes it possible to visualise and measure real time images of the microcirculation, without fluorescent dyes or transillumination. It has yet to be used on the kidney but the technology can not give information on the deep vasculature at this stage.

Intravital microscopy involves inspection a flat piece of tissue placed on a microscope slide (usually a skin flap or the *vas deferens* of a small mammal) and is thus not possible to perform on renal tissue.

Blood flow to the renal cortex has also been measured using radioactive microspheres (Stein, J.H. *et al.*, 1973). Although this allows an absolute value for cortical blood flow to be measured, the portal nature of the renal vasculature (see 2.2.1) means that microspheres will only lodge in the cortical small vessels and not be able to pass into the medulla. Although a quantitative measure of intra-renal flow is possible, the distribution between cortex and medulla is not measurable by this technique.

Laser Doppler flow (LDF) studies on the other hand, allow measurements to be taken at any level of the kidney. A fuller description of LDF is provided in the Methods chapter. It is an established and reliable method for the measurement of the microcirculation in clinical and laboratory situations (Roald, A.B. *et al.*, 2002), (Liss, P. *et al.*, 1999a), (Agmon, Y. *et al.*, 1993), (Agmon, Y. and Brezis, M., 1993), (Atkins, J.L. and Lankford, S.P., 1991), (Dobrowolski, L. *et al.*, 2000), (Flemming, B. *et al.*, 2000), (Mattson, D.L. *et al.*, 1993), (Millar, C.G. and Thiemermann, C., 1997), (Smits, G.J. *et al.*, 1986). The drawback with LDF is that it does not give absolute regional flow values and can only provide changes in local flow. By maintaining a probe in the same position and continually measuring during physiological derangement, short-term variations in local tissue flow may be monitored, but because of the unitless nature of LDF, only percentage changes (rather than absolute values) are reported.

2.4.2.1 Laser Doppler studies

Some of the very early validation studies performed with LDF used rat renal cortex. Stern *et al* (Stern, M.D. *et al.*, 1977) described a feasibility study carried out using light from a helium-neon laser illuminating a 1 mm area of human skin and rat renal cortex and monitored changes in LDF over time. By 1990, LDF was still being described as 'a new method' (Oberg, P.A., 1990) and it was not much longer before it was put to use measuring changes in renal flow.

Paired measurements of pig renal cortical PtO_2 and LDF were described in 1990 (Sandin, R. *et al.*, 1990) to validate the timing of microsphere injection. Analysis of the LDF output was not performed. The first true renal application of LDF was performed by Brezis's group to assess the effects of adenosine receptor agonists and antagonists (Agmon, Y. *et al.*, 1993). Endogenous adenosine is secreted locally by the kidney during tissue hypoxia and induces heterogeneous renal haemodynamic responses. They found that intrarenal adenosine reduces cortical blood flow via A1 receptors and increases medullary flow through A2 receptors.

Brezis then published paired papers '*Determinants of intrarenal oxygenation. I. Effects of diuretics'* (Brezis, M. *et al.*, 1994a) and *'Determinants of intrarenal oxygenation. II. Hemodynamic effects'* (Brezis, M. *et al.*, 1994b) elaborating on tissue oxygen work carried out earlier in the 1990s and using LDF to confirm that regional flow was maintained during various insults. When furosemide was used, they noted a fall in medullary flow and a rise in the PtO_2 confirming the 'oxygen sparing' effects of loop diuretics. Shortly after, Dobrowolski (Dobrowolski, L. *et al.*, 2000) also demonstrated that furosemide decreased medullary flow.

In the results of previous whole animal models described above (Table 2-1), there were significant differences in the experimental technique of each of the models. Similarly, the model presented in this thesis also varies from those described previously. Small variations in experimental technique may account for the large differences in PtO_2 noted.

Differences in nomenclature may also be one very simple explanation to account for some of the differences found. Brezis's group, for example, frequently measured cortical PtO_2 from 2 mm and greater below the surface (Brezis, M. *et al.*, 1994b), (Brezis, M. *et al.*, 1994a) – a depth Liss would regard as the outer stripe of the medulla (Liss, P. *et al.*, 1997a) (see Figure 2-1).

2.4.3 The influence of experimental design on intra-renal haemodynamics and oxygenation

2.4.3.1 The influence of anaesthesia

A variety of anaesthetic agents have been used in animal models that have studied intrarenal haemodynamics and oxygen tensions. All have relied on an intermittent injection technique (intravenous, intramuscular or intraperitoneal) which offers a far less stable environment than a constant infusion or flow of anaesthetic agent. Assessment of the depth of anaesthesia is very difficult and usually involves monitoring of cardiorespiratory parameters (e.g. blood pressure, pulse and respiratory rate as well as gas exchange, in particular carbon dioxide tensions). As a major and valid criticism of previous studies, such monitoring has usually been lacking.

Most intermittent techniques simply re-dose the animal every 30 minutes. Variability between individual animals means that some will be excessively sedated with intermittent boluses while others may abruptly awaken during the study. Blood pressure may fluctuate markedly, with either hypotension from anaesthetic overdose, or an 'alpine-vista' blood pressure profile where the animal's BP rises as the anaesthetic wears off only to fall again when the next anaesthetic dose is administered. Kotajima and colleagues (Kotajima, F. *et al.*, 2005) noted changes in cerebral vascular tone with changes in ventilation during REM and non-REM sleep. In anaesthetised, spontaneously breathing subjects, carbon dioxide tensions will also vary considerably as awareness under anaesthesia is associated with hyperventilation and deep anaesthesia with hypoventilation (Miller, R.D., 2004). Changes in arterial pCO_2 have major consequences on pulmonary (Dorrington, K.L. and Talbot, N.P., 2004), peripheral (Rothe, C.F. *et al.*, 1990) and cerebral vasculature (Cox, B.F. and Brody, M.J., 1989). Although experimental data does not exist, changes in arterial pCO_2 may be predicted to also affect intra-renal blood flow. If the kidney is representative of other organ beds high arterial pCO_2 levels will result in vasodilatation, while low levels cause vasoconstriction. In addition, awareness while under anaesthesia is associated with surgical stress, resulting in an increased output from the sympathetic system with systemic release of adrenergic agonists (epinephrine and norepinephrine). The kidney has a sympathetic nerve supply and is therefore under the influence of both local and systemic adrenergic systems. For all the above reasons, it is thus highly likely that overdose or emergence from anaesthesia prior to the next administered dose would alter intra-renal haemodynamics and affect both local flow and PtO_2.

According to some authors (Evans, R.G. *et al.*, 2004), the medulla is relatively insensitive to vasoconstrictors (as might be expected from the 'portal' nature of the *vasa recta*), though changes in sympathetic output do alter cortical blood flow.

Although inhalational anaesthesia overcomes many of the problems listed above, especially when the animal is adequately monitored, it does carry some potential drawbacks. Vapour anaesthesia causes vasodilatation and hypotension in the unresuscitated subject (animal or human). Both Liss (Liss, P. *et al.*, 1997a) and Brezis (Brezis, M. *et al.*, 1994b) noted that vasodilatation with intravenous glyceryl trinitrate (GTN) caused convergence between cortical and medullary PtO_2. As a NO donor, however, GTN may also be modulating cell respiration in addition to causing vasodilatation so this finding may not be significant.

Inhalational agents are also associated with a reduction in oxygen consumption in many tissue beds, including the kidney (Miller, R.D., 2004). In addition, isoflurane has been shown to induce pre-conditioning in brain (Zheng, S. and Zuo, Z., 2005), spinal cord (Park, H.P. *et al.*, 2005), myocytes (De Hert, S.G. *et al.*, 2005) and reduces the extent of myocardial infarction (Haessler, R. *et al.*, 1994). Isoflurane may therefore be protective during ischaemia/reperfusion. Unfortunately, pre-conditioning is beyond the scope of this thesis but investigation may certainly be possible through the use of this model.

2.4.3.2 The influence of an intact or removed renal capsule

The kidney is surrounded by a fibrous capsule. When breached during our experiments, the capsule tore implying that the tissues underneath were under pressure. The compartmental pressure within the capsule will affect renal perfusion pressure and therefore intra-renal haemodynamics according to the formula shown in Figure 2-6. No studies have examined the effects of an intact/removed capsule on intra-renal haemodynamics. This should be the subject of further studies.

$$RPP = MAP - CVP - ICpP$$

Figure 2-6: Formula to calculate the compartmental perfusion pressure

(RPP = Renal Perfusion Pressure, MAP = Mean Arterial Pressure, CVP = Central Venous Pressure, ICpP = Intra-Capsular Pressure)

2.4.3.3 The influence of fluid resuscitation

The model described in this thesis also varies from other models in both the volume and type of resuscitation fluid used.

The influence of type

Although commonly known as 'normal' saline, 0.9% Sodium Chloride solution contains 154 mmol sodium and 154 mmol chloride dissolved completely as ions in one litre of water. The concentrations of both sodium and chloride administered when infusing this solution are far in excess of those found physiologically (Table 2-2). Although not specifically studied by authors, Liss and colleagues (Liss, P. *et al.*, 1997b) noted that injection of Ringer's solution did not change intra-renal tissue oxygen when used as control in a study of the effects of contrast solutions.

Intravenous fluid	mmol/l				
	Na^+	K^+	HCO_3^-	Cl^-	Ca^{2+}
Normal plasma values	**142**	**4.5**	**26**	**103**	**2.5**
Sodium Chloride 0.9%	150	-	-	150	-
Compound Sodium Lactate (Hartmann's)[+]	131	5	29	111	2
Ringer's Solution[*]	147	4	22	156	2.2
Sodium Chloride 0.18% and Glucose 4%	30	-	-	30	-
Potassium Chloride 0.3% and Glucose 5%	-	40	-	40	-
Potassium Chloride 0.3% and Sodium Chloride 0.9%	150	40	-	190	-

Table 2-2: Electrolyte concentrations—intravenous fluids

+ Lactate used for buffer - Hartmann's Solution is also known as Lactated Ringer's Solution

*** Phosphate used for buffer**

The influence of volume

As described in the Methods chapter, our animal model received enough fluid resuscitation to optimise aortic flows. As anaesthesia of all types is associated with vasodilatation and hypotension in the under-resuscitated subject, fluid optimisation may restore adequate blood pressure. Fluid resuscitation is the cornerstone of therapy in patients presenting with compromised renal function. In a study of critically ill oliguric patients (Marik, P.E., 1993), 200 patients were screened and only nine enrolled. Many oliguric patients were excluded because of an improvement in their urine output after fluid challenge.

Mattson (Mattson, D.L. *et al.*, 1993) examined the autoregulation of blood flow in different regions of the renal cortex and medulla in volume-expanded or water-restricted anaesthetised rats. At renal perfusion pressures greater than 100 mmHg, renal blood flow (measured by electromagnetic flowmetry), and superficial cortical blood flow and deep cortical blood flow (both measured by laser Doppler flowmetry) were all well autoregulated in both volume-expanded and hydropenic rats. Inner and outer medullary blood flows were also well autoregulated in the water-restricted rats, but blood flow in these regions was poorly autoregulated in volume-expanded animals. Below a perfusion pressure of 100 mmHg, all regions of the kidney had reduced flows. The authors concluded that the animal maintained autoregulation in the renal cortex but that fluid resuscitated animals lost autoregulation in the medulla.

This interesting conclusion is discussed further in chapter 5. Of note, however, medullary flow is dependent on cortical flow through the portal nature of the

post-glomerular vasculature. Therefore, under-resuscitation probably caused the animals to demonstrate cortical flow-dependent medullary flow. I would suggest that under-resuscitation may compromise the medulla and that autoregulation should not necessarily be a feature of medullary flow.

There are also issues relating to excess fluid administration. By providing a high sodium load to the tubules, an additional energetic burden may be placed upon the filtration and reabsorption systems. This could then increase local oxygen consumption and cause a fall in tissue oxygen should the extra burden not be matched by an increase in blood supply.

Species	Anaesthetic	Fluid Resus	Capsule On/Off	Kidney in Cup? Yes/No	Mode of PO_2 Measurement	Ref
Dogs		None	Off	No	Silastic tonometers	(Nelimarkka, O., 1984)
Lewis DA rats	Inactin - thiobarbital	Ringers' Solution	?	Yes	Clark Electrode	(Liss, P. *et al.*, 1997a)
Sprague -Dawley Rat	Inactin - thiobarbital	Normal Saline with 4% Albumin	Off	Yes	Clark Electrode	(Brezis, M. *et al.*, 1994b)
Mice	Awake – allowed to drink water freely	No IV access	*In vivo study*	N/A	Electron Paramagnetic Resonance (EPR)	(James, P.E. *et al.*, 1996)
Wistar Rat	Vapour	Compound Ringer's Lactate Solution	On	No	Ruthenium fluorescence	Current thesis

Table 2-3: Summary of experimental techniques used in the study of renal tissue oxygen measurements

2.5 Pathophysiology

2.5.1 Renal hypovolaemic responses

In an organ so closely aligned with fluid homeostasis, significant changes in PtO_2 and intra-renal flow may be expected during hypovolaemic stress. However, in early studies using radioactive microspheres, Szabo and colleagues (Szabo, G. *et al.*, 1977) failed to reveal evidence of either autoregulation of renal blood flow or selective renal vasoconstriction. They only observed a moderate shift of blood flow from the outer to the inner cortex with a small increase in medullary ^{133}Xe wash-out but could not show redistribution of renal blood flow.

Early experiments studying flow (Aukland, K. and Wolgast, M., 1968) and PtO_2 (Kwan, M.R. and Hunt, T.K., 1973), (Carriere, S. and Daigneault, B., 1970), concentrated on the feasibility of the techniques employed rather than the study of renal oxygenation mechanisms. Nelimarkka (Nelimarkka, O., 1984), (Nelimarkka, O. *et al.*, 1982), (Nelimarkka, O. and Niinikoski, J., 1986) studied renal cortical and medullary tissue oxygen tension in dogs during graded haemorrhage and re-infusion of shed blood. Measurements were made through implanted Silastic tubes but no flow measurements were made. 40% blood loss caused significant falls in both cortical and medullary PtO_2 which returned to pre-haemorrhage levels in the medulla following re-transfusion with a transient

increase in cortical PtO_2. In a subsequent study, however, Nelimarkka demonstrated that the mixed venous saturation of blood in the renal vein during acute haemorrhage remained constant until the PtO_2 reached a critical level (Nelimarkka, O. and Niinikoski, J., 1986). This implies that oxygen extraction is reduced in the face of a decreasing oxygen delivery.

In contrast, Brezis (Brezis, M. *et al.*, 1994b) showed that acute hypotension (by controlled haemorrhage) paradoxically increased medullary pO_2 but decreased cortical pO_2 and that laser-Doppler studies indicated a reduction of cortical blood flow while medullary blood flow was unchanged or increased. These results are placed in context in chapter 5. It is proposed that differences in experimental technique could contribute to such different results.

2.5.2 The kidney in sepsis

2.5.2.1 Histological changes seen in sepsis

Although the term *'acute tubular necrosis'* (ATN) is colloquially applied to the renal dysfunction of sepsis, histology fails to reveal either necrosis or signs of tubular damage (Hotchkiss, R.S. *et al.*, 1999). No uniform diagnostic criteria for ATN exist (Thadhani, R. *et al.*, 1996). One definition of toxic acute tubular necrosis is roximal tubular epithelium necrosis (loss of nuclei, intense eosinophilic homogenous cytoplasm, but preserved shape). Necrotic cells fall

into the tubule lumen, obliterating it, and determining acute renal failure. The basement membrane remains intact, so that tubular epithelium regeneration is possible. Glomeruli are not affected. Clinically, ATN is characterised by a sudden decline in glomerular filtration rate (GFR); accumulation of nitrogenous wastes; and an inability of the kidney to regulate the balance of sodium, electrolytes, acid, and water. This loose definition applies to many patients with renal dysfunction. However, the commonest cause of ARF in hospital is ischaemic or so-called 'toxic' ATN (Liano, F. and Pascual, J., 1996).

In one paper (Richman, A.V. *et al.*, 1981), rhesus monkeys were given endotoxin, either as a 10 mg/kg bolus or by prolonged infusion at a rate of 10 mg/kg/hr. Only minor morphological changes were seen in those animals receiving the endotoxin bolus. Those receiving endotoxin infusion showed sequestration of neutrophils and monocytes in the peritubular capillaries and, to a lesser extent, in the glomeruli; however, no sequestration was seen in the tubules. These changes were associated with occasional fibrin deposits and extensive endothelial cell damage with focal capillary disruption. Only in the advanced stages, when the endotoxin infusion had been running for 22 hours in animals not resuscitated with fluid, were changes seen that included prominent interstitial oedema and focal necrosis of tubular epithelium. Endothelial cell changes seen in the glomeruli were far less severe than those observed in the peritubular capillaries.

Histological data from septic patients are even less common in the literature. In an important post-mortem study of patients dying of multiple organ failure,

Hotchkiss *et al* (Hotchkiss, R.S. *et al.*, 1999) observed; *"histologic findings in kidneys from control patients revealed no acute changes. Surprisingly, despite the high prevalence of clinical renal dysfunction (65%) ... only one septic patient had evidence of kidney necrosis. No renal tubular nor glomerular cell apoptosis was seen in any septic patient. Hence, in patients without pre-existing renal disease, renal histology did not reflect the severity of renal injury indicated by the decrease in kidney function."* Also noteworthy was the lack of comment on the presence of microvascular thrombosis.

The presence of normal-looking kidneys under light microscopy points towards a lack of overt inflammatory activity that could be responsible for renal dysfunction. However, this feature is not simply isolated to sepsis. Early studies of biopsies taken at *post mortem* and from patients with "acute tubular necrosis" failed to find overt tubular necrosis (Finckh, E.S. *et al.*, 1962), (Brun, C. and MUNCK, O., 1957), though subsequent studies using electron microscopy did reveal some ultrastructural changes (Olsen, T.S. *et al.*, 1985). This latter study examined biopsies taken from 24 patients diagnosed with ATN following sepsis, post-partum haemorrhage, surgery or trauma. Despite the wide range of underlying causes, cellular disintegration was very rare in both recovering and active ATN. They further noted that apoptosis was not present in the proximal tubules of the controls and was rare in acute renal failure (only 1.6-2.1% of cells studied). This would be insufficient in itself to account for changes in renal function.

These findings also explain the failure to find sloughed epithelial cells in sepsis-induced renal failure. Although true ATN is associated with sloughing of epithelial cells and occlusion of the tubular lumina by casts and cellular debris (Whitworth, J.A. *et al.*, 1994), (Esson, M.L. and Schrier, R.W., 2002), this is not an apparent feature of the histological findings quoted above (Hotchkiss, R.S. *et al.*, 1999), (Finckh, E.S. *et al.*, 1962), (Brun, C. and MUNCK, O., 1957), (Olsen, T.S. *et al.*, 1985).

2.5.2.2 Renal PtO_2 in sepsis

In health, the renal cortex has a higher blood flow than the medulla (Brezis, M. and Rosen, S., 1995). This is partly to ensure adequate plasma clearance by the glomeruli. Furthermore, to maintain an osmotic gradient within the medulla, a lower flow must exist in this region so that the solutes that constitute the gradient are not washed out. In an organ as sensitive to relative hypovolaemia, it would be logical to assume a vascular component would contribute to sepsis-induced ARF. However, one study (Camacho, M.T. *et al.*, 2001) failed to ameliorate organ failure in an animal model by aggressive resuscitation with albumin.

Characterisation of intra-renal haemodynamics is hampered by current technology. As outlined above, laser Doppler studies exist (Brezis, M. *et al.*, 1994b), (Heyman, S.N. *et al.*, 2000a), but can only express changes in regional flow (or, more precisely, flux) rather than absolute values. Linking absolute

flow to tissue pO_2 may allow estimation of regional oxygen delivery. However, all that can be noted at present is that tissue pO_2 differences between cortex and medulla tend to converge under septic conditions. Assuming passive diffusion of oxygen between vessels and tissue, the rise in medullary tissue pO_2 in sepsis noted by several authors (James, P.E. *et al.*, 1996),(Heyman, S.N. *et al.*, 2000a), may be due to changes in flow and/or the inability of the cells to use available oxygen (so called cellular dysoxia).

Renal cellular dysoxia is poorly described in the literature. Robin (Robin, E.D., 1977) first used the term 'dysoxia' in 1977 but it was only brought into the vernacular with the introduction of gastric tonometry and the realisation that there was more to resuscitation in sepsis than the maintenance of blood pressure (Gutierrez, G. and Brown, S.D., 1995), (Brown, S.D. and Gutierrez, G., 1996). Rises in renal tissue oxygen in the face of documented maintenance of intra-renal flow have yet to be described in the literature. I believe that my model demonstrates the first example of renal disruption of oxygen consumption in the face of adequate supply.

Hypotension is a common accompaniment of sepsis due to a combination of hypovolaemia, vasodilatation, a variable degree of myocardial depression, and vascular hyporeactivity. At the very least, hypotension will decrease the pressure gradient across the glomerulus and hence the filtration pressure within the capsule. However, this cannot be the sole cause of ARF as it may develop in the absence of any obvious haemodynamic perturbation. The septic insult also leads to production of a range of cytokines and vasoactive mediators that

produce regional microcirculatory pockets of vasodilatation and vasoconstriction. The acute stress response initiated by shock results in activation, among others, of the sympathetico-adrenal system (with increased levels of catecholamines), the renin-angiotensin system, and a rise in vasopressin. The multi-modal effects of vasopressin could have advantageous, deleterious and, ultimately, unpredictable effects on renal function. A review by Holmes *et al* (Holmes, C.L. *et al.*, 2001) summarised that plasma vasopressin levels at 10-20 pg/ml could cause antidiuresis through V2 receptors (V2R) receptors within the kidney. However, by acting through V1 receptors (V1R), a diuresis could be achieved at any level (between 1 and 1000 pg/ml). These receptors are also responsible for decreasing renal blood flow. Similarly, stimulation of the sympathetic system leads not only to an outpouring of epinephrine that may enhance renal flow, but also norepinephrine that causes vasoconstriction in the unresuscitated subject.

In sepsis, changes thus occur at both macro- and microcirculatory levels. Intra-renal haemodynamics have not been characterised in man while a confounding feature in many animal models is the co-existence of hypovolaemia due to inadequate resuscitation and the type of anaesthesia used (see earlier). This may account in part for the wide variation in reported results (Khan, R.Z. and Badr, K.F., 1999), not to mention differences in the type of model chosen, animal species, choice and degree of insult and number/severity of surgical procedures. Even in hyperdynamic septic models, variable renal blood flow responses have been seen (Ravikant, T. and Lucas, C.E., 1977), (Cronenwett, J.L. and Lindenauer, S.M., 1978), suggesting that selective renal vasoconstriction

maintains a normal renal blood flow in the face of an increasing cardiac output (Ravikant, T. and Lucas, C.E., 1977).

Several studies have characterised the oxygen gradient that exists within the kidney (Liss, P. *et al.*, 1997a), (Brezis, M. *et al.*, 1994b), (Leichtweiss, H.P. *et al.*, 1969), (Lubbers, D.W. and Baumgartl, H., 1997). Absolute values of cortical and medullary pO_2 vary between studies; as with intra-renal haemodynamics, this may also be contingent upon variations within the model and measuring technique (Table 2-1). There is, however, general agreement that the corticomedullary region has the lowest tissue pO_2 value. The juxtamedullary and outer medullary areas contain a high density of energy dependent Na^+/K^+ and Na^+/H^+ pumps that require high oxygen extraction. The partial pressure of oxygen at any point is the balance between local oxygen delivery and oxygen consumption. Regions of low tissue pO_2 may then be assumed to have low oxygen delivery and/or high oxygen extraction. Inhibition of Na^+/K^+-ATPase pumps by a loop diuretic (furosemide) caused a rise in medullary pO_2; this may also contribute to a reduction in tubular damage (Heyman, S.N. *et al.*, 1994). This was tested in human volunteers using Blood Oxygenation Level-Dependent Magnetic Resonance Imaging (BOLD MRI) (Epstein, F.H. and Prasad, P., 2000). In an *in vitro* model, unstimulated medullary kidney cells had a lower oxygen consumption compared with cortical cells but were able to raise their VO_2 to comparable levels when stimulated by endotoxin (James, P.E. *et al.*, 1995).

2.5.2.3 Distribution of blood flow

Brezis et al (Brezis, M. *et al.*, 1994b) showed how the NO donor sodium nitroprusside increased flow to the renal medulla and elevated medullary tissue pO_2. Administration of a loop diuretic under these conditions did not cause a further rise in medullary pO_2. The same group found that an endotoxin infusion resulted in maintained total renal flow, an increase in cortical flow but no change in outer medullary flow (Heyman, S.N. *et al.*, 2000a). These changes were blocked by the relatively non-specific nitric oxide synthase (NOS) inhibitor, N^G-nitro-*L*-arginine methyl ester (*L*-NAME), suggesting an important role for nitric oxide in the regulation of intra-renal blood flow. Furthermore, pre-treatment 24 hours prior with a single dose of endotoxin, a stimulator of nitric oxide production, globally reduced systemic and renal flows. Again, the effect was attenuated by *L*-NAME. In addition, other vasoactive mediators may act on renal blood flow via NO production; for example, vasopressin administration appeared to *increase* renal blood flow, an effect blocked by *L*-NAME (Holmes, C.L. *et al.*, 2001).

2.6 Renal pharmacology

2.6.1 Loop diuretics

The loop-active diuretic furosemide has been the standard treatment for heart failure for several decades. Apart from its diuretic action, furosemide also has effects on the cardiovascular system. In heart failure, its systemic administration has been reported to relieve the symptoms of pulmonary oedema immediately, even before diuresis sets in (Dikshit, K. *et al.*, 1973), through vasodilatation.

Furosemide conveys its diuretic effects by inhibiting sodium and chloride reabsorption in the proximal part of the ascending loop of Henle. Blocking the reabsorption of sodium, increases its excretion and water follows by osmosis. Blocking the ATP-dependent channels reduces local energy expenditure and ATP consumption, and thus should reduce oxygen consumption (Cunarro, J.A. and Weiner, M.W., 1978). As PtO_2 represents the balance between local oxygen delivery and regional cellular consumption, the PtO_2 should rise (Brezis, M. *et al.*, 1994a), (Brezis, M. *et al.*, 1984e). The PtO_2 should also rise if oxygen delivery increases. Contemporaneous measurement of flow and pO_2 allows changes in regional cellular consumption (VO_2) to be thus extrapolated. Results studying tissue oxygen should be interpreted in the knowledge that it is a combined measure of signals acquired from arteriolar, capillary and venule

blood balanced against the consumption by renal cells, vascular endothelium, immunological and interstitial cells.

Furosemide may inhibit many Na/K ATPases and has been used to alter pump activity in eosinophils (Perkins, R.S. *et al.*, 1992), rat parotid acini (Nauntofte, B. and Poulsen, J.H., 1986), rat liver (Anwer, M.S. and Clayton, L.M., 1985) and guinea pig cochlear cells(Komune, S. *et al.*, 1985). Furosemide inhibits mitochondrial respiration in rat liver, renal cortex and renal medulla (Orita, Y. *et al.*, 1983) and also causes vasodilatation (Dikshit, K. *et al.*, 1973), (Wallach, S. *et al.*, 1982), (Suehiro, K. *et al.*, 2001). It also reduces oxygen consumption in isolated renal tubules (Cunarro, J.A. and Weiner, M.W., 1978). Tissue oxygen tension rose following the administration of furosemide to both an isolated kidney preparation (Brezis, M. *et al.*, 1994a) and also to anaesthetized animals (Liss, P. *et al.*, 1999b). However, one human study using BOLD MRI revealed that furosemide did not alter medullary oxygen in older subjects (Epstein, F.H. and Prasad, P., 2000).

There are no studies measuring both tissue oxygen and local flow in the same volume of tissue following furosemide administration. As furosemide also vasodilates, any increase in tissue oxygen tension may be accounted for, in part, through local vascular effects and an increase in oxygen delivery, and in part through direct effects on cellular metabolism.

2.6.2 Inhibitors of the angiotensin converting enzyme (ACE)

Enalaprilat is the active metabolite of enalapril, an inhibitor of the angiotensin converting enzyme. ACE inhibition prevents conversion of angiotensin I into the potent vasoconstrictor, angiotensin II. Enalapril is used clinically for hypertension and to alleviate the symptoms of cardiac failure. It is also protective following myocardial infarction (Swedberg, K. *et al.*, 1992). Enalaprilat is a vasodilator and specifically relaxes vasoconstriction of the post-glomerular arteriole. It may therefore preferentially increase flow to the outer regions of the kidney. In addition, oxygen consumption is reduced in isolated rat kidneys slices (Adler, S. and Huang, H., 2002) suggesting a flow-independent effect on cellular metabolism. Angiotensin II inhibition also augmented renal cortical microvascular pO_2 (Norman, J.T. *et al.*, 2003) in a set of experiments performed without matching flow measurements.

2.7 Effects of hypoxaemia and hyperoxia

Oxygen is a cornerstone of the treatment of acutely ill patients. It is routinely used to give symptomatic relief of hypoxaemia and to improve tissue oxygenation by elevating blood oxygen tensions and thus improving oxygen delivery to the tissues.

Although a first-line drug in patient resuscitation, oxygen is not a benign drug. Though hypoxaemia is harmful, there are also inherent dangers in giving excessive amounts of oxygen. For example, hyperoxia causes pulmonary and ocular damage in mammals; in the early days of neonatal intensive care, babies were blinded through retrolental fibroplasia caused by the administration of high concentrations of oxygen.

The effects of changing FiO_2 on the kidney are poorly described in the literature. Hyperoxic reperfusion has been shown to exacerbate renal dysfunction following ischaemia in uninephrectomised, male mongrel rabbits (Zwemer, C.F. *et al.*, 2000). Antioxidant activity (of superoxide dismutase [SOD], catalase and glutathione peroxidase) was also reduced when breathing 100% O_2 compared with air following renal artery clamping in the rat (Sela, S. *et al.*, 1993). The latter study proposes that inactivation of these enzymes accounts for increases in ROS during hyperoxia.

Hyperoxic damage and cell death derive from enhanced intracellular formation of reactive oxygen species (ROS) upon exposure to air. These ROS are probably of mitochondrial origin though there is controversy on this point. Hyperoxia increases H_2O_2 release by lung mitochondria and microsomes (Turrens, J.F. *et al.*, 1982) and increases free radical production (Freeman, B.A. and Crapo, J.D., 1981). It is, however, highly likely that the degree of ROS production, and the response to these radicals, may differ between *in vitro* models and the *in vivo* situation.

2.8 Summary

Investigation of the physiological and pathophysiological responses to varying insults requires a multi-modal approach. Cellular and sub-cellular experiments offer a controlled environment in which to assess the response to a single variable but may be complicated by the response to high concentrations of oxygen when exposed to air and, in the case of cell lines and primary cultures, their establishment and growth in a much higher oxygen environment compared to similar cells *in vivo*. Furthermore, *in vivo* models are frequently dogged by a multitude of responses to an insult and that different cell types within a single organ may respond to insults in different ways. This is particularly true of the kidney, an organ containing numerous renally derived cells, vascular and immune cells each under the influence of the sympathetic, renin-angiotensin and vasopressin feedback control systems.

Previous *in vivo* animal models have reported wide differences in PtO_2 values and some may have compromised the renal physiology as a result of their experimental methodology. In this thesis, an original *in vivo* model of matched rat renal perfusion and tissue oxygen has been developed which attempts to ensure physiological stability throughout. The model is consistent between control experiments and assesses intra-renal regional changes through a variety of physiological and pharmacological challenges. The kidney is manipulated as little as possible and checks are in place to ensure that haematomas forming around the tip of the probe are detected. This thesis presents what is believed to

be the first attempt to quantify cellular respiration *in vivo* and to localise the site of acute renal damage.

The pathophysiology underlying ARF remains a conundrum. Treatment directed at correcting hypovolaemia and improving systemic blood flow may still not avert renal dysfunction. The ARF seen in sepsis and other shock conditions may be a deliberate attempt by the organ to preserve its long-term integrity in the face of a short-term insult. Teleologically, this makes sense. The ability of an organism to survive the initial acute insult, only to be killed in the medium term by irrecoverable renal failure runs counter to evolutionary theory. It may be that by reducing the amount of intracellular work, the kidney could reduce its ATP utilization, thereby maintaining ATP levels above the trigger for cell death (apoptosis or necrosis).

In order to move away from studies using cells, investigators have used whole animals. However, in many cases, although large changes in PtO_2 have been noted, these have rarely been linked to changes in regional flow. Until now, the technology has not existed to match flow with PtO_2. Previous experimental models varied in genus, species, mode of anaesthesia, degree and type of fluid resuscitation. As a result, wide varieties of values were obtained for PtO_2. I believe that vital to the physiological study of ARF is a robust animal model, such as that presented in this thesis.

3 Methods

3.1 Equipment used

In our model, measurements were made by using the OxyLite™ in combination with a laser Doppler flow probe, the OxyFlo™ (both Oxford Optronix, Oxford, UK). These are combined with a thermistor into a single 450 micron probe to allow measurement of local pO_2, net blood flow and temperature. Measurements of whole body and whole kidney flow were made using Doppler ultrasonic flow probes around the infra-renal aorta and renal arteries (both Transonics, Ithaca, NY). Arterial blood gas analysis was undertaken using an ABL70 blood gas analyser (Radiometer, Copenhagen, Denmark).

3.1.1 OxyLite ™

The OxyLite device uses the principle of ruthenium fluorescence to measure PtO_2. A ruthenium crystal, sited at the tip of a glass fibre 2 metres in length, fluoresces when excited by a blue LED light at a frequency of 485 Hz. The probe then measures the decay of the fluorescence at 600 Hz returned down the same fibre. Fluorescence quenching is related directly to the local oxygen tension according to the Stern-Volmer equation (Figure 3-1).

$$\frac{I_o}{I} = \frac{\tau_o}{\tau} = 1 + \tau_o K_q [O_2]$$

Figure 3-1: The Stern-Volmer equation

(I and I_0 are the measured signal intensity and signal intensity at time zero respectively, τ and τ_0 are the signal lifetime at the time of measurement and time zero, Kq is the bimolecular rate constant for the dynamic reaction of the quencher with the fluophore, τ_0Kq is the Stern-Volmer constant)

In the Stern-Volmer Equation, I_0 is the initial signal intensity, I is the measured signal intensity. τ and τ_0 are the signal lifetime, in the presence and absence of quencher respectively. Kq is the bimolecular rate constant for the dynamic reaction of the quencher with the fluophore. The product of $\tau_0 Kq$ is referred to as the Stern-Volmer constant or K_{SV}. One advantage of fluorescence techniques is that concentrations may be measured without the need to know the concentration of fluophore in the tissue in question. At constant temperature and atmospheric pressure, the concentration of oxygen is directly proportional to the partial pressure.

The OxyLite has advantages over conventional polagraphic probes in several ways:

- There is virtually no oxygen consumption

  Unlike the Clark electrode, fluorescence-based techniques consume much smaller amounts of oxygen and sample in short bursts. Any oxygen consumed during the course the light reaction should be replaced by the time of the next flash. This is in contrast to the Clark electrode where oxygen consumption is continuous but not constant. As outlined in Chapter 1, the rate of reaction for consumption at the Clark cathode is dependent upon many factors, not least the concentration of oxygen itself at the probe tip. It also varies as the anode becomes coated with silver chloride (isolation of the anode). As a result, calculation of very low concentrations of oxygen by the Clark electrode is impossible because of the unmeasurable and unknown proportion of oxygen lost to consumption.

- It becomes more accurate at lower partial pressures of oxygen.

  Since the fluorescence decay is lengthened at low partial pressures of oxygen, the decay half-life is longer and therefore more accurately measured. Fluorescent techniques therefore become more accurate at lower pO_2. At low partial pressures of oxygen, the Clark electrode's consumptive portion becomes relatively bigger and therefore more significant.

- Multi-channel

  The OxyLite™ is available in 2 or 4 channel configurations allowing simultaneous monitoring at multiple tissue sites. Advantage was made of this during the following set of experiments as measurements were made from three different regions of the kidney.

- Pre-calibrated Probes

  OxyLite™ eliminates the time consuming set-up and calibration procedures. Probes are supplied pre-calibrated with a unique bar-code containing the calibration information.

- Integrated Temperature Compensation

  The probes used in these set of experiments contained an integrated temperature sensor. Not only did this allow measurement of the tissue temperature but also allowed for automatic compensation of the pO_2 signal.

The OxyLite however, does not have true continuous oxygen monitoring. It emits 3 pulses of light and calculates the pO_2 from the average of the signals. Readings may be taken as frequently as every second. This maintains a balance between monitoring of physiological events such as oxygen decay curves following termination of experiments and bleaching of the fluophore. In contrast, polargraphic techniques are truly continuous (albeit causing oxygen consumption) as the concentration of oxygen dictates the rate of reaction at the electrode.

Other problems are associated with fluorescence techniques. Although measurements may be made every second, more frequent stimulation of the fluophore risks blanching of the fluophore within the tissues and a decrease in the signal returning; many of the fluophores are toxic and unsuitable for human use.

3.1.2 OxyFlo ™

The OxyFlo™ uses laser Doppler flowmetry (LDF) for continuous measurement of microcirculatory red blood cell flux, a variable assumed to be representative of local microcirculatory flow. LDF is established as an effective and reliable method for the measurement of the microcirculation in clinical and laboratory situations (Roald, A.B. *et al.*, 2002), (Liss, P. *et al.*, 1999a), (Agmon, Y. *et al.*, 1993), (Agmon, Y. and Brezis, M., 1993), (Atkins, J.L. and Lankford,

S.P., 1991), (Dobrowolski, L. *et al.*, 2000), (Flemming, B. *et al.*, 2000), (Mattson, D.L. *et al.*, 1993), (Millar, C.G. and Thiemermann, C., 1997), (Smits, G.J. *et al.*, 1986). LDF is reported in unitless perfusion units, the result being a net vector flow in line with the direction of the in-coming, Doppler-shifted signal. The returning signal will comprise of components from vessels of all sizes and at all angles to the probes. Insertion of the probe into different positions of the same kidney but also different insertions into different subjects, brings about a large variation in the results obtained because of the extreme variability in size, proximity and angle of return of vessels. Correlation of perfusion units with local flow can only be performed on a large experimental population. However, it is possible to measure the effect of an intervention by keeping the probe in the same position and recording the changes that occur. Because of the unitless nature of LDF, percentage changes (rather than the absolute value) are therefore noted.

The OxyFlo uses LDF for continuous measurement of microcirculatory red blood cell flux and provides a real time display of the returned signal or 'backscatter'. Backscatter is the percentage of the outgoing signal returning. An example of the experimental trace obtained is shown in Figure 3-2. Should the backscatter fall below 5%, results are known to be unreliable and were therefore not used. In the presence of obstruction of the probe tip, the pulsatile signal is flattened and the backscatter reduced.

The biggest criticism of the OxyLite system is the size of the probe. In contrast to the Clark electrode, combination of an OxyLite with OxyFlo probe and a

thermistor, as used in these experiments, forms a probe that is 450 μm in diameter and risks greater tissue trauma: Tissue haematoma formation could impair oxygen diffusion and is irritant to blood vessels possibly causing vasoconstriction (Wilson, S.R. *et al.*, 2005). Dampening of signal caused by haematoma can be detected by combining the OxyLite with an OxyFlo probe. Failure to receive an adequate backscatter signal or OxyFlo pulsatile variation may herald haematoma formation around the tip of the probe and thus leading to results being abandoned. As a result, it is possible to confidently detect the presence of significant haematoma around the probe tip with this model.

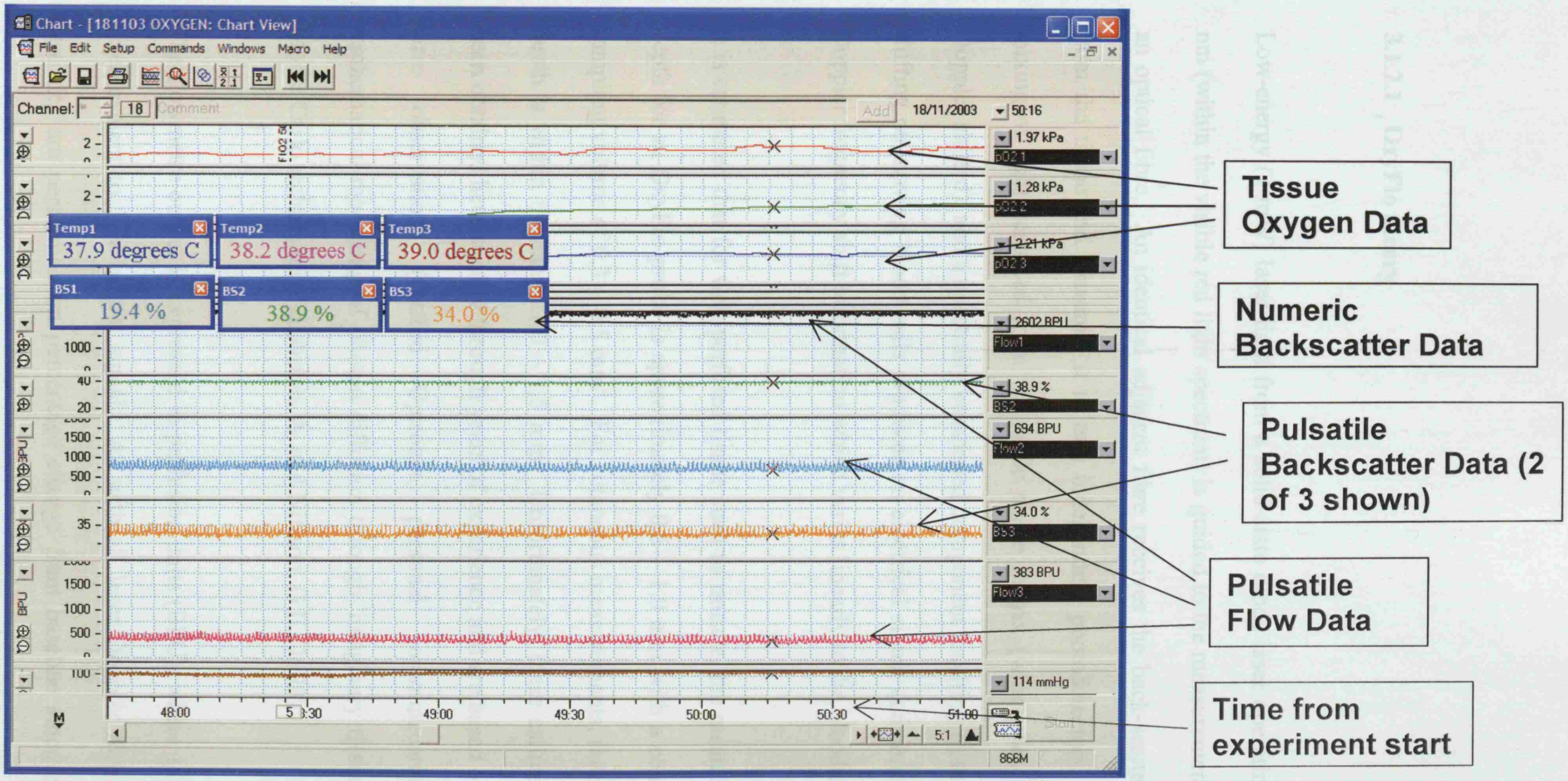

Figure 3-2: Example data screen capture for these sets of experiments

3.1.2.1 OxyFlo theory

Low-energy (2 mW) laser light from a solid-state diode laser operating at 780 nm (within the visible red light spectrum) is guided to the measurement site via an optical fibre. An identical adjacent fibre receives the back-scattered light from the tissue and transmits it to two independent photodetectors. Optical mixing of light scattered from the static tissue matrix (which has not been Doppler shifted), and a spectrally broadened component resulting from Doppler shifting on moving blood cells produces an electrical signal containing all the Doppler frequency shift information which varies linearly to the blood cell flow.

It is estimated that for well-perfused tissue such as muscle, the mean sampling depth for an OxyFlo probe is approximately 0.5 – 1.0 mm with a concomitant sampling volume of 0.3 – 0.5 mm^3. For cutaneous measurements, the sampling depth is within the range 1.0 – 1.5 mm. Unfortunately, these estimates have been obtained heuristically through years of experience and are based on both *in vitro* observations (Oxford Optronix, personal communication) and mathematical modelling of photon diffusion through 'imaginary tissues' using Monte Carlo techniques (Jakobsson, A. and Nilsson, G.E., 1993).

The flowmetre output is expressed in perfusion units (BPU), where 1,000 BPU is equivalent to 1 V output signal. As with all laser Doppler flow studies, statistics are performed on percentage change from baseline since perfusion

signals obtained vary widely, according to their proximity to large vessels and the vector to the signal.

Combination of these technologies into a single probe allows simultaneous sampling of both flow and pO_2 data from an area of tissue approximately 0.7 – 1.0 mm^3 (data from Oxford Optronix). Sampling from a wide volume within the kidney allows a representation of the whole region to be measured rather than the small specific signals that vary greatly within a few microns (Baumgartl, H. *et al.*, 2002) obtained from the Clark electrode.

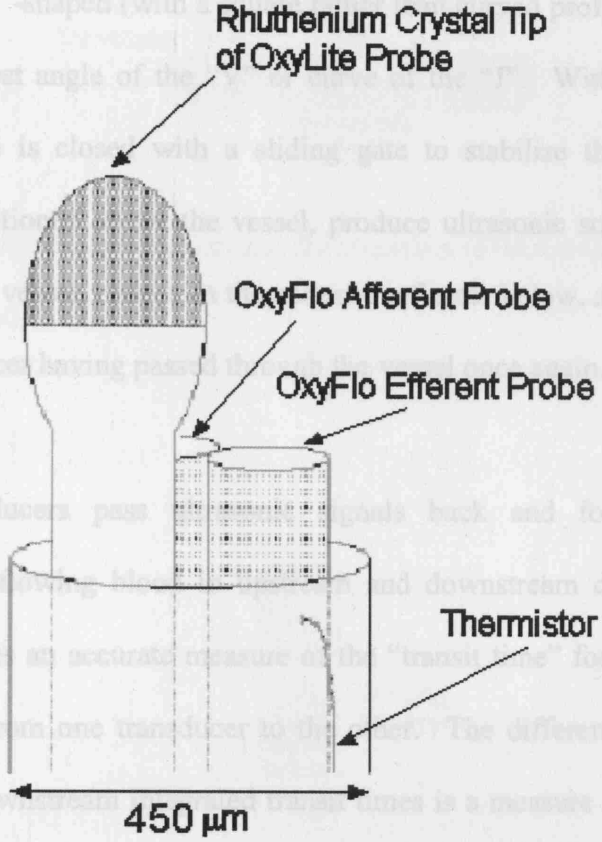

Figure 3-3: Combined OxyLite/OxyFlo and thermisor probe

3.1.3 Ultrasonic perivascular flow probe (Transonic™)

Probes are supplied in various sizes and shapes according to the size of the animal and vessel under investigation. Probes consist of a body which houses ultrasonic transducers and a fixed acoustic reflector so that the whole probe is either "V"- or "J"-shaped (with a square rather than curved profile). The vessel sits in the deepest angle of the "V" or curve of the "J". With larger probes, [2SB] the curve is closed with a sliding gate to stabilise the vessel. The transducers, positioned above the vessel, produce ultrasonic sound waves that pass through the vessel, reflect on the acoustic reflector below, and return to the opposite transducer having passed through the vessel once again.

The two transducers pass ultrasonic signals back and forth, alternately intersecting the flowing blood in upstream and downstream directions. The flowmeter derives an accurate measure of the "transit time" for the ultrasound wave to travel from one transducer to the other. The difference between the upstream and downstream integrated transit times is a measure of volume flow rather than velocity.

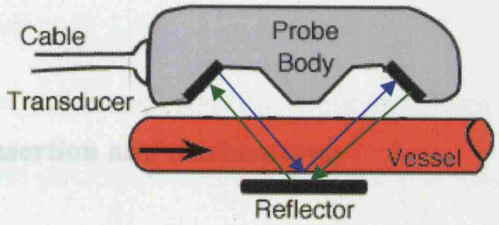

Figure 3-4: Bidirectional wide beam illumination (side view) (Diagram from Transonics)

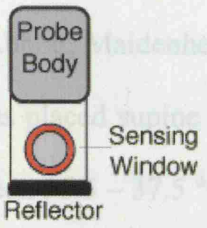

Figure 3-5: Bidirectional wide beam illumination (end view) (Diagram from Transonics)

3.2 Basic model instrumentation and set-up

3.2.1 Renal tissue oxygen and flow

3.2.1.1 Cannula insertion and tracheostomy

Experiments were performed under United Kingdom Home Office approval according to the Animals (Scientific Procedures) Act 1986. Male Wistar rats of 300 – 350 g body weight were given free access to food and water until the time of surgery. Anaesthesia was induced by placing the rats in a plastic tank and introducing 5% isoflurane (Baxter Healthcare Ltd, Northampton, UK) in air by a pump driving a Tec 4 vaporiser (Abbott, Maidenhead, UK). Once anaesthesia had been established, the animal was placed supine on a heated operating table to maintain rectal temperature between 36.5 – 37.5 °C. During instrumentation, anaesthesia was maintained with 2% isoflurane via a face mask or tracheostomy, once inserted. Thereafter, isoflurane was administered at a dose of 1.5% continuously throughout the experimental period. The animal was allowed to remain spontaneously breathing on room air throughout the experiment with normoxaemia and normocapnia confirmed in the stable baseline state by arterial blood gas analysis (ABL70, Radiometer, Copenhagen, Denmark).

Neck dissection was performed and vascular lines were inserted into jugular vein and carotid artery using polyethylene catheters of 0.9 mm outside diameter. Catheters were stretched over a heat source to reduce the diameter of the ends. The right internal jugular venous line was used to administer fluids while the left common carotid artery cannula allowed continuous blood pressure monitoring (Powerlab AD Instruments, Oxford, UK), withdrawal of blood during hypovolaemia, and blood sampling. A tracheostomy was also sited (2.08 mm external diameter polythene tubing) and cut to a length approximating to anatomical dead space and to secure the airway. This was then connected to a t-piece for administration of anaesthetic for the rest of experiment.

3.2.1.2 Laparotomy

A midline laparotomy was performed with the incision running from the xiphisternum to approximately 1 cm above the base of the penis. The bladder was exposed and a small incision made in its avascular dome through which a drainage cannula was passed. The large and small intestines were wrapped in a saline-soaked tissue, sealed with cling film and brought out of the abdomen to sit on the animal's right side (opposite to the experimental kidney).

Half-way along the laparotomy incision, a transverse incision was made in the animal's left abdominal wall. The stomach, pancreas, omentum and spleen were gently retracted to expose the left kidney. A thermistor was placed over the kidney and a warming light was placed over the exposed abdominal organs

to ensure a constant temperature between 36.5 – 37.5 °C through the course of the experiment. The kidney was kept moist with warmed Hartmann's solution dripped over the kidney whenever it appeared that the moisture had evaporated. After renal instrumentation (see below), the exposed abdomen was covered with cling-film and aluminium foil to reduce evaporative/convective fluid and heat losses. Because the returned signal from the OxyLite and OxyFlo probes were easily overwhelmed by the bright light from the warming light, the aluminium foil also kept the abdomen dark. To correct for fluid losses and to optimize cardiac output whilst under the vasodilatory effects of vapour anaesthesia, 7.5 ml/kg Hartmann's solution was given over five minutes: This figure was obtained during control whole body flow experiments and shown to maximise aortic flow following experimental set-up.

3.2.1.3 Insertion of OxyLite probes

Following cannula insertion, tracheostomy and laparotomy, small incisions were made in the renal capsule with a 25 Gauge needle to allow easy passage of three 450 μm diameter dual-purpose fibreoptic probes (Product Code BF/OFT, Oxford Optronix, Oxford, UK) into the parenchyma. To minimize the likelihood of haematoma formation at the region of interest, the probes were inserted 3 mm beyond their final depth. After 30 minutes they were withdrawn to the required depth (0.5, 1.5 and 3.5 mm), marked on the probe with indelible ink. These depths were chosen as they correspond anatomically to cortex, cortico-medullary junction (CMJ) and outer medulla on post-mortem

histological examination (personal communication, Dr M Novelli, Reader in Histopathology, UCL). The first two probes were placed perpendicular to the kidney surface. The medullary probe was placed through half-way down the lateral edge of the kidney parallel to its caudal plane. The CMJ probe was placed caudally from the first, in the same plane. This consistent placement assured that the same depth was always measured between animals. The most superficial probe was placed on the lower pole of the kidney slightly higher than the previous two, towards the upper surface (Figure 3-7 & Figure 3-8). By placing the probe in this way, the probe could be inserted to a depth of 1 mm but was actually sampling from a perpendicular depth of 0.5 mm. The probes were connected to OxyLite and OxyFlo monitors (OxyFlo 4000, Oxford Optronix, Oxford, UK) to enable continuous monitoring of PtO2 and microvascular blood flow. As the bright warming light overwhelmed the relatively weak signal from the OxyLite, the aluminium foil placed over the abdomen also acted as an extraneous light shield. To ensure model stability, the animals were monitored for 30 minutes after instrumentation and prior to the experimental intervention (outlined below).

Following termination of the model, the probes were withdrawn and the kidney removed from the abdominal cavity. The kidney was bisected through its perpendicular plane and the tract formed by the probe inspected. By this technique, parallel insertion of the probe was assured and excessive tissue haemorrhage noted.

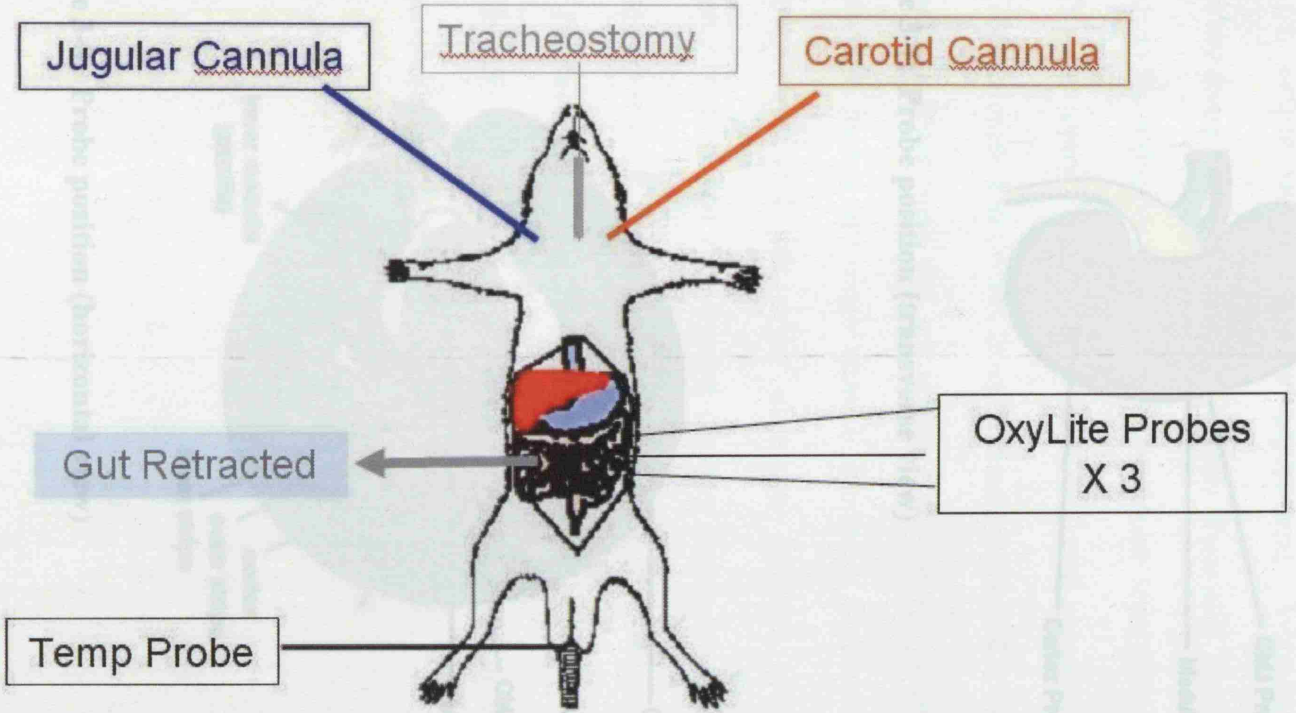

Figure 3-6: Diagram of basic experimental setup

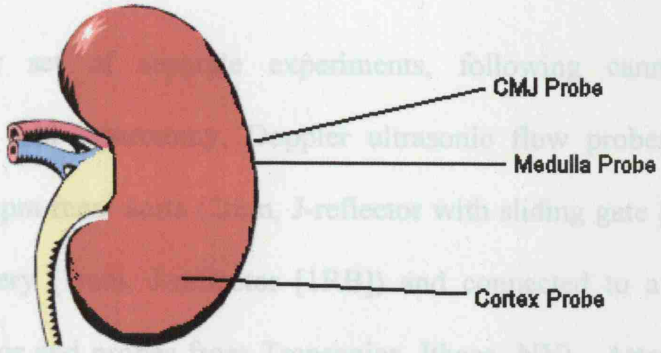

Figure 3-7: Probe position (transverse view)

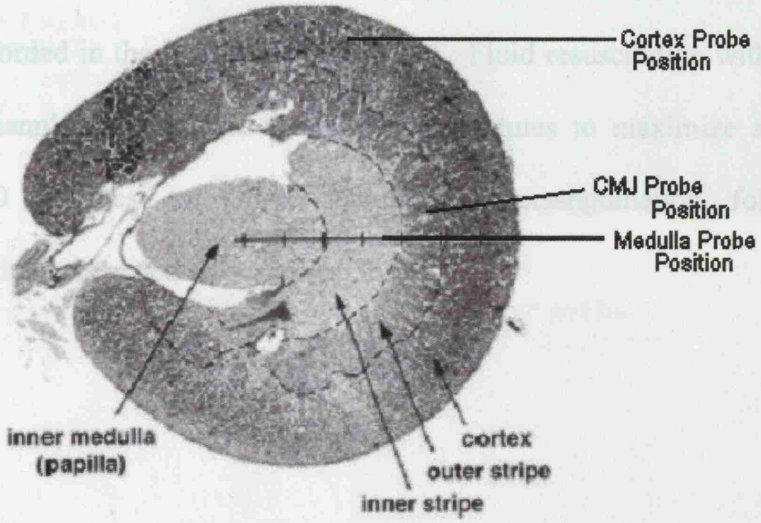

Figure 3-8: Probe position (horizontal view)

3.2.2 Whole body flow experiments

In a further set of separate experiments, following cannula insertion, tracheostomy and laparotomy, Doppler ultrasonic flow probes were placed around the supra-renal aorta (2mm, J-reflector with sliding gate [2SB]) and the left renal artery (1mm, J-reflector [1RB]) and connected to a flow monitor (T206; monitor and probes from Transonics, Ithaca, NY). Attempts had been made to place both the ultrasonic renal artery probe and the intra-renal flow/PtO_2 probes in a single animal. However, inadequate space, a prolonged set-up time, and additional, excessive surgical stress resulted in renal haemodynamic and oxygenation changes that were significantly different to those recorded in the less monitored model. Fluid resuscitation with 7.5 ml/kg of Hartmann's solution was given over 5 minutes to maximize aortic flow. After 30 minutes to allow stabilisation, exsanguination followed by resuscitation proceeded as described above.

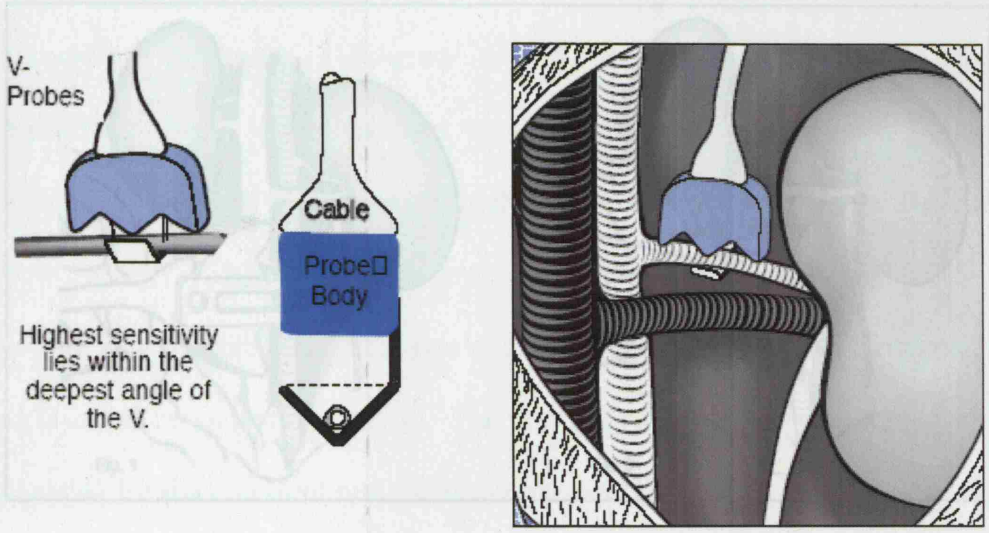

Figure 3-9: Surgical placement of a renal artery probe

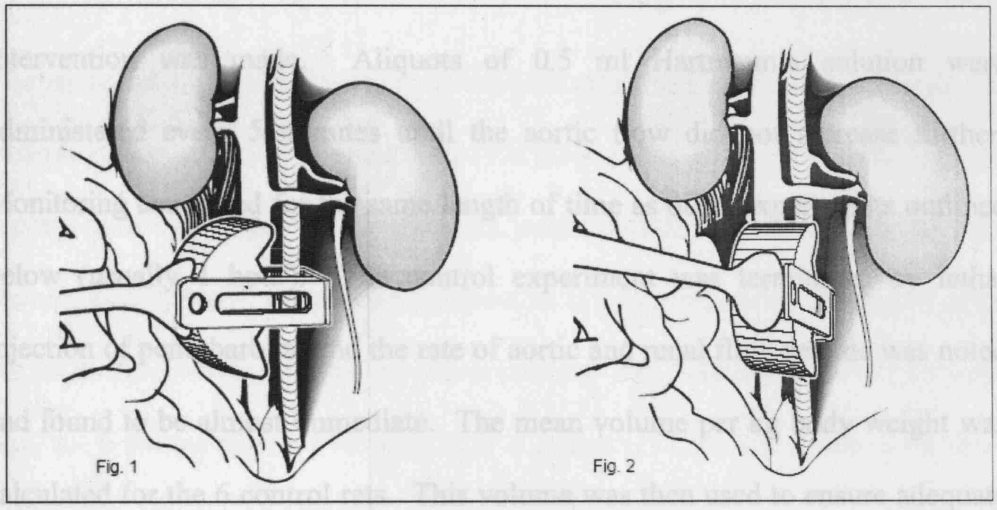

Figure 3-10: Surgical approach to the abdominal aorta (infra-renal measurements shown)

3.3 Experimental Technique

3.3.1 Whole kidney flow control experiments

A set of control experiments were performed to document baseline whole organ flows. The animal was instrumented as above (Section 3.2.2) but no other intervention was made. Aliquots of 0.5 ml Hartmann's solution were administered every 5 minutes until the aortic flow did not increase further. Monitoring continued for the same length of time as other experiments outlined below (usually 1 hour). The control experiment was terminated by lethal injection of pentobarbital and the rate of aortic and renal flow decline was noted and found to be almost immediate. The mean volume per kg body weight was calculated for the 6 control rats. This volume was then used to ensure adequate fluid resuscitation for the following experiments.

3.3.2 Control experiments

A set of control experiments were performed to document baseline PtO_2 and intra-renal flows. The animal was instrumented as above (Section 3.2.1) and fluid resuscitated (Section 3.3.1) but no other intervention was made. Monitoring continued for the same length of time as other experiments outlined

below (usually 1 hour). The control experiment was terminated by lethal injection of pentobarbital. Tissue oxygen tensions were monitored in the absence of flow for the next two minutes. Intra-renal flow cessation was confirmed to be almost immediate.

3.3.3 Withdrawal experiments

The tissue oxygen model was set up as outlined above (Section 3.2.1) with the exception that only a single unmarked OxyLite probe was placed deep into the kidney midway between each pole and perpendicular to the workbench. The probe was set onto a microscope platform with a Vernier scale. Having allowed a tract to form over 30 minutes, the probe was then withdrawn in 1 mm steps with the readings allowed to settle over 5 minutes. This was repeated on three occasions along the same tract.

The final reading before the tip of the probe emerged from the kidney was used as the reference point at 0.5 mm depth. The previous reading taken was therefore at 1.5 mm depth, the one before that was located at 2.5 mm depth and so on. Having plotted the results from six rats, two striking features became apparent. Firstly, the PtO_2 in cortex and medulla were persistently lower than those reported by Brezis (Brezis, M. *et al.*, 1994b), (Brezis, M. *et al.*, 1994a). Secondly, there was a region of very low tissue oxygen between 1.5 and 2.5 mm. Microscopic investigation revealed that this region corresponded to the CMJ (Dr Marco Novelli, Reader in Histopathology, UCL, personal

communication). This finding lead to the investigation of three renal regions (the cortex, CMJ and medulla) rather than two.

3.3.4 Hypovolaemia/Resuscitation

The model was set up as detailed in Section 3.2.1. After control readings were taken, 10% of estimated circulating blood volume (calculated on the basis of 70 ml/kg total blood volume) was withdrawn through the arterial cannula under its own pressure. The cannula was flushed with a small amount of heparinised saline to prevent intra-luminal clotting. After a further 10 minutes, an arterial blood gas sample of 150 µl was drawn, followed by a further removal of 10% circulating volume. On each occasion, heparin (1000 IU/kg) was added to the drawn blood and the sample placed in a water bath heated to 37°C. After a further 10 minutes, another arterial blood gas sample was taken and the kept blood transfused by slow intravenous injection over three minutes. The jugular venous catheter was then flushed with compound sodium lactate solution (Hartmann's Solution).

3.3.5 Aortic occlusion

In separate experiments, the experiment was set-up as outlined in Section 3.2.1 with the exception that pressure was measured from the right femoral artery

(rather than the right carotid artery) and a vascular occluder of 2 mm diameter (Cat No: AH 62-0109, Harvard Apparatus Ltd, Edenbridge, Kent) placed above the junction of the aorta and renal arteries, but below the hepatic artery. After instrumentation and a 30 minute period for stabilization, the balloon of the occluder was inflated sequentially so that the pressure detected in the femoral artery was reduced by 10 mmHg at each step. It was assumed that the decrease in pressure with the occluder was directly proportional to the decrease in flow in the aorta below the occluder. Once stable readings had been achieved over a 10 second period, the balloon was inflated further to achieve another fall in measured pressure of 10 mmHg. This was repeated until the balloon was maximally inflated. The balloon was not deflated between steps. Intra-renal microvascular flow was recorded at baseline and at each pressure step.

Whole organ flows could not be performed with the vascular occluder as there was no space around the aorta for both the ultrasonic probes and the occluder. Furthermore, the occluder caused slight movements in the renal vessels; this caused a change in the angle of the vessel within the ultrasonic probe and for the signal to be read at an angle rather than along the line of the vessel. This frequently lead to loss of returned signal or a greater decrease in flow and the technique had to be abandoned.

3.3.6 The effect of furosemide

The experiment was set up as outlined in Section 3.2.1. After the stabilisation period, an intravenous bolus dose of furosemide (1.5 mg/kg) was given. Readings were taken for 30 minutes and an arterial blood gas drawn. A further dose of 1.5 mg/kg was then given and readings taken for another 30 minutes. At the end of this time, another arterial blood gas was drawn before concluding the experiment. OxyLite readings were continued for 2 minutes following termination of the experiment in order to monitor the decline in tissue pO_2.

3.3.7 The effect of enalaprilat

The experiment was set up as outlined in Section 3.2.1. After the stabilisation period, an intravenous bolus dose of enalaprilat (3 mg/kg) was given. Readings were taken for 30 minutes and an arterial blood gas drawn. A further dose of 3 mg/kg was then given and readings taken for another 30 minutes. At the end of this time, another arterial blood gas was drawn before concluding the experiment. OxyLite readings were continued for 2 minutes following termination of the experiment in order to monitor the decline in tissue pO_2.

3.3.8 Whole organ flow during enalaprilat and furosemide

The animal was instrumented as above (Section 3.2.2). Doses of either furosemide or enalaprilat were administered according to the same schedules outlined in Sections 3.3.6 and 3.3.7 above and the changes in aortic and renal artery blood flows noted.

3.3.9 Administration of lipopolysaccharide (LPS)

Following set up according to the protocol outlined in sections 3.2.1 and 3.2.2, *Klebsiella* LPS (L4268, Sigma-Aldrich Company Ltd, Gillingham, Dorset, UK) at a dose of 40 mg/kg was administered as an intravenous infusion over 30 minutes. Changes were monitored both during the infusion and for 60 minutes after infusion end. In addition to the initial fluid resuscitation, Hartmann's solution at 25 ml/kg/hr was also commenced with the LPS infusion and continued throughout the course of the experiment in recognition of the severe insult and vasodilatation induced by this dose of LPS.

3.3.10 Alterations in inspired fraction of oxygen

The animal was instrumented as above (Section 3.2.1). Rather than breathing room air, pressurised nitrogen and oxygen from cylinders were administered

through anaesthetic rotameters so that the amount of oxygen in the inspired gas could be controlled. Following the stabilisation period, the gas mixture was added to the vapouriser and administered through plastic tubing 8 mm external diameter. A further 150 cm of piping was connected before the combined supply entered the vaporiser to ensure adequate admixture of the gases. A three way tap was inserted after the vaporiser so that the fraction of inspired oxygen (FiO_2) could be sampled. The rotameters were adjusted to achieve the desired FiO_2 which was sampled and analysed through the ABL70 blood gas analyser (Radiometer, Copenhagen, Denmark).

Animals breathed either air (21%), followed by 15%, then 10% oxygen for 5 minutes each before readings were taken. In between each reading, the animal was returned to breathing air so that the FiO_2 could be adjusted for the next step. The FiO_2 was then increased along the same steps for a repeat set of measurements. The FiO_2 was increased incrementally to 30%, 50% and 100% respectively with a settling period of 5 minutes in between. The same FiO_2 values were then used during a step-down with the exception that 10 minutes was allowed between measurements to ensure full washout of the oxygen from tubing and the residual volume in the lungs and blood. Again, the animal was allowed to breathe room air before setting the next FiO_2 level. However, after three experimental protocol set-ups, it became apparent that exposure of the animal to low FiO_2 for long periods of time caused irreversible changes in PtO_2 and so, for half of the set-ups, the FiO_2 was increased first then decreased.

3.3.11 Use of different anaesthetic agents and concentrations

The model was instrumented as outlined in Section 3.2.1 using isoflurane as induction and maintenance anaesthetic. During four of the experiments, the vaporiser was adjusted so that the concentration of inspired isoflurane was increased from 1.5% to 2% and 30 minutes allowed to pass for the system to equilibrate. The concentration was then increased to 2.5% and another 30 minutes allowed to pass.

In a second set of experiments, a second general anaesthetic agent was introduced (either pentobarbitone or Hypnorm [Fentanyl citrate 0.315 mg/ml with Fluanisone 10 mg/ml]) during the stabilisation period, and the isoflurane withdrawn. The model was monitored for 1 hour, maintained with intermittent intravenous boluses of anaesthetic agent.

3.3.12 Removal of capsule

The model was instrumented as outlined in Section 3.2.1 except that rather than making a small incision in the capsule, the whole of the capsule was removed. The OxyLite probes were then inserted into the kidney parenchyma without difficulty.

3.4 Data collection

All physiological data were collected using a 16-Channel Powerlab 16PC system (AD Instruments, Oxford, UK) sampling at 10Hz to an Apple iMAC computer running AD Instruments 'Chart' software. Mean data were collected using the algorithm from this software and analysed by Excel Spreadsheet (Microsoft, Seattle, WA, USA).

3.4.1 Analysis of results

3.4.1.1 Intra-renal flow

As mentioned above, BPU output for Doppler laser flow is non-parametric and can therefore only be compared against baseline. Non-parametric statistical analysis can be applied but requires much larger numbers for analysis. As such, flow results are presented as percentage changes in regional flow rather than absolute values. For P:F ratios, the raw BPU output was divided into the PtO_2 at baseline and this was compared with the P:F ratio following intervention. The percentage change was then calculated. It is unlikely that there is a linear relationship between flow and PtO_2 as many authors agree that cell respiration is highly regulated. However, a decrease in cell respiration with constant blood

flow within the tissue would cause an increase in P:F. Similarly, an increase in cell respiration during otherwise constant conditions would cause a decrease in PtO_2 and a decrease in P:F.

PtO_2, percentage changes in flow, and the ratio of PtO_2 to microvascular flow (PtO_2:F ratio) in the three intra-renal regions were analyzed using Student's t-test. Analysis of variation (ANOVA) was performed on all other sequential results (BP, percentage changes in flow and PtO_2:F ratios). Values are reported as mean ± standard error. Significant values are reported for p values <0.05.

3.4.1.2 Oxygen decay

OxyLite readings were continued following cessation of blood flow as measured by loss of blood pressure and cessation of intra-renal flow. By suddenly halting the flow of oxygen in to the tissues, the initial local oxygen consumption of the surround cells could be extrapolated from the initial decline in PtO_2. A simple exponential decay half-life curve was fitted using the sum of least squares to the signal obtained from the OxyLite device over the first 15 seconds following loss of blood pressure and flow.

Statistics were performed on the time constant rather than the half-life of the curve as this is calculated from the curve fit and the half-life ($t_{½}$) is calculated by dividing this into the natural logarithm of 2. However, the mean half-life and standard errors are also reported.

$$[C]_t = [C]_0 \times e^{-k_{el}t}$$

Figure 3-11: Formula to calculate concentration [C] at time (t) using a single compartment model knowing the elimination constant (k_{el})

$$t_{1/2} = \frac{\ln(2)}{k_{el}}$$

Figure 3-12: Calculation of half-life constant from the elimination constant (k_{el}) for a one compartment model

Decay of the oxygen signal following this fitted a double exponential curve with a greater correlation; this decay was very slow from 25 seconds onwards. Once flow to the tissues had ceased, two major influences come into play. Firstly, the ability to acutely control local oxygen consumption will affect the rate of PtO_2 decline in the first instance (assuming that this is a rapidly acting mechanism). Secondly, it may be that the dual exponential nature of the curve reflects diffusion from outside the kidney to the inside. The PtO_2 was measured for up to 5 minutes and settled at 0.2 kPa. For this reason, any significant bias caused by external diffusion of oxygen during experimentation was discounted.

4 Results

4.1 Whole kidney blood flow - control experiments

Six rats were instrumented and given aliquots of 0.5 ml Hartmann's solution every 5 minutes until flow in the aorta was maximised. A volume of 2.42 ± 0.2 ml (mean ± SEM, n=6) was administered, equivalent to 7.5 ml/kg. This volume by weight was used to optimise the cardiac status of the animals by fluid resuscitation in subsequent experiments.

4.2 Withdrawal of OxyLite probes through renal parenchyma

Withdrawal of a single OxyLite probe through the kidney revealed a persistent area of very low PtO_2 approximately 1.5 mm below the surface. Histologically, this region correlates to the cortico-medullary junction (CMJ). Cortical and outer medullary regions were also defined histologically as 0.5 mm and 3.5 mm depth (Dr Marco Novelli, Reader in Histopathology, UCL, personal communication). Attention was therefore focussed on these regions for the duration of the experiments.

Figure 4-2 shows the PtO_2 values (mean ± SEM) obtained. Baseline cortical values were 1.8 ± 0.3 kPa, CMJ was 1.0 ± 0.1 kPa and outer medulla was 3.6 ± 0.3 kPa by this method.

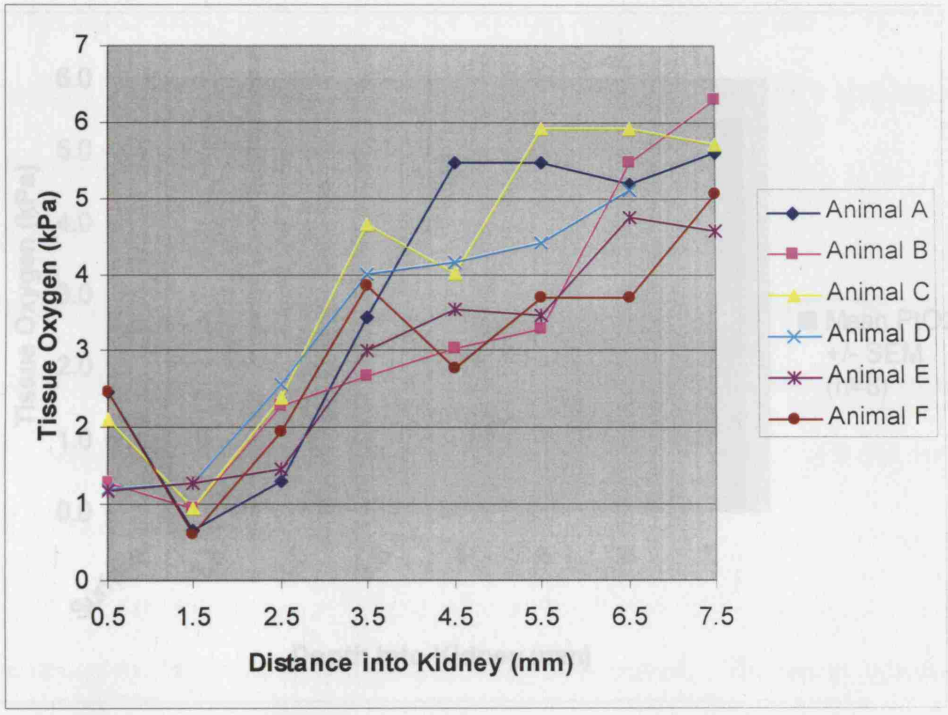

Figure 4-1: Individual PtO_2 profiles across renal parenchyma

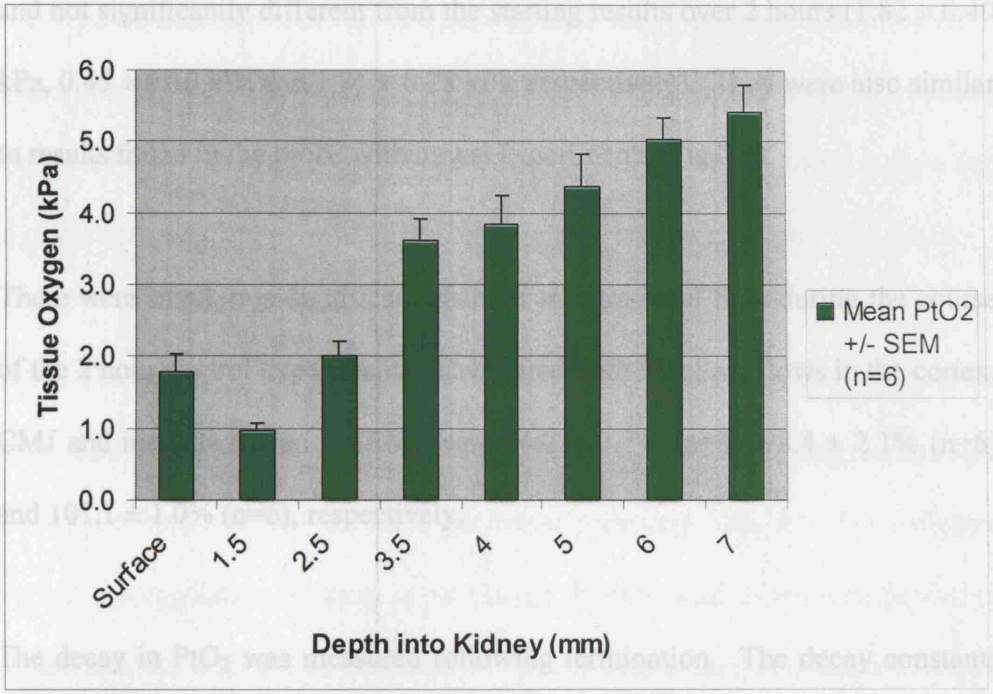

Figure 4-2: Mean PtO_2 at increasing renal depths

4.3 Control results using static OxyLite probes

Baseline tissue oxygen tensions (mean ± SEM) using static probes in the cortex, corticomedullary junction and outer medulla were 1.94 ± 0.32 kPa (n=6), 0.55 ± 0.11 kPa (n=6) and 1.75 ± 0.38 kPa (n=6), respectively. These remained stable and not significantly different from the starting results over 2 hours (1.82 ± 0.40 kPa, 0.45 ± 0.10 kPa and 1.81 ± 0.28 kPa, respectively). They were also similar to results found in the probe withdrawal experiments (Fig 4.2).

There were small, non-significant changes in intra-renal flow during the course of the 2 hour control experiments. Compared with baseline, flows in the cortex, CMJ and medulla (mean ± SEM) were 94.2 ± 3.2% (n=6), 98.4 ± 2.1% (n=6) and 101.1 ± 1.0% (n=6), respectively.

The decay in PtO_2 was measured following termination. The decay constants (mean ± SEM) were calculated as 0.119 ± 0.025 sec^{-1} in the cortex, 0.077 ± 0.11 sec^{-1} in the CMJ and 0.030 ± 0.11 sec^{-1} in the medulla. These values were used to compare against changes found during physiological challenges. The decay half-lives (mean ± SEM) were 5.8 ± 1.0 sec in the cortex, 9.0 ± 1.1 sec in the CMJ and 23.3 ± 6.1 sec in the medulla.

4.4 Aortic constriction

4.4.1 Changes in intra-renal flow

Restricting flow to the kidney during aortic constriction revealed complex responses in regional flow. The cortex and CMJ both displayed an ability to autoregulate and maintain regional flow as renal artery pressure fell in the early stages (Figure 4-3). Mean cortical flow did not differ significantly from initial values until the femoral BP had fallen by 40-59%. The intra-medullary flow fell significantly and immediately, but was relatively preserved at very low flows.

Strick (Strick, D.M. *et al.*, 1994) defined the efficiency of autoregulation of intra-renal flows by calculating an 'autoregulatory index' (AI) using the formula AI = (%Δ blood flow)/(%Δ renal perfusion pressure). An AI of 0 indicates perfect autoregulation as there is no change in flow with decreasing perfusion pressure, while an index of 1 indicates a system with a fixed resistance. Using a cut-off of a 50% reduction in femoral pressure, linear regression analysis was applied to the data plotted on a graph of change in flow (y-axis) against change in blood pressure (x-axis) in a similar manner to Strick's analysis: A perfectly autoregulated system would produce a graph with a line parallel to the x-axis.

A plot of the 'best fit' line (Figure 4-4) showed that the line was almost parallel to the x-axis with a gradient of 0.124 ± 0.07 (mean ± SEM) with an r^2 of 0.084.

This is close to zero, implying independence of flow from BP. Confidence limits for the line gradient were -0.017 to +0.266, straddling a gradient of zero.

In a separate analysis, regression analysis suggested that regional flow was independent of BP across the range of BP changes to which the model was applied. When each individual point was also compared with 1 using a paired t-test, cortical flow ratio did not alter significantly from unity (p=0.08).

This finding was not so strong in the CMJ (Figure 4-5). Initial values differed significantly from unity (paired t-test, p=0.028) implying that flow did fall significantly as the femoral pressure was reduced, although the r^2 value for the linear regression was 0.134. The mean gradient was 0.261 ± 0.112 (mean ± SEM). Confidence intervals for the gradient were 0.034 to 0.489, not straddling a gradient of zero.

There was reduced maintenance of flow in the face of reduced organ pressure in the medulla (Figure 4-6). There was a steep decline in flows (gradient 0.32) but the gradient increased (to 1.32) at pressures below 50% of initial.

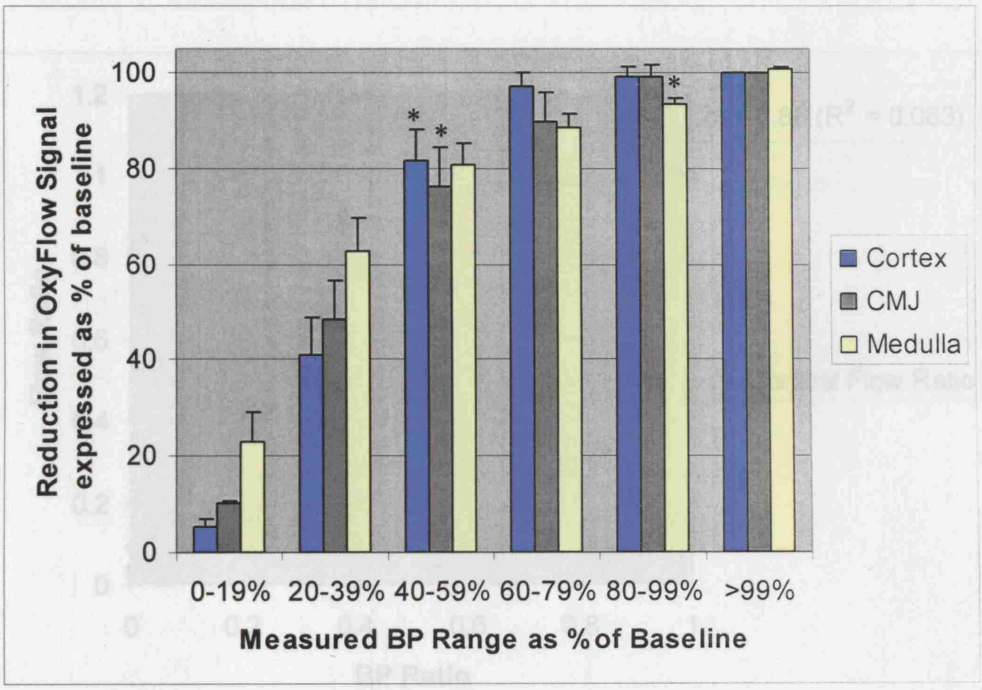

Figure 4-3: Percentage change (mean ± SEM, n=6) in regional flow plotted against percentage change in femoral pressure with aortic constriction.

*** is the first flow to be significantly different from baseline ($p<0.05$)**

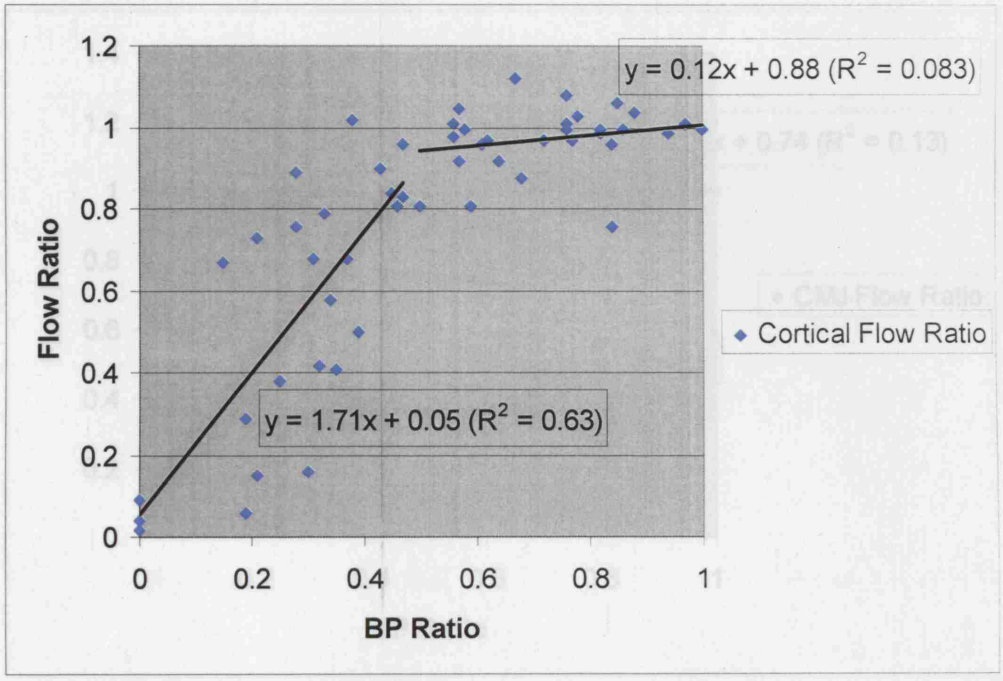

Figure 4-4: Plot of change in flow against change in perfusion pressure within the cortex (n=6)

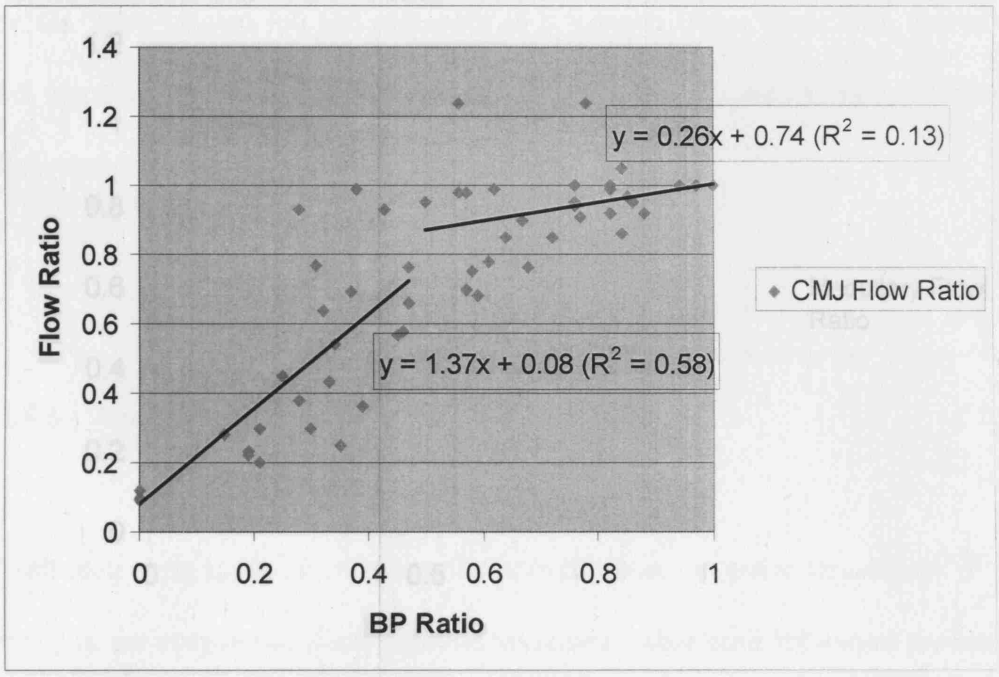

Figure 4-5: Plot of the change in flow against change in perfusion pressure for CMJ (n=6)

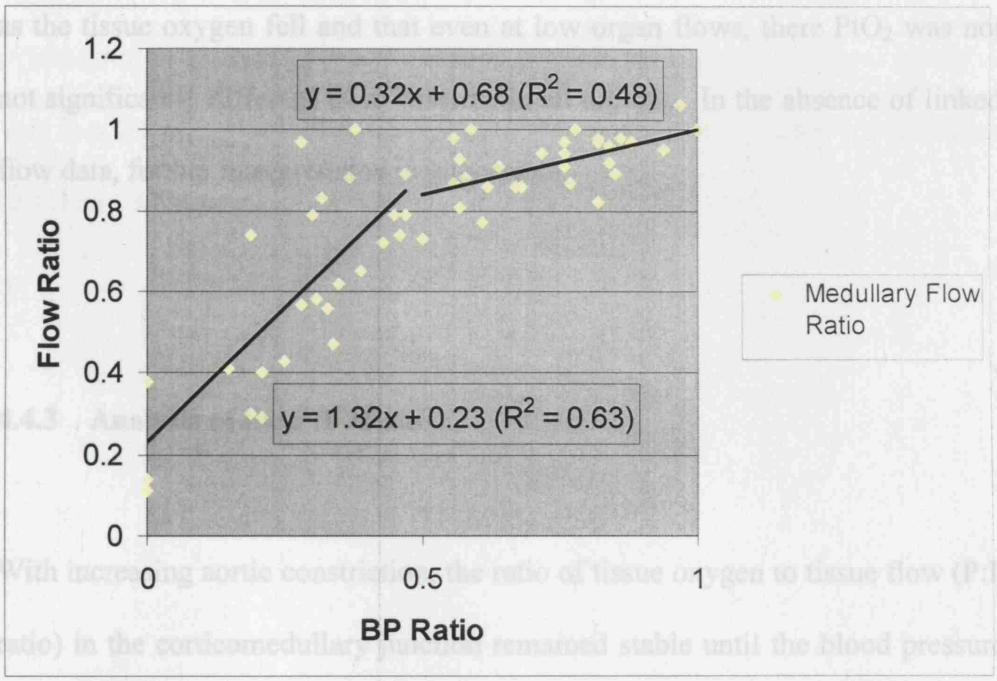

Figure 4-6: Plot of change in flow against change in perfusion pressure for the medulla (n=6)

4.4.2 Changes in renal tissue oxygen

Aortic constriction caused a decline in the PtO_2 (Figure 4-7) in all regions of the kidney. As can be seen from Figure 4-7, there was a progressive fall in PtO_2 in all regions with increasing constriction. Unfortunately, there was wide variation as the tissue oxygen fell and that even at low organ flows, there PtO_2 was not not significantly different from baseline in all regions. In the absence of linked flow data, further interpretation is impossible.

4.4.3 Analysis of the P:F Ratio

With increasing aortic constriction, the ratio of tissue oxygen to tissue flow (P:F ratio) in the corticomedullary junction remained stable until the blood pressure had fallen below 40% of baseline values, at which point the P:F ratio rose (Figure 4-8). The P:F ratio (mean ± SEM) in the cortical and medullary regions fell significantly soon after aortic constriction was commenced - from 1 to 0.71 ± 0.07 and 0.60 ± 0.12 for 60-79% and 40-59% of baseline BP in the cortex, and from 1 to 0.59 ± 0.1 and 0.55 ± 0.09 in the medulla. However, with severe constriction, values returned towards baseline. As regional PtO_2 was relatively maintained in the cortex and medulla, the fall in the P:F ratio appears almost entirely due to a fall in local oxygen consumption and not necessarily through decreased oxygen delivery alone.

In considering these results, there is another factor that should be considered. During the experimental protocol, to achieve a level of blood pressure that was 40% of normal took 15 minutes to attain, thereby causing the kidney to be ischaemic for several minutes. It may be that the intra-cellular adaptations reducing oxygen consumption can only protect cells for a certain amount of time and the rise in P:F ratio noted at very low flows was actually due to the exhaustion of protective mechanisms. Alternatively, at the extreme insult of very low flows, other protective mechanisms may take over. This is considered further in the discussion chapter.

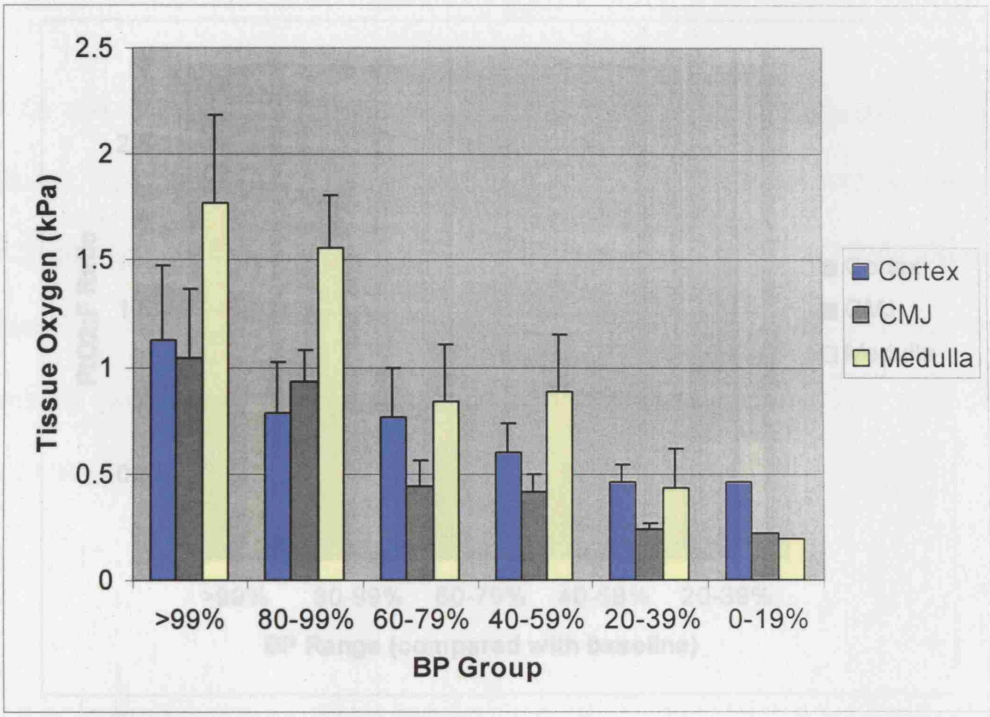

Figure 4-7: Changes in PtO_2 with aortic constriction (Mean ± SEM, n=6 except for group 0-19% where n=1)

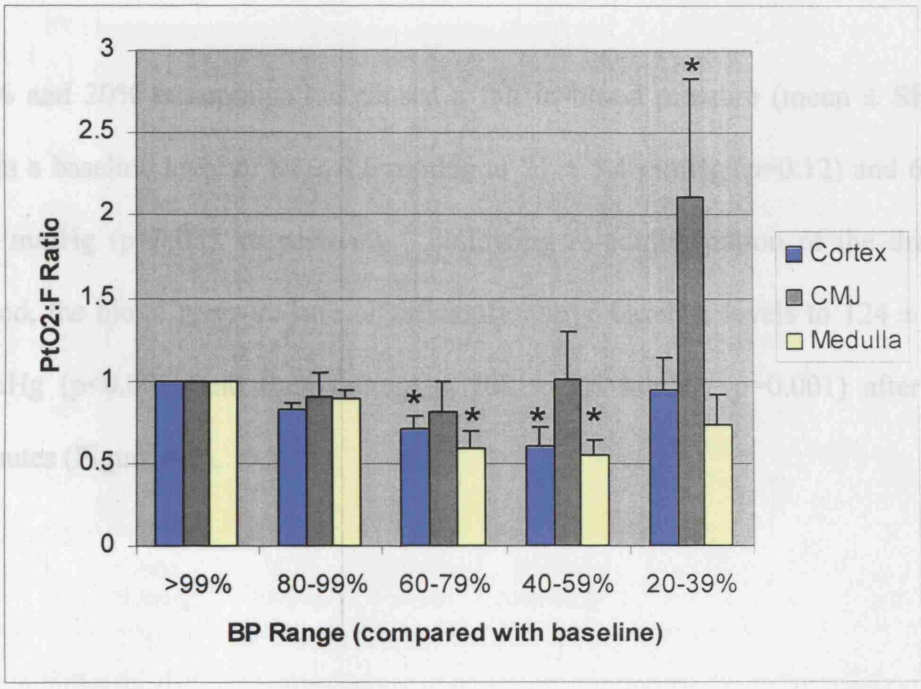

Figure 4-8: P/F Ratios (Mean ± SEM, n=6, *p<0.05) during aortic constriction compared with baseline (shown ≡ 1)

4.5 Exsanguination and subsequent resuscitation with drawn blood

4.5.1 Changes in BP and whole organ flow

10% and 20% exsanguination caused a fall in blood pressure (mean ± SEM) from a baseline level of 82 ± 4.6 mmHg to 71 ± 5.4 mmHg ($p=0.12$) and 66 ± 5.8 mmHg ($p=0.03$), respectively. Following re-administration of the drawn blood, the blood pressure rose significantly above baseline levels to 124 ± 4.6 mmHg ($p<0.001$) and then falling to 108 ± 3.6 mmHg ($p=0.001$) after 10 minutes (Figure 4-9).

4.5.2 Changes in intra renal flow

Intra-renal flow was initially preserved during withdrawal of 10% of circulating blood volume. On 20% exsanguination, flow to the cortex of the kidney fell, CMJ flow was well preserved while, paradoxically, flow to the inner part of the kidney *rose* by 19.1% ($p=0.016$) (Figure 4-9). The rise in medullary flow significantly differs from flows noted during similar falls in BP during aortic constriction.

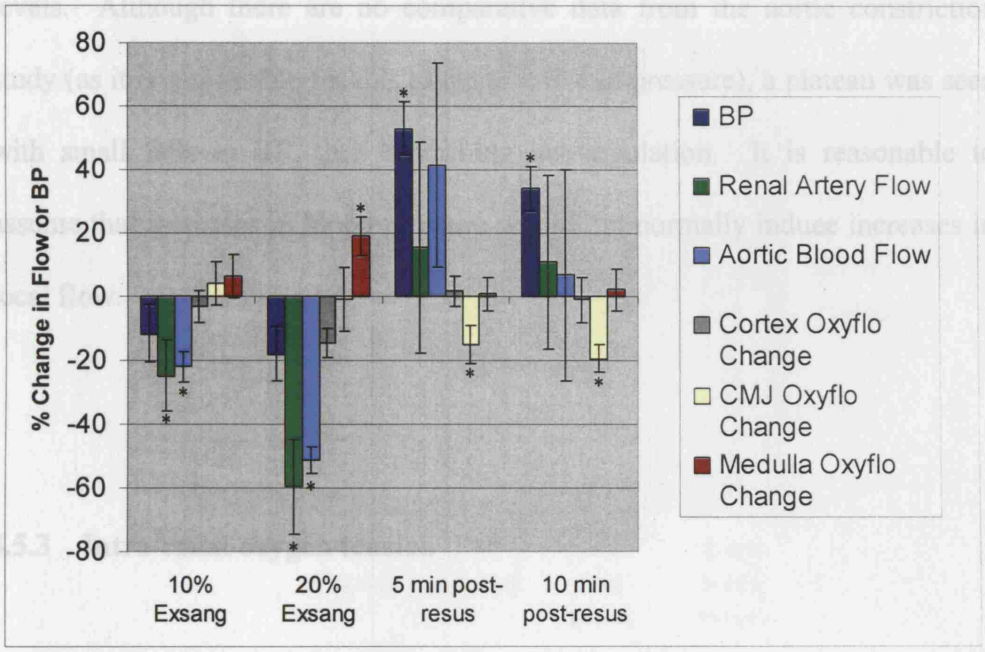

Figure 4-9: Percentage change in blood pressure, aortic flow, renal artery flow and intra-renal flow during exsanguination-resuscitation

(*significantly different values at $p<0.05$, Student's t-test)

Following resuscitation, flow in the CMJ continued to fall (15% ± 6.0 mean ± SEM, p=0.01), despite restoration of cortical flow and an increase in blood pressure. This trend worsened in the minutes following resuscitation; after 10 minutes the flow (mean ± SEM) in this region was reduced by 19.3 ± 4.2% ($p<0.001$) compared with baseline. Flow to the medulla returned to baseline levels. Although there are no comparative data from the aortic constriction study (as it is impossible for this to cause a rise in pressure), a plateau was seen with small falls in BP, thus describing autoregulation. It is reasonable to assume that increases in blood pressure would not normally induce increases in local flow.

4.5.3 Intra-renal oxygen tension

Baseline tissue oxygen tensions (mean ± SEM) (Figure 4-10) were 1.59 ± 0.32 kPa in the cortex, 0.55 ± 0.11 kPa in the CMJ, and 1.05 ± 0.38 kPa in the outer medulla. There were no significant changes in oxygen tension in any region of the kidney during the period of exsanguination. Following re-infusion of the shed blood, significant rises in tissue pO_2 were seen immediately in the cortex (to 4.03 ± 0.94 kPa, p=0.02) and medulla (to 2.40 ± 0.39 kPa, p=0.039), and later in the CMJ (to 1.70 ± 0.35 kPa, p=0.007).

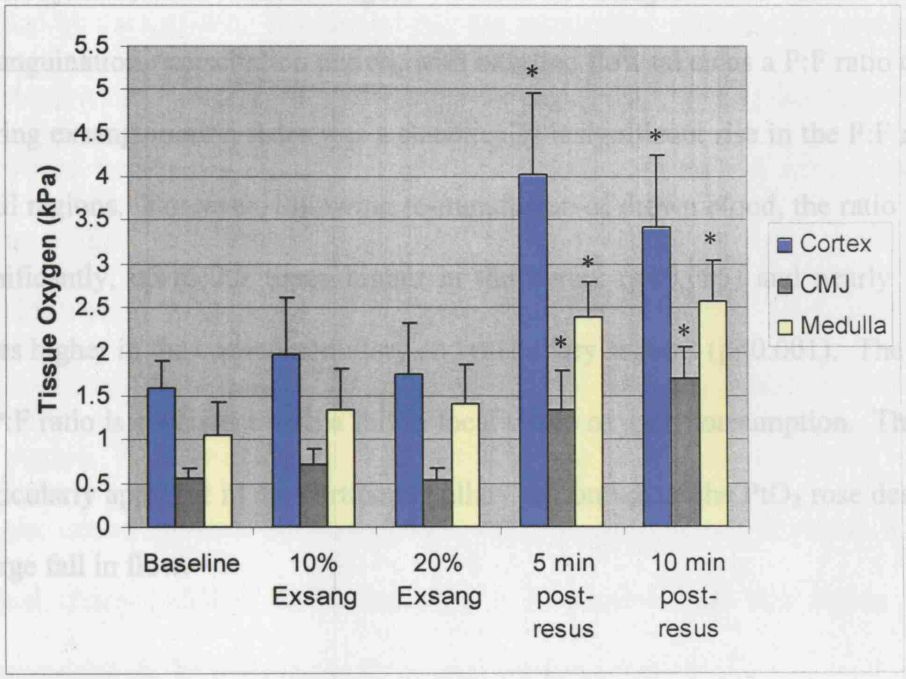

Figure 4-10: Intra-renal tissue pO_2 (mean ± SEM) during and immediately following exsanguination (p values are those significantly different from baseline)

4.5.4 Analysis of P:F Ratio

Having measured temporal changes in flow and tissue oxygen, the P:F ratio was calculated for each individual animal at baseline and following the haemodynamic intervention. Figure 4-11 shows changes in P:F ratio over the exsanguination-resuscitation period, with baseline flow taken as a P:F ratio of 1. During exsanguination there was a statistically insignificant rise in the P:F ratio in all regions. However, following re-transfusion of drawn blood, the ratio rose significantly, up to 2.5 times higher in the cortex ($p<0.005$) and nearly four times higher in the corticomedullary and medullary regions ($p<0.001$). The rise in P:F ratio is consistent with a fall in local tissue oxygen consumption. This is particularly apparent in the corticomedullary region where the PtO_2 rose despite a large fall in flow.

4.5.5 Analysis of oxygen decay following termination

A simple exponential decay half-life curve was fitted using the sum of least squares to the signal obtained from the OxyLite during the first 15 seconds following cessation of cardiac output (and therefore oxygen delivery), as measured by loss of blood pressure and cessation of intra-renal flow. It is interesting to note that 25 seconds after death, decay of the oxygen signal became very slow indeed. This is unlikely to be from diffusion from the

surrounding air as the intermediate layer (the CMJ) remained lower than the medulla, and therefore a gradient has not been created from the outer layers to the inner.

Table 4-2 shows the mean half-life of oxygen decay following termination of the animal. The oxygen consumption time constant is equal to the log of 2 divided by the half-life. Because of this log association, statistics are applied to the oxygen consumption time constant. Exsanguination and resuscitation was associated with a significant fall in the oxygen consumption time constant (mean ± SEM) in the cortex (from 0.119 ± 0.025 to 0.067 ± 0.011 sec^{-1} [n=6, $p<0.035$]) and CMJ (from 0.077 ± 0.11 to 0.042 ± 0.014 sec^{-1} [n=6, $p<0.05$]) and confirms that the rate of oxygen consumption has significantly reduced in this region. Measurements are difficult at slower oxygen decays (or at lower oxygen consumptions); although there was a non-significant increase in the oxygen decay half-life in the medulla, it is possible that this region also possesses the ability to decrease its oxygen consumption.

Dividing the rate constants into the log of 2 allowed mean half-lives to be calculated. The cortical oxygen decay half-life almost doubled from 5.8 ± 1.0 to 10.4 ± 1.4 sec (n=6).

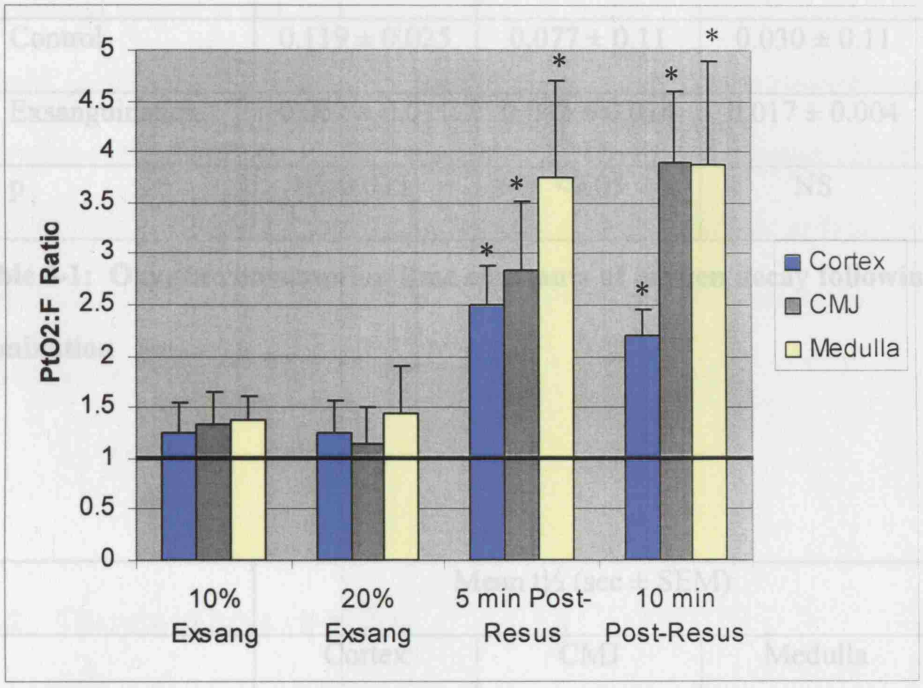

Figure 4-11: P:F Ratios during exsanguination and following resuscitation (*p<0.05, n=6)

	Time constant (sec^{-1} ± SEM)		
	Cortex	CMJ	Medulla
Control	0.119 ± 0.025	0.077 ± 0.11	0.030 ± 0.11
Exsanguination	0.067 ± 0.011	0.042 ± 0.014	0.017 ± 0.004
p	<0.035	<0.05	NS

Table 4-1: Oxygen consumption time constants of oxygen decay following termination

	Mean t½ (sec ± SEM)		
	Cortex	CMJ	Medulla
Control	5.8 ± 1.0	9.0 ± 1.1	23.3 ± 6.1
Exsanguination	10.4 ± 1.4	16.6 ± 4.2	39.7 ± 7.9

Table 4-2: Half-life of oxygen decay following termination

4.6 Furosemide and enalaprilat

4.6.1 Changes in BP and whole organ flow

Furosemide caused a fall in aortic blood flow from 21.3 ± 1.8 to 14.3 ± 1.1 ml/min, [p=0.007, n=4], but had no significant effect on blood pressure or renal artery flow (Figure 4-12). Enalaprilat caused a fall in blood pressure (from 101 ± 4.5 to 73 ± 2.8 mmHg, [p<0.001, n=6]), a significant increase in renal artery flow from 6.1 ± 0.3 to 9.3 ± 0.7 ml/min [p<0.001, n=4] (Figure 4-13), but no change in aortic flow.

4.6.2 Changes in intra renal flow

Flow within the renal cortex fell by 8% (p<0.05) with 0.5 mg furosemide but regained baseline values thereafter (Figure 4-14). No significant changes in microvascular flow were seen in either corticomedullary junction or medulla on administration of furosemide. Enalaprilat 0.5 mg caused a significant rise in the intra-renal flow (mean ± SEM) to the CMJ by 28 ± 10% (p<0.05, n=6), although there was a less impressive (and non-significant) rise of 9 ± 5.6% (n=6) in flow to the cortex (Figure 4-15).

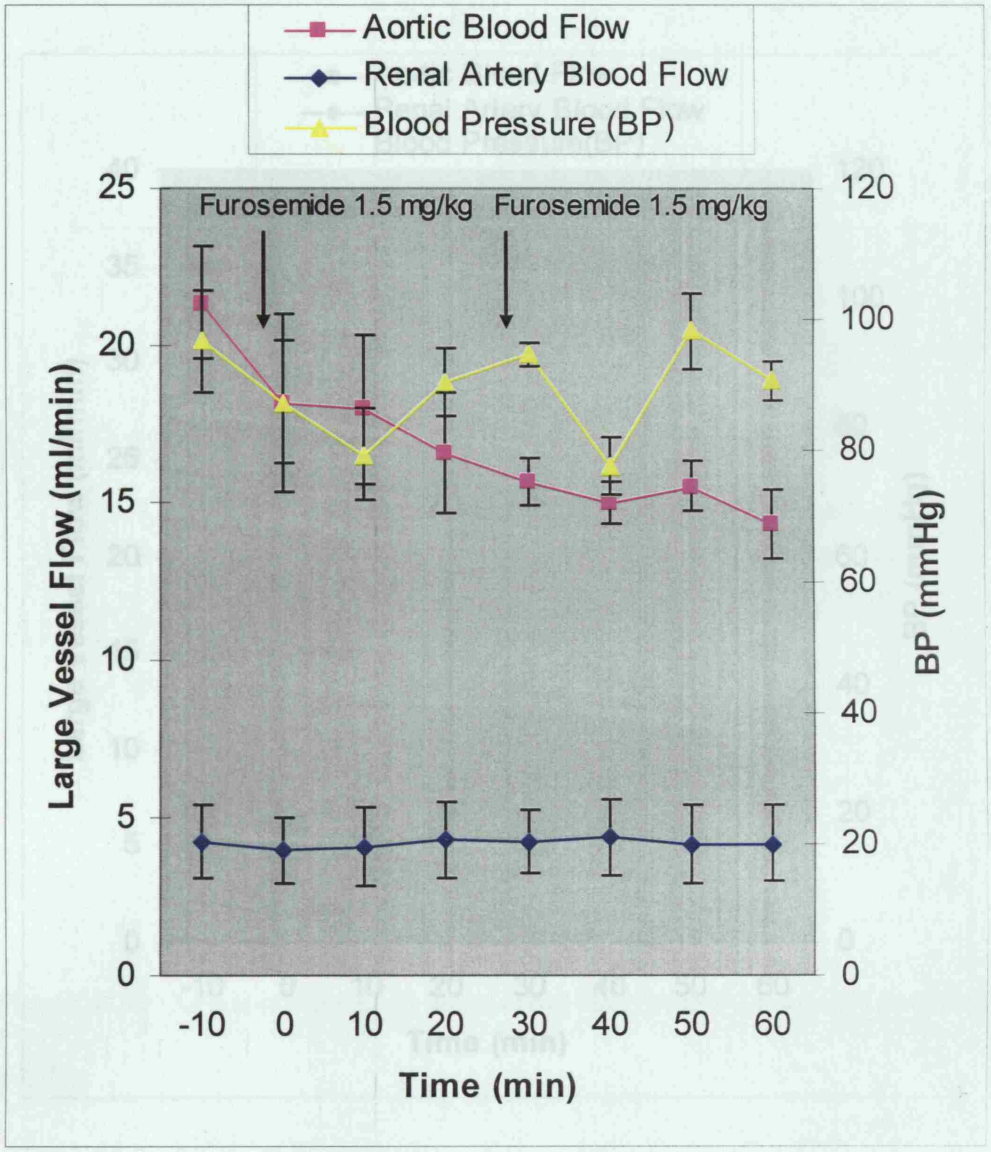

Figure 4-12: BP and large vessel flow changes with Furosemide (n=6)

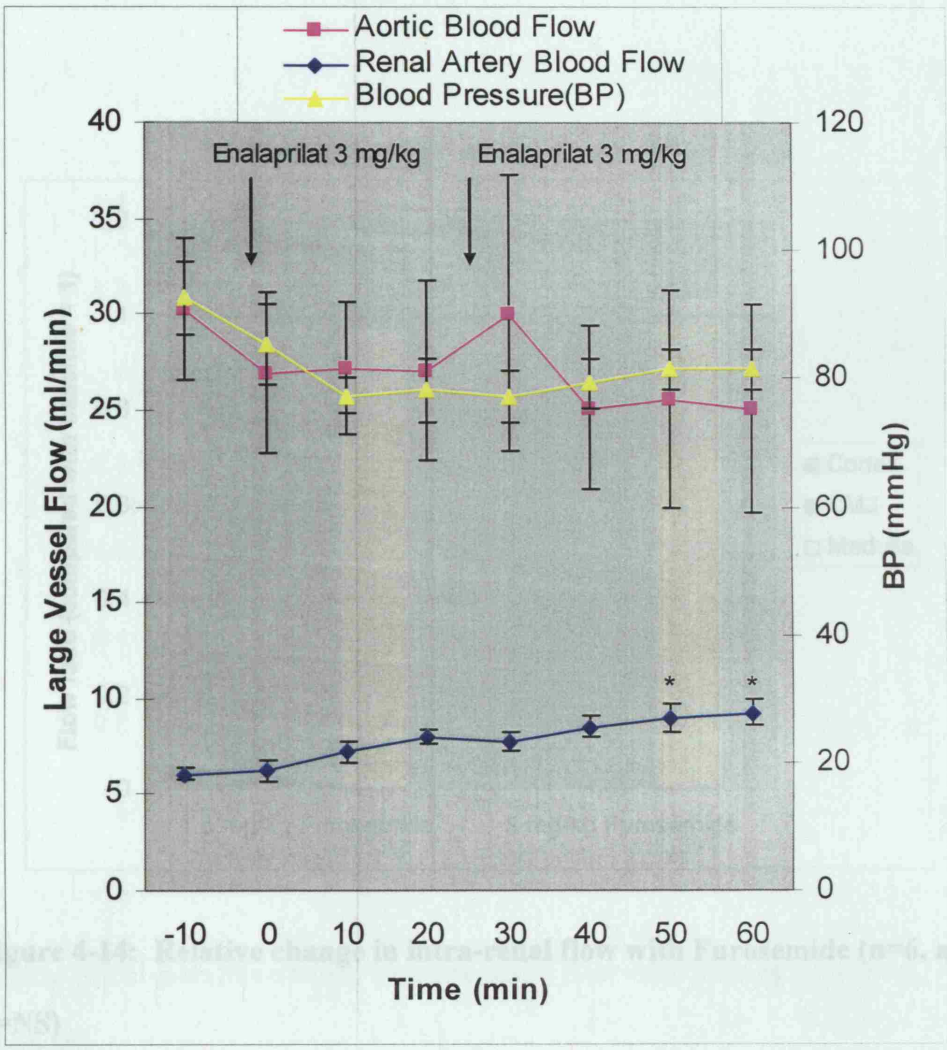

Figure 4-13: BP and large vessel flow with Enalaprilat (Mean ± SEM, n=6, * $p<0.05$)

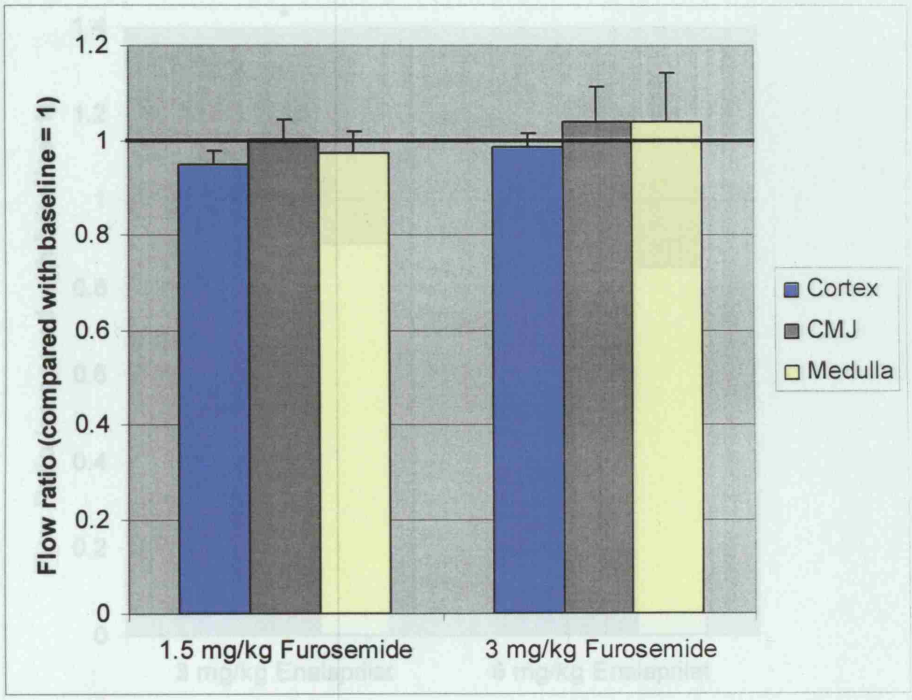

Figure 4-14: Relative change in intra-renal flow with Furosemide (n=6, all p=NS)

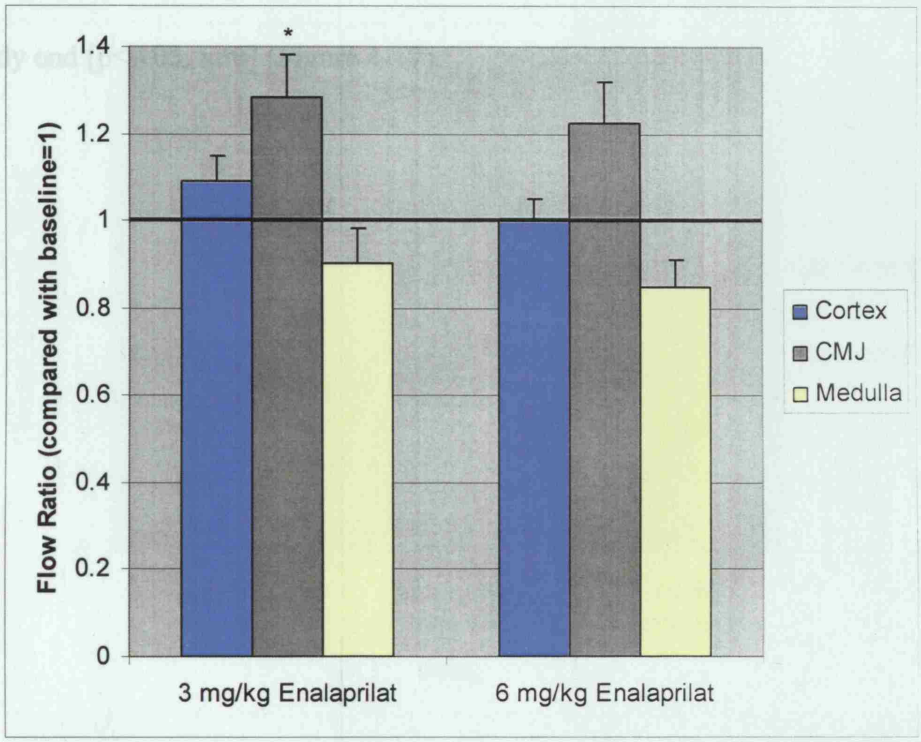

Figure 4-15: Relative change in intra-renal flow with Enalaprilat (n=6, *p<0.05)

4.6.3 Intra-renal oxygen tension

Furosemide produced a significant rise in medullary PtO_2 from 1.2 ± 0.3 to 2.3 ± 0.2 kPa at study end ($p<0.01$, n=6) (Figure 4-16), whereas enalaprilat induced a rise in cortical PtO_2 from a baseline value of 1.27 ± 0.2 to 1.89 ± 0.3 kPa at study end [$p<0.05$, n=6] (Figure 4-17).

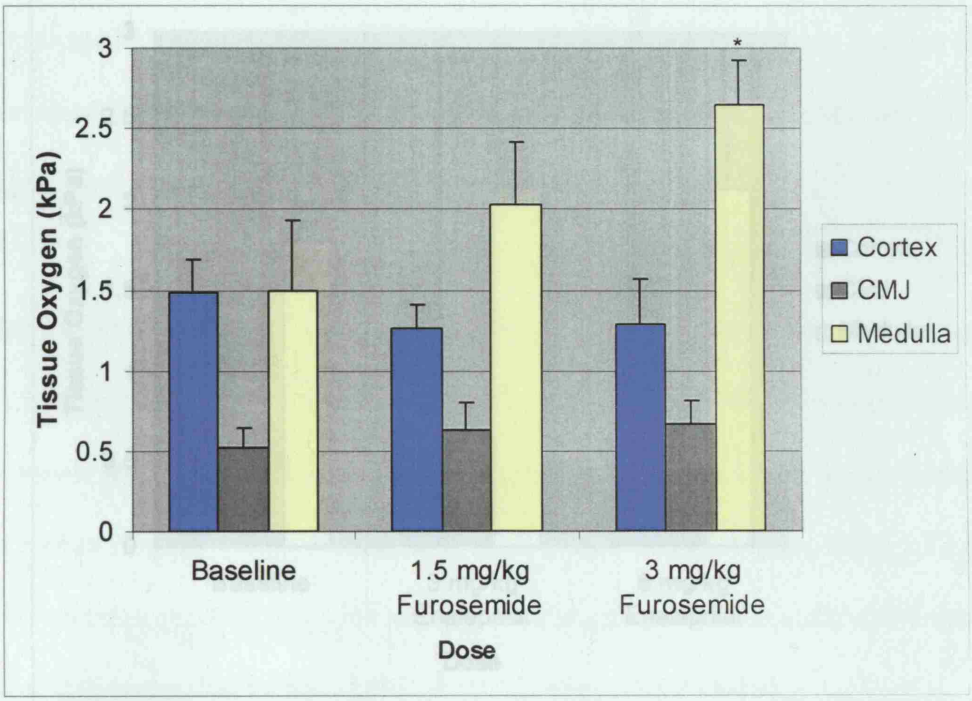

Figure 4-16: Changes in PtO_2 with increasing doses of Furosemide (n=6, *p<0.05)

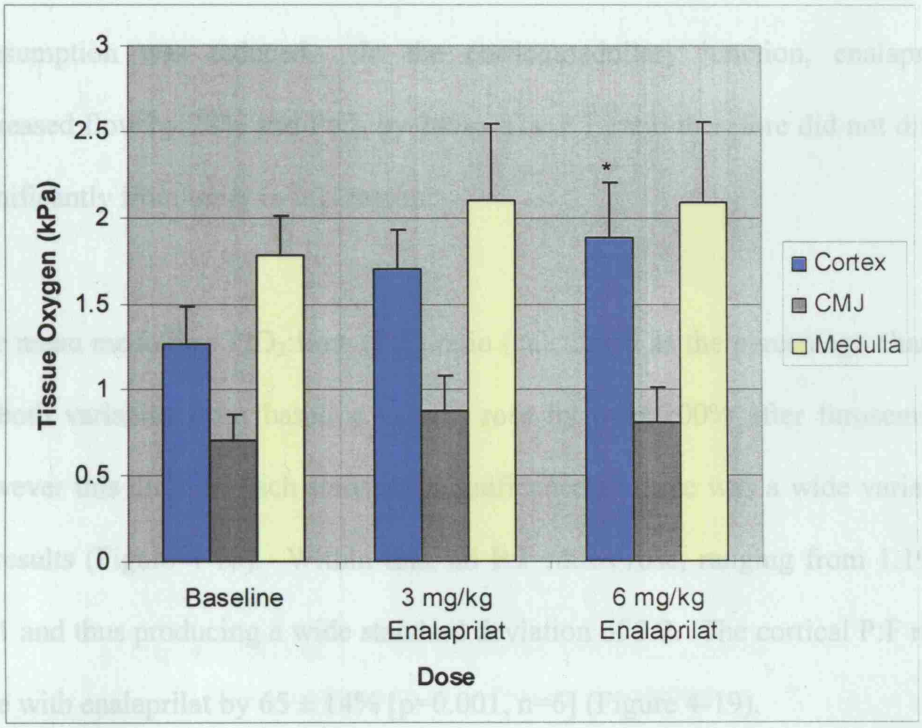

Figure 4-17: Changes in PtO_2 with increasing doses of Enalaprilat (n=6, *p<0.05)

4.6.4 Analysis of P:F Ratio

There was a non-significant rise in medullary PtO_2 (from 1.77 ± 0.23 to 2.08 ± 0.46) but a decrease in flow by 15% following 1 mg enalaprilat. The P:F ratio rose but did not reach statistical significance; but does imply that local oxygen consumption was reduced. In the corticomedullary junction, enalaprilat increased flow by 28% and PtO_2 by 24%. The P:F ratio therefore did not differ significantly from unity in this region.

The mean medullary PtO_2:flow (P:F) ratio (calculated as the percentage change in both variables from baseline values) rose by over 200% after furosemide, however this did not reach statistical significance as there was a wide variance in results (Figure 4-18). Within this, all P:F ratios rose, ranging from 1.19 to 9.41 and thus producing a wide standard deviation of 3.2. The cortical P:F ratio rose with enalaprilat by 65 ± 14% [p=0.001, n=6] (Figure 4-19).

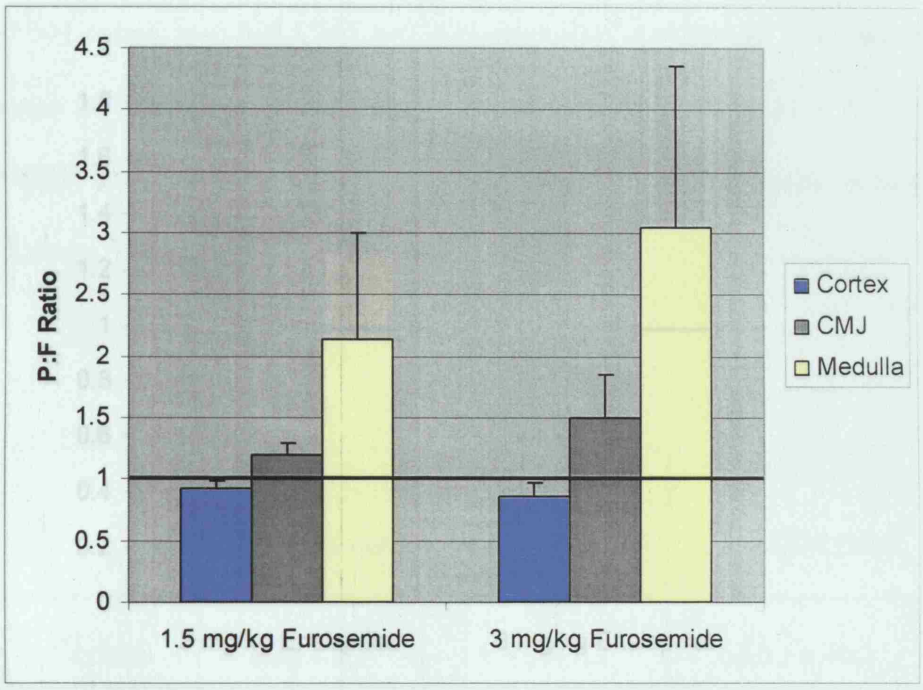

Figure 4-18: Changes in P:F Ratio with furosemide (n=6, p=NS)

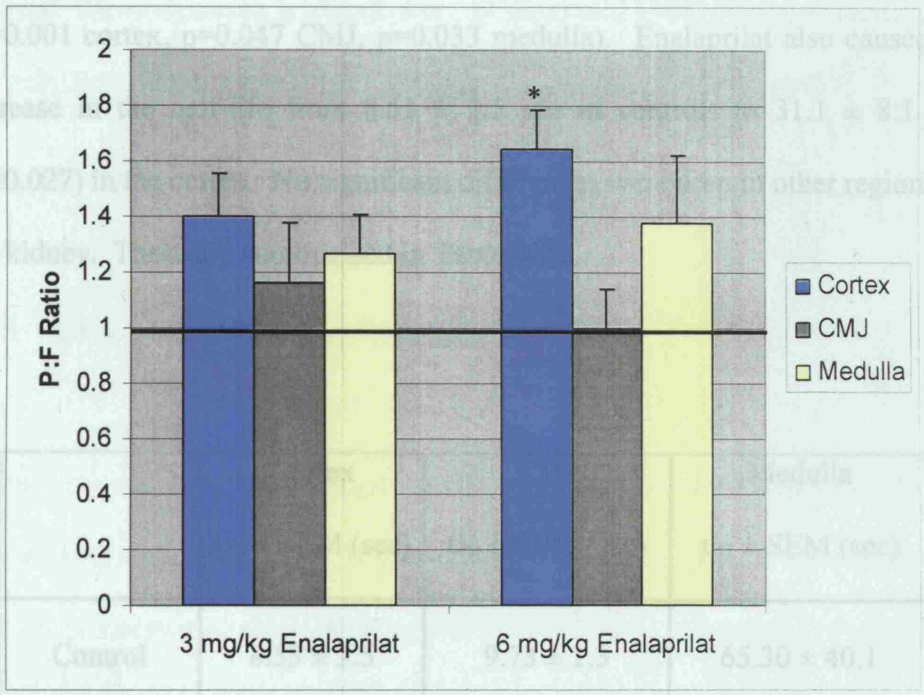

Figure 4-19: Changes in P:F Ratio with enalaprilat (n=6, *p<0.05)

4.6.5 Analysis of oxygen decay following termination

On termination of the experiment, the half-life of the tissue oxygen tension decay curve increased with the use of furosemide in all regions of the kidney (p=0.001 cortex, p=0.047 CMJ, p=0.033 medulla). Enalaprilat also caused an increase in the half-life from 8.53 ± 3.5 sec in controls to 31.1 ± 8.1 sec (p=0.027) in the cortex. No significant differences were seen in other regions of the kidney. These are summarised in Table 4-3.

	Cortex t½ ± SEM (sec)	CMJ t½ ± SEM (sec)	Medulla t½ ± SEM (sec)
Control	8.53 ± 3.5	9.73 ± 1.3	65.30 ± 40.1
Enalaprilat	31.14 ± 8.1 (p=0.027)	17.98 ± 8.2 (p=0.234)	26.32 ± 12.3 (p=0.499)
Furosemide	89.87 ± 13.3 (p=0.001)	80.82 ± 26.0 (p=0.047)	307.3 ± 77.0 (p=0.033)

Table 4-3: Oxygen decay half-life with furosemide and enalaprilat

4.7 Endotoxaemia

Eleven animals were studied; three died within an hour and two more became so sick that they hyperventilated and the probes moved or fell out of the kidney. Previous experience with this model has shown that this dose of LPS constitutes a severe haemodynamic insult (Rosser, D.M. *et al.*, 1995). Data reported here are only from those animals who survived the two-hour study period.

4.7.1 Changes in BP and whole organ flow

There were no significant changes in BP after two hours of lipopolysaccharide in surviving animals (LPS). The initial mean (± SEM) BP of 83 ± 3 mmHg (n=6) was maintained throughout so that the BP was 81 ± 6 mmHg (n=6) after 2 hours. Aortic and renal artery flows fell during separate control experiments. I believe that the extra fluid resuscitation received during the protocol protected the rat from hypotension and thus the effects seen are related directly to the endotoxaemia rather than hypotension *per se*.

4.7.2 Changes in intra-renal flow and tissue oxygen

LPS caused a significant fall in intra-renal blood flows in all regions of the kidney (Figure 4-20). By the end of the LPS infusion (at time 30 min), mean (± SEM) flow to the cortex had fallen by 42.3 ± 10%, to the CMJ by 27.0 ± 8.6% and to the medulla by 37.5 ± 5.7% (n=6). Flows did not change significantly from these levels for the duration of the experiment.

At the same time, PtO_2 rose in the CMJ but fell in the other two regions (Figure 4-21). Although absolute figures only reached significance at the 5% level after 45 minutes in the medulla because of a wide variance, percentage changes in PtO_2 were highly significant throughout (Figure 4-22). By the end of the infusion the PtO_2 had fallen by a mean (± SEM) of 37.7 ± 6% in the cortex, fallen by 62.5 ± 13% in the medulla, but risen by 95.0 ± 55% in the CMJ (n=6 throughout).

4.7.3 Analysis of P:F ratio

Consequently, the P:F ratios (Figure 4-23) in the CMJ were raised but showed a wide variation. Although a significance value of less than 5% was not achieved, the confidence limits for most results were above zero (for example, 32-344 % rise after 75 minutes) and most of the individual results also showed a rise. In face of the recorded falls in intra-renal flow, it is reasonable to infer that the CMJ has reduced its oxygen consumption.

P:F ratios in the cortex rose by between 7-34% (p=NS) but fell in the medulla (-23 to -45%, p=NS). It thus appears that the cortex had also reduced its oxygen consumption although the findings in the medulla are less easy to interpret.

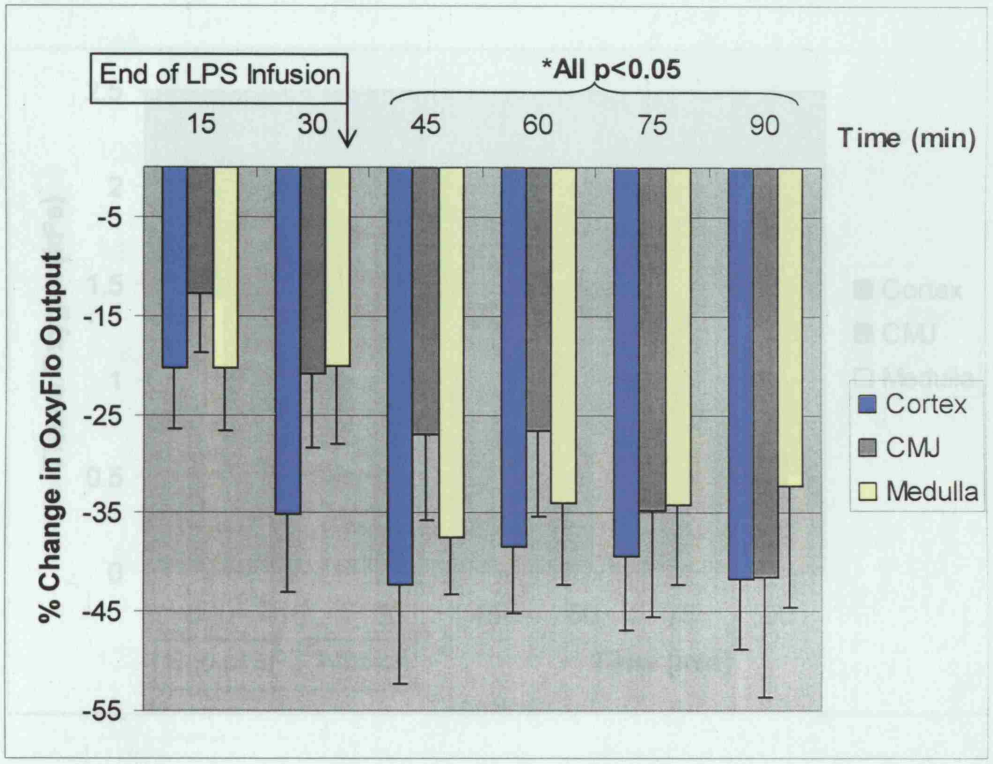

Figure 4-20: Changes in intra-renal flow during and following the administration of LPS

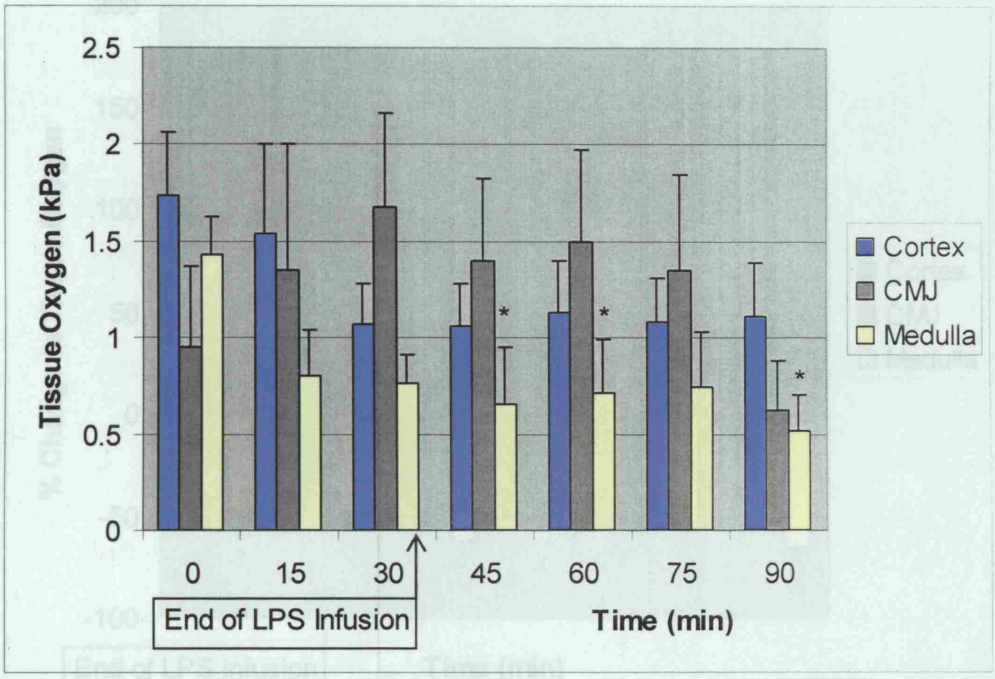

Figure 4-21: Changes in intra-renal PtO_2 during and following the administration of LPS (n=6, *p<0.05)

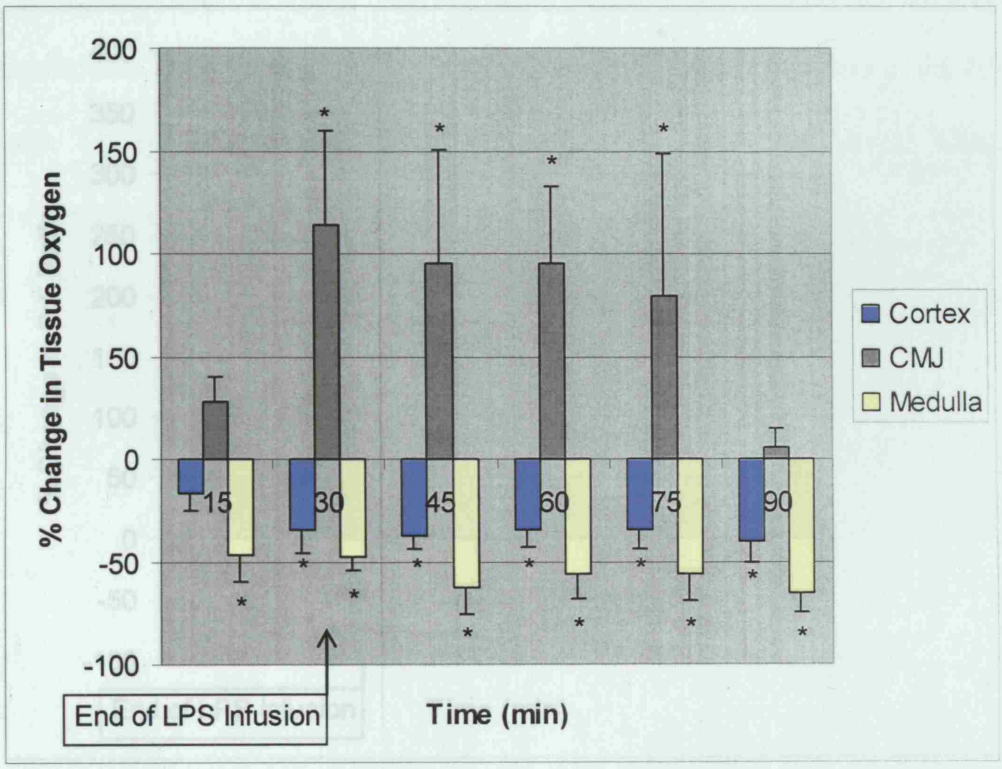

Figure 4-22: Percentage change in intra-renal PtO_2 during and following the administration of LPS (n=6, *p<0.05)

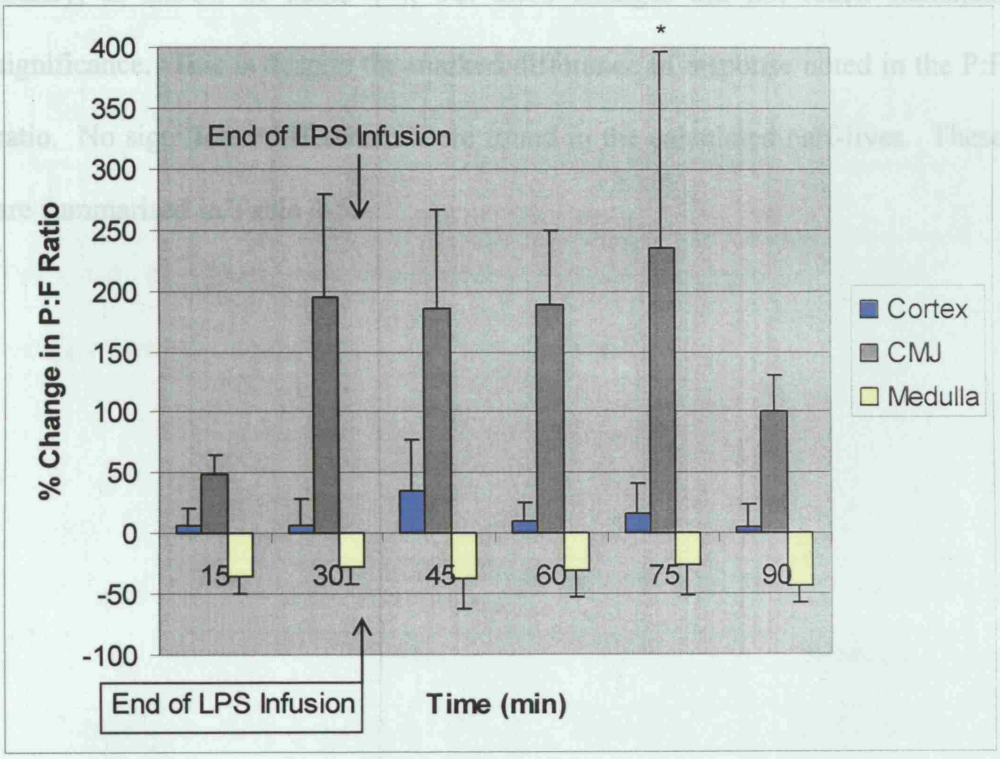

Figure 4-23: Changes in P:F ratio during and following the administration of LPS (n=6, *p<0.05)

4.7.4 Analysis of oxygen decay following termination

On termination of the experiment, the decay time of the tissue oxygen tension decay curve increased following endotoxaemia in the outer regions of the kidney, as shown in Table 4-4, but these changes did not reach statistical significance. This is despite the marked difference in response noted in the P:F ratio. No significant differences were found in the calculated half-lives. These are summarised in Table 4-5.

	Time constant (sec^{-1} ± SEM)		
	Cortex	CMJ	Medulla
Control	0.119 ± 0.025	0.077 ± 0.11	0.030 ± 0.11
Septicaemia	0.09 ± 0.018	0.036 ± 0.02	0.028 ± 0.02
p	All NS		

Table 4-4: Oxygen consumption time constants of oxygen decay after termination following septicaemia experiments

	Mean t½ (sec ± SEM)		
	Cortex	CMJ	Medulla
Control	5.8 ± 1.0	9.0 ± 1.1	23.3 ± 6.1
Septicaemia	7.7 ± 1.4	19.2 ± 3.1	24.8 ± 5.4

Table 4-5: Half-life of oxygen decay after termination following septicaemia experiments

4.8 Changes in tissue oxygen during exposure to varying inspired oxygen concentrations

Analysis for this section proved to be difficult. The PtO_2 differed whether a particular FiO_2 target was approached from either above or below. 10% FiO_2 resulted in a long-term increase in PtO_2 when the FiO_2 of room air (21%). However, a similar response was also noted when 100% FiO_2 was administered. This would imply that local oxygen consumption was reduced. The PtO_2 frequently remained raised for more than 45 minutes, implying that this was not simply because of washout of excess oxygen.

In other experiments, once the FiO_2 had been established and the PtO_2 stabilised, the PtO_2 inexplicably increased and did not return to baseline levels. An example of this is shown in Figure 4-24. In order to ensure that dampened PtO_2 findings were not due to haematoma, the backscatter from the OxyFlo probes were continuously monitored (and showed that a good proportion of the outward signal was being returned) and, in addition, a visual inspection of a section through the kidney was made at the end of the experiment.

Hyperoxia causes pulmonary and ocular damage in mammals. In the early days of neonatal intensive care, babies were blinded through retrolental fibroplasia caused by the administration of high concentrations of oxygen. The mechanisms for this were elucidated in the 1970s. In the present study,

exposure of the animal to high concentrations of inspired oxygen for long periods of time caused an increase in aortic flow and a decrease in blood pressure; these are similar changes to those seen during septicaemia or the recovery phase following exsanguination-resuscitation. I thus believe that the kidney is extremely sensitive to hyper- and hypoxia with decreases in local oxygen consumption induced by this simple challenge. This sensitivity also has implication for interpretation of *ex vivo* cell studies which entails exposing cells to room air having extracted them from physiological oxygen concentrations.

As oxygen delivery is dependent upon oxygen saturation (SpO_2), SpO_2 is used in the following graphs. SpO_2 is calculated rather than measured. The algorithm in the arterial gas machine calculated saturations greater than 100% in some cases.

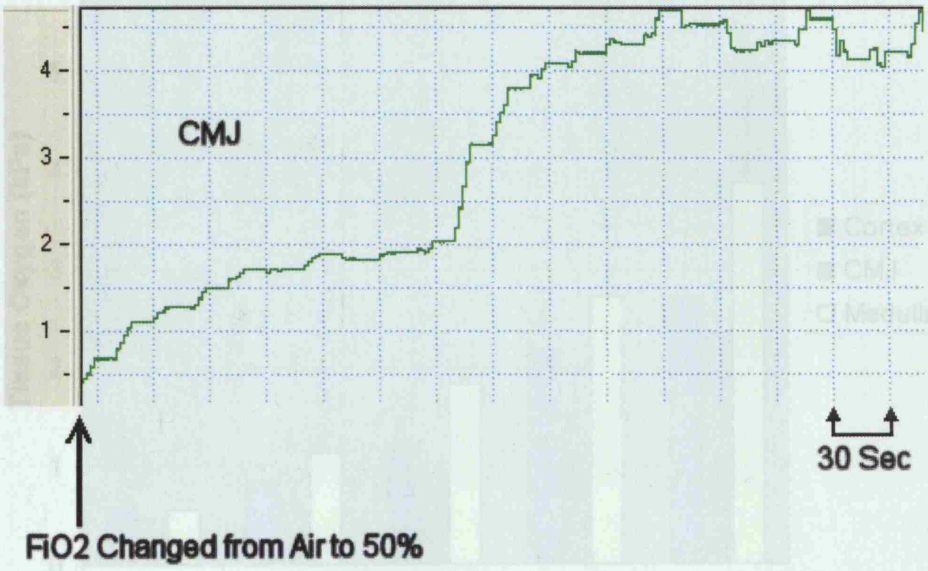

Figure 4-24: Figure showing an example of a sudden increase in PtO_2 during experimentation

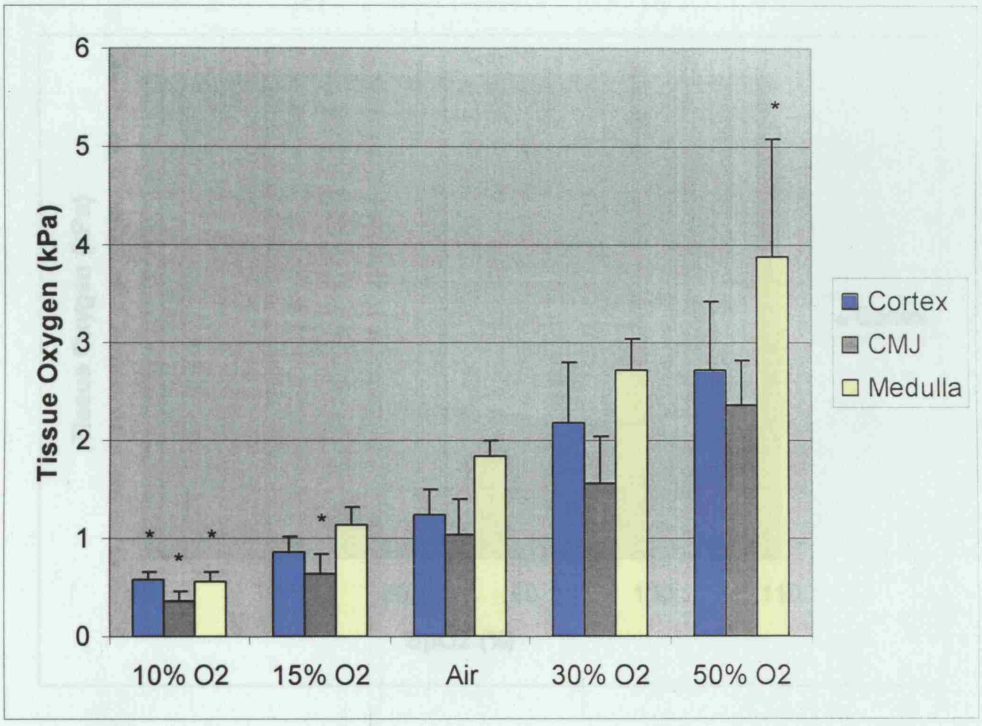

Figure 4-25: Mean PtO_2 against grouped FiO_2 (includes all data points, *p<0.05)

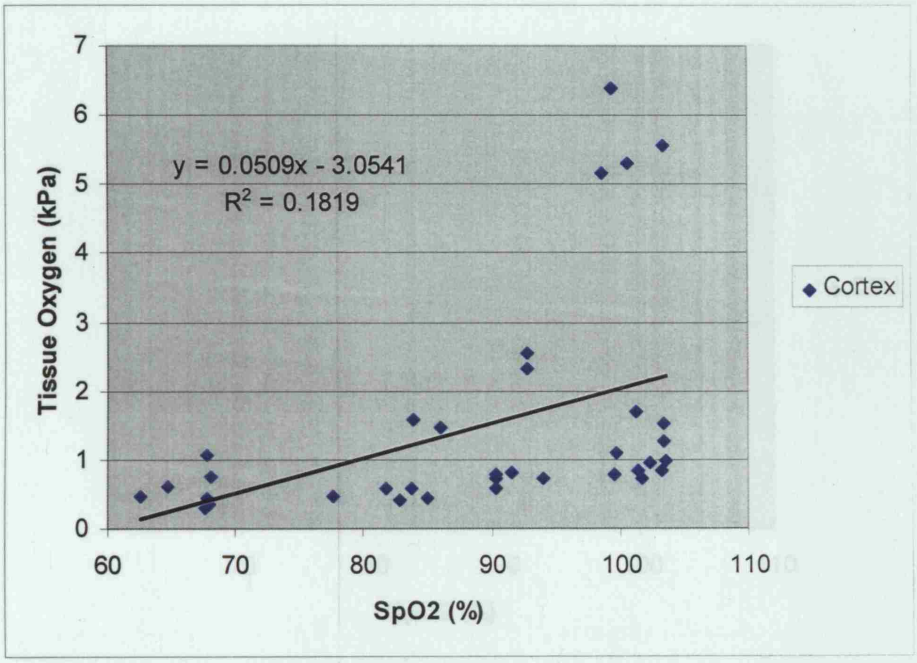

Figure 4-26: Changes in cortical tissue oxygenation plotted against arterial blood saturation during varying inspired oxygen concentrations

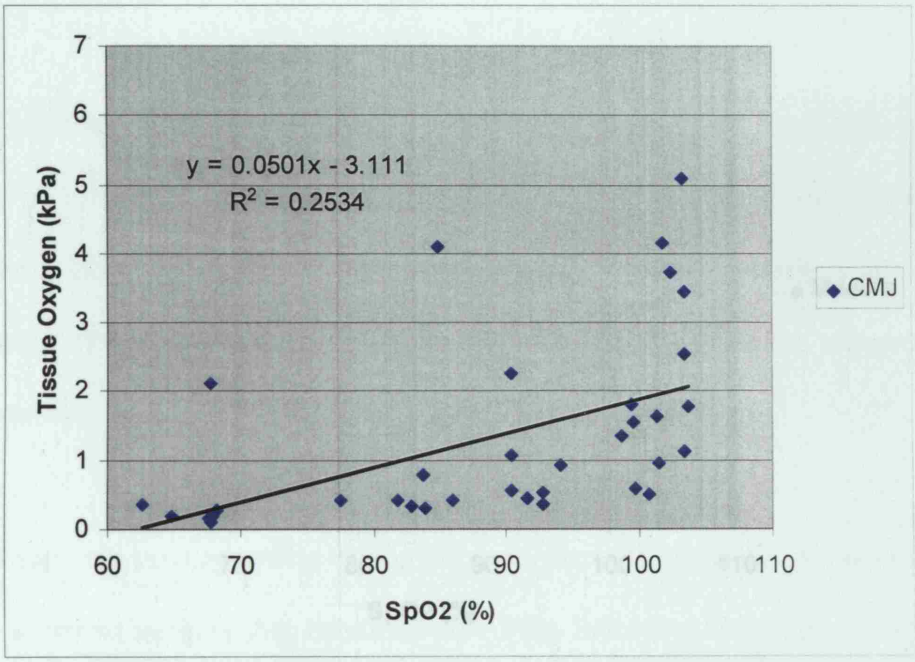

Figure 4-27: Changes in CMJ tissue oxygenation plotted against arterial blood saturation during varying inspired oxygen concentrations

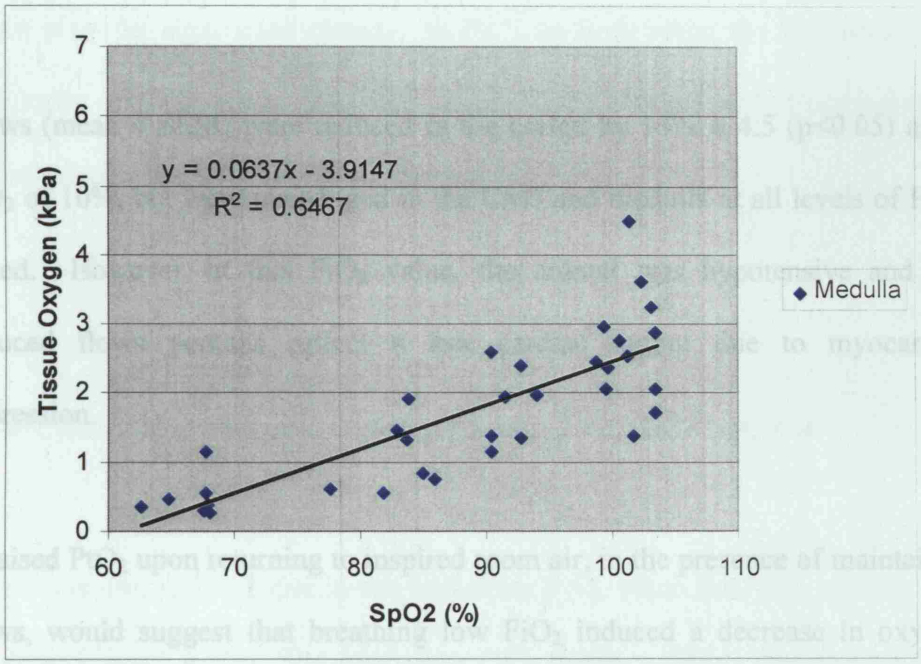

Figure 4-28: Changes in medulla tissue oxygenation plotted against arterial blood saturation during varying inspired oxygen concentrations

There is a correlation between arterial blood saturation and tissue oxygen tension at all levels of the kidney. The gradients of the slopes are very similar, implying that all regions respond in a similar way during the early part of exposure to a change in inspired oxygen concentration. The linear regression results are difficult to perform because of the numerous outliers (as explained above).

Flows (mean ± SEM) were reduced in the cortex by 15% ± 4.5 ($p<0.05$) at an FiO_2 of 10%, but were unchanged in the CMJ and medulla at all levels of FiO_2 tested. However, at this FiO_2 value, the animal was hypotensive and the reduced flows perhaps reflect a low cardiac output due to myocardial depression.

A raised PtO_2 upon returning to inspired room air, in the presence of maintained flows, would suggest that breathing low FiO_2 induced a decrease in oxygen consumption which persisted when the FiO_2 was restored to 21% (air). The combination of this finding with the discovery that oxygen eventually 'broke through' to the tissues despite good pulsatile backscatter, is against conventional wisdom and that our understanding of oxygen flow and delivery through the tissues *in vivo* is far from complete. It may also be that the experimental protocol was mimicking a reperfusion injury. I believe that these responses merit further investigation.

4.9 The effects of different anaesthetic agents

There were no significant changes in BP, intra-renal flows or PtO_2 when the isoflurane was increased from 1.5% to 2% and from 2% to 2.5%.

There were no significant changes in PtO_2 or flow when the isoflurane was withdrawn and Hypnorm (Fentanyl citrate 0.315 mg/ml with Fluanisone 10 mg/ml) was used as the sole anaesthetic agent.

4.10 Changes in tissue oxygen following capsule removal

There was a significant rise in the medullary PtO_2 when the renal capsule was removed (Figure 4-29). The medullary PtO_2 (mean ± SEM) rose from 1.65 ± 0.37 kPa to 3.35 ± 0.57 kPa (n=6, p=0.038, 2-tailed t-test). However, there were no significant changes in medullary intra-renal flow (which fell by 5 ± 16%, n=4). A significant fall was seen in flow to the CMJ which fell by 28 ± 5% (n=4, $p<0.001$), though cortical flow rose only by 8% (p=ns).

As a result, the P:F ratio in the CMJ increased significantly by 173 ± 74% (n=4, p=0.03). This implies that local regional oxygen consumption within the CMJ and medulla was significantly reduced. It may be that the extra surgical stress and time taken to set the experiment may have contributed to these surprising

results rather than capsule removal affecting cell respiration directly. This is discussed further in Chapter 6.

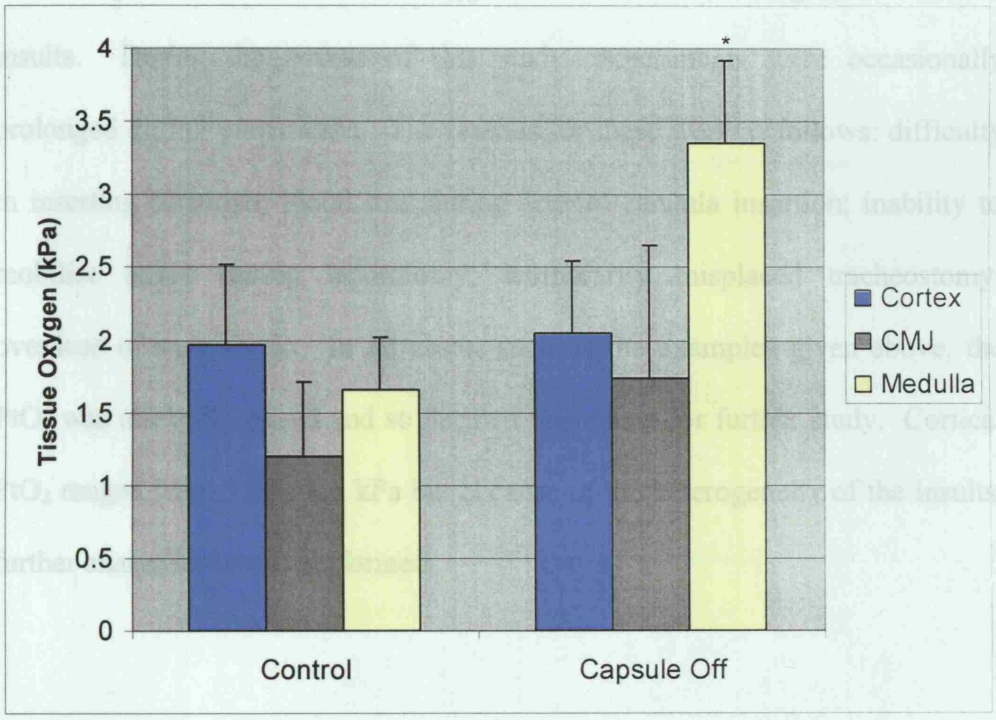

Figure 4-29: Changes in PtO_2 when the renal capsule was removed (*p<0.05)

4.11 Other results

Over 150 animals were anaesthetised of which fewer than 10% did not complete the full experimental protocol. There was good concordance of baseline PtO_2. Data not presented in this thesis suggest that the kidney is highly sensitive to insults. During the course of this study, experiments were occasionally prolonged during preparation. The reasons for these were as follows: difficulty in inserting cannulae; blood loss during arterial cannula insertion; inability to mobilise tissue during laparotomy; temporarily misplaced tracheostomy; overdose of anaesthetic. In all cases, such as the examples given above, the PtO_2 was markedly raised and so deemed unsuitable for further study. Cortical PtO_2 ranged from 3.7 to 8.1 kPa but because of the heterogeneity of the insults, further analysis was not performed.

4.12 Results summary

Intervention	Cortex		CMJ		Medulla	
	% Change in P:F Ratio	O_2 Half-Life (sec^{-1})	% Change in P:F Ratio	O_2 Half-Life (sec^{-1})	% Change in P:F Ratio	O_2 Half-Life (sec^{-1})
Control	-	5.8 ± 1.0	-	9.0 ± 1.1	-	23.3 ± 6.1
Resuscitation	121.3 ± 25.0 *	10.4 ± 1.4 *	2.88.8 ± 70.2 *	16.6 ± 4.2 *	288.2 ± 1.8 *	39.7 ± 7.9
Furosemide	-14.6 ± 11.2	89.9 ± 13.3 *	49.8 ± 36.0	80.8 ± 26.0 *	204 ± 30.3 *	307.3 ± 77.0 *
Enalaprilat	64.6 ± 15.3 *	31.1 ± 8.1 *	0.3 ± 61.3	18.0 ± 8.2	37.4 ± 67.8	26.3 ± 12.3
Endotoxin	15.6 ± 24.8	7.7 ± 1.4	236 ± 160 *	19.2 ± 3.1	-27.1 ± 25.0	24.8 ± 5.4

Table 4-6: Quantitative summary of results (*p<0.05)

Intervention	Cortex		CMJ		Medulla		Conclusion
	PtO_2	Flow	PtO_2	Flow	PtO_2	Flow	
Aortic Clamp	↓	↓↓	↓	↓↓	↓	↓	Relative preservation of medullary flow
Hypoxaemia	↓	↓↓	↓	↓	↓	↓	Difficult to interpret. VO_2 may be reduced in the cortex
Exsanguination	↓	↓↓	↔	↔	↔	↑	VO_2 may be reduced in the cortex
Resuscitation	↑↑	↔	↑	↓	↔	↔	VO_2 reduced in cortex and CMJ
Furosemide	↔	↔	↔	↔	↑	↔	VO_2 reduced in medulla
Enalaprilat	↑	↔	↔	↑	↔	↔	VO_2 probably reduced in cortex
Endotoxin	↑	↓	↑↑	↓	↓	↓	VO_2 reduced in CMJ

Table 4-7: Qualitative summary of results

5 Discussion

5.1 Model overview

The model described in this thesis placed three probes at different levels of the kidney and monitored changes in PtO_2 and LDF following various interventions. In general, changes in LDF were used as absolute values vary widely (Lien, B. *et al.*, 1992). To be able to carry out population statistics on the raw LDF data, many more animal experiments would have been necessary (Lien, B. *et al.*, 1992).

By concurrently measuring intra-renal flow together with PtO_2, I believe that I have demonstrated *in vivo* decreases in oxygen consumption during increases in PtO_2 in the face of maintained flow.

As shown in Table 2-1, reported values of intra-renal tissue oxygen tensions vary greatly. This is likely to be predominantly related to methodological differences due to the use of species (rats, mice and dogs), kidney preparation and instrumentation, anaesthesia regimens, and the degree and constituents of fluid resuscitation. The depth at which measurements were taken was variable in some studies (Brezis, M. *et al.*, 1994b), while others investigators removed the renal capsule during instrumentation. Some models placed the kidney extraperitoneally (James, P.E. *et al.*, 1996) or in a cup (Liss, P. *et al.*, 1997a),

while the degree of intraperitoneal warming (if not cupped) was not reported (Gunther, H. *et al.*, 1974), (James, P.E. *et al.*, 1996).

Many previous studies concentrated simply on the differences in tissue oxygenation between cortex and medulla. Growing evidence suggests that the corticomedullary junction (or juxtamedullary region in some papers) may be the source of renal failure (Adler, S. and Huang, H., 2002), (Roald, A.B. *et al.*, 2002). My data suggest that the PtO_2 does not steadily decline from the cortex towards the medulla but, instead, a nadir is seen at the corticomedullary junction. This site also exhibited the largest changes during haemorrhage/reperfusion.

The gap I found between cortical and medullary PtO_2 is narrow, but when compared with some other groups, it is the cortical PtO_2 that appears to be disproportionally low. However, as discussed in chapter 4, higher cortical PtO_2 values are possible to achieve under certain physiological stresses and the presence of a low but constant cortical PtO_2 with predictable responses may still offer useful results.

5.1.1 Removal of capsule

I found that PtO_2 changed with removal of the kidney capsule. In the introduction, I speculated that removal of the capsule may alter intra-renal flows by affecting compartmental pressures and thus intra-renal vascular resistance.

However, I found that intra-renal flows were not affected by this procedure. Therefore it would appear that there has been a reduction in regional oxygen consumption when the capsule is removed, though the mechanism for this is unclear and merits further investigation. The kidney is under the influence of a complex interplay of mediators including the renin-angiotensin system, the sympathetic system, prostaglandins and NO. The sympathetic supply must penetrate the capsule and it may be that this supply is disrupted by its removal. I also note that *any* disruption of the physiological norm caused a rise in PtO_2; this may also be a contributing factor as lifting the kidney to remove the posterior segment of the capsule may kink the blood vessels and disrupt the blood supply.

5.1.2 Exsanguination/Resuscitation

Despite similar falls in blood pressure, I found different intra-renal haemodynamic responses when comparing sequential aortic constriction and haemorrhage. With aortic constriction, autoregulation existed in the cortical and corticomedullary regions, maintaining flow until the blood pressure fell by approximately 50%. Flow was significantly decreased in the medulla once perfusion pressure fell below 80% of baseline. These findings are in distinct contrast to those obtained during exsanguination where flow to the medulla rose. The P:F ratio showed a decrease in cortical and medullary regions during progressive aortic constriction but an increase during exsanguination and subsequent resuscitation. The PtO_2 was virtually unchanged during

exsanguination but fell in proportion to the fall in perfusion pressure during aortic constriction. The reason for this is unclear but implies that exsanguination induced a reduction in cell respiration that continued during immediate resuscitation with drawn blood. Although both insults involve reductions in organ flow in the first instance, the time course of the exsanguination experiments was longer and may have given the cells more time to respond to the insult. The only region that appeared to respond consistently was the corticomedullary junction. The generalised systemic effect of exsanguination on release of mediators and hormones may also contribute to the differences seen. Mattson *et al* (Mattson, D.L. *et al.*, 1993) previously studied autoregulation of blood flow in the cortex and medulla in a variety of both volume-expanded and unresuscitated animals under anaesthesia. Blood flow in the renal cortex was autoregulated in both volume-expanded and unresuscitated animals, unlike the medulla where blood flow was poorly autoregulated in volume-expanded animals. They suggested that this disparity was due to changes in resistance in the post-glomerular circulation of deep nephrons. I have extended this work further by simultaneously monitoring the corticomedullary region during two distinct insults compromising the renal circulation.

The paradoxical rise in medullary PtO_2 identified by Brezis (Brezis, M. *et al.*, 1994b) during haemorrhage in rats is probably explained by the experimental methodology used. Rats were exsanguinated an average of 3.9 ± 0.2 ml (range 1.7-8 ml) in order to induce a fall in mean blood pressure to 80 mmHg. Such a wide range of blood withdrawal is as much a test of the cardiovascular fitness of

an individual rat rather than applying a constant insult to a group, and took no account of the starting blood pressure.

I found that the P:F ratio was maintained during blood withdrawal in all regions of the kidney, yet increased markedly during subsequent resuscitation, particularly in the deeper regions. A linear relationship is unlikely to exist between flow and PtO_2 as cell respiration is highly regulated (Beltran, B. *et al.*, 2000). However, a decrease in cell respiration with constant blood flow within the tissue would cause an increase in the P:F ratio, and *vice versa*. The rise in P:F ratio seen on blood withdrawal and, particularly, following resuscitation implies that the cells in that particular region have reduced their oxygen consumption. This was found throughout the kidney, and even in the corticomedullary region where PtO_2 *rose* despite a significant decrease in flow. I also confirmed these findings by showing that the initial decay in PtO_2 on death was slower in regions where the P:F ratio was increased out of proportion to any increase in local flow.

This presumptive fall in oxygen consumption is likely to have arisen from decreased mitochondrial respiration as ATP production constitutes over 90% of total cellular oxygen consumption (Clementi, E. *et al.*, 1998). Whether this fall is due to a direct inhibition of mitochondrial enzymes from nitrogen and oxygen free radicals released during both the periods of tissue hypoxia and reperfusion (Turrens, J.F. *et al.*, 1982), (Freeman, B.A. and Crapo, J.D., 1981), and/or a decrease in energy-requiring metabolic processes such as solute and water re-absorption remains to be determined. The probes were measuring from a

greater volume of tissue than some other models and so consideration of all metabolically active cells should be made. For example, the vascular endothelium is considered a major contributor to regional oxygen consumption (Tsai, A.G. *et al.*, 1998).

The findings during post-exsanguination resuscitation are in accord with previous studies measuring tissue oxygen tension in the bladder epithelium. The tissue pO_2 fell during haemorrhage (Singer, M. *et al.*, 1996) and hypoxaemia (Stidwill, R.P. *et al.*, 1998) but increased in both high and low output endotoxaemia (Rosser, D.M. *et al.*, 1995). The haemorrhage study protocol (Singer, M. *et al.*, 1996) also included a resuscitation step after the first blood withdrawal; of note, the bladder epithelial pO_2 increased non-significantly over its pre-haemorrhage value while aortic and renal blood flow only recovered to 70% of baseline.

My recorded cortical:medullary pO_2 ratio of 1.6 is, nevertheless, very similar to three previous studies (Nelimarkka, O., 1984), (Liss, P. *et al.*, 1997a), (James, P.E. *et al.*, 1996) but much lower than the approximate 4:1 ratio reported by Gunther (Gunther, H. *et al.*, 1974) and Brezis (Brezis, M. *et al.*, 1994b). However, Duling and Berne (Duling, B.R. and Berne, R.M., 1970) measured a pO_2 of 1.1 ± 0.3 kPa in a hamster hind limb model.

5.1.3 Furosemide and enalaprilat

Despite a fall in aortic blood flow, no flow changes were noted either to or within the kidney with furosemide. As blood pressure was also maintained, this suggests that autoregulation is still maintained with flow redistribution from other organs compensating for the decrease in total blood flow. However, the near-doubling of medullary PtO_2 in the presence of an unchanged medullary flow is strongly suggestive of a reduction in local oxygen consumption. Rises in medullary PtO_2 with furosemide have been previously noted by many authors in various species including man (Brezis, M. *et al.*, 1994a), (Epstein, F.H. and Prasad, P., 2000), (Prasad, P.V. *et al.*, 1996), (Heyman, S.N. *et al.*, 1989), (Nuutinen, L.S. and Tuononen, S., 1976), (Priatna, A. *et al.*, 1999). Other groups have noted a reduction in oxygen consumption (Manuel, M.A. and Weiner, M.W., 1976), (Eknoyan, G. *et al.*, 1975). Interestingly, Eknoyan and colleagues (Eknoyan, G. *et al.*, 1975) found a reduction in oxygen consumption in both cortical and outer medullary cells which was not apparent until the model was terminated. Though no significant changes were seen with furosemide on cortico-medullary and cortical PtO_2, the delayed oxygen decay curve on cessation of flow suggests that oxygen consumption is actually reduced to all levels of the kidney. As mitochondrial energy production is the main consumer of oxygen, this implicates a direct effect of furosemide on mitochondrial respiration. Indeed, this finding has been previously reported in both renal cortex and medulla (Orita, Y. *et al.*, 1983), (Manuel, M.A. and Weiner, M.W., 1976).

Nilsson and Friberg (Nilsson, A.B. and Friberg, P., 2000) previously reported that enalapril maintained renal blood flow in the neonatal pig despite a 10% reduction in blood pressure. Dukacz and Kline (Dukacz, S.A. and Kline, R.L., 1999) had made similar findings in a spontaneously hypertensive rat model. I found, however, that the active metabolite enalaprilat produced an *increase* in total renal blood flow. Of note, the major effect on intra-renal haemodynamics was noted at the corticomedullary junction.

Our group previously reported in a similar rat model (Norman, J.T. *et al.*, 2003) that enalaprilat increased cortical PtO_2, but did not match these with local flow measurements. Our current finding of an approximate 65% increase in cortical PtO_2 matched by a similar increase in P:F ratio and in the presence of constant microvascular flow suggests a reduction in local oxygen consumption. This has been previously shown by Adler *et al* in renal cortical tissue slices taken from mice (Adler, S. *et al.*, 2001). We believe ours is the first *in vivo* demonstration of this effect in the renal cortex. Adler *et al* also noted that the effects on the reduction of oxygen consumption were reversed when a free radical scavenger (Tempol, 4-hydroxy-2,2,6,6-tetramethyl piperidine-1-oxyl) was added to their model (Adler, S. and Huang, H., 2002). Enalapril was also noted to increase mitochondrial nitric oxide synthase activity in rat heart and liver (Boveris, A. *et al.*, 2003). As with most cells, the mitochondrion is responsible for 90% of cellular oxygen consumption, thus the prolonged decay in cortical tissue oxygen tension seen on cessation of flow in the enalaprilat-treated animals adds further support to a direct effect on mitochondrial respiration. This may be an

important mechanism of enalapril-induced renal protection and clearly warrants further study.

5.1.4 The kidney in sepsis

5.1.4.1 Renal mitochondrial dysfunction in sepsis

A number of animal models have been used to investigate mitochondrial function in sepsis (Brealey, D. and Singer, M., 1999). Little consistency was seen in short-term models though studies lasting in excess of 12 hours consistently showed decreased mitochondrial activity and/or mitochondrial damage. Few studies have been performed on renal tissue or cells. Fry's group found no uncoupling of mitochondrial respiration (Asher, E.F. *et al.*, 1983) nor significant alterations in State 3 and State 4 respiratory rates (Garrison, R.N. *et al.*, 1982) in liver and kidney mitochondria isolated from endotoxic rats five hours after injection. However, Mela performed a series of investigations on mitochondrial function and ultrastructural change in rat and guinea pig models. Kidney and brain mitochondrial O_2 utilization and ATP synthesis were significantly depressed 24 hrs after induction of sepsis (Mela, L., 1981). High-dose steroids prevented this deterioration in mitochondrial function and completely abolished the 60% mortality seen in untreated animals (Mela, L. and Miller, L.D., 1983). A long-term faecal peritonitis rat model developed by our

group confirmed a decrease in renal cellular respiration (Brealey, D. *et al.*, 2004).

5.1.4.2 Nitric oxide and the kidney

NO may be an important regulator of renal oxygen consumption in both health and disease. The value for half-maximal NO-mediated inhibition of respiration was virtually identical to that found in isolated mitochondria (Koivisto, A. *et al.*, 1999). A direct correlation has long been recognised between sodium reabsorption and oxygen consumption. This is probably a reflection of the large proportion of oxygen consumption expended on sodium excretion compared with other renal cellular functions. Blocking NO production with the NO synthase inhibitor L-NMMA increased sodium excretion in dogs (Seeliger, E. *et al.*, 2001). In theory, changes in sodium excretion may be closely linked to the rate of mitochondrial respiration.

Over-production of NO has been implicated in the organ dysfunction developing in septic animal models although human data remain scanty. All three isoforms of NO synthase are produced in the kidney: neuronal (nNOS), inducible (iNOS) and endothelial (eNOS) (Millar, C.G. and Thiemermann, C., 1997). Endotoxaemia causes expression of iNOS and increases the activity of eNOS (Bachmann, S. *et al.*, 1995) though affects on nNOS are reported. The excessive vasodilatation and hypotension associated with circulatory shock can be reversed by inhibitors of the inducible form of NO synthase, though without

necessarily improving the accompanying organ dysfunction (Schwartz, D. *et al.*, 2001), (Wray, G.M. *et al.*, 1998). NO is involved in all mechanisms currently implicated in the development of ARF, namely intra-renal flow distribution, control/inhibition of cellular respiration and oxygen consumption, damage to mitochondria, and apoptosis and cell death.

5.1.4.3 Control of cellular respiration

At low concentrations for short periods, NO reversibly inhibits mitochondrial Complex IV (cytochrome c oxidase) by competing with O_2 (Brown, G.C., 2000). Complex IV is a key enzyme involved in generation of ATP and the only step in the whole oxidative phosphorylation pathway at which oxygen is consumed. Indeed, this one enzyme accounts for approximately 90% of total body VO_2 (Babcock, G.T. and Wikstrom, M., 1992). NO is thus considered to be an important physiological regulator of O_2 consumption in health. In pathological states such as sepsis, the larger amounts of NO are produced over long durations. Their production may out strip anti-oxidant mechanisms and it may combine with oxygen free radical to produce peroxynitrite ($ONOO^{\bullet -}$). Peroxynitrite is also a free radical and may produce a longer-acting, if not irreversible, inhibition of the electron transport chain, as well as direct damage to the mitochondria. In addition, oxygen free radical production may be enhanced by inhibition of the electron transport chain by NO (predominantly occurring at complexes I and IV).

5.1.4.4 Apoptosis

NO is an important mediator for inducing apoptosis (Beltran, B. *et al.*, 2000). Although apoptosis has not been shown to be a histological feature of ARF in sepsis (Hotchkiss, R.S. *et al.*, 1999), it should be borne in mind that apoptotic cells are rapidly cleared; further studies may be needed before excluding loss of cells as a contributory factor to acute renal failure

5.1.5 Changes in inspired oxygen

In general, I did find a correlation between arterial oxygen saturation and tissue oxygen tensions. Because of the shape of the oxygen dissociation curve (Figure 5-1), at PaO_2 values above 8 kPa, the saturations approximate to 100% and the dissolved component is the only was to increase oxygen carrying capacity of the blood (Figure 5-2). At high FiO_2 and assuming the local oxygen consumption remains constant, then the PtO_2 will rise linearly with the FiO_2.

At lower FiO_2, blood saturation becomes much more important than the dissolved component in calculating the carrying capacity of the blood. I may have demonstrated a reduction in local oxygen consumption on reducing FiO_2 but further study would be necessary to confirm this preliminary finding.

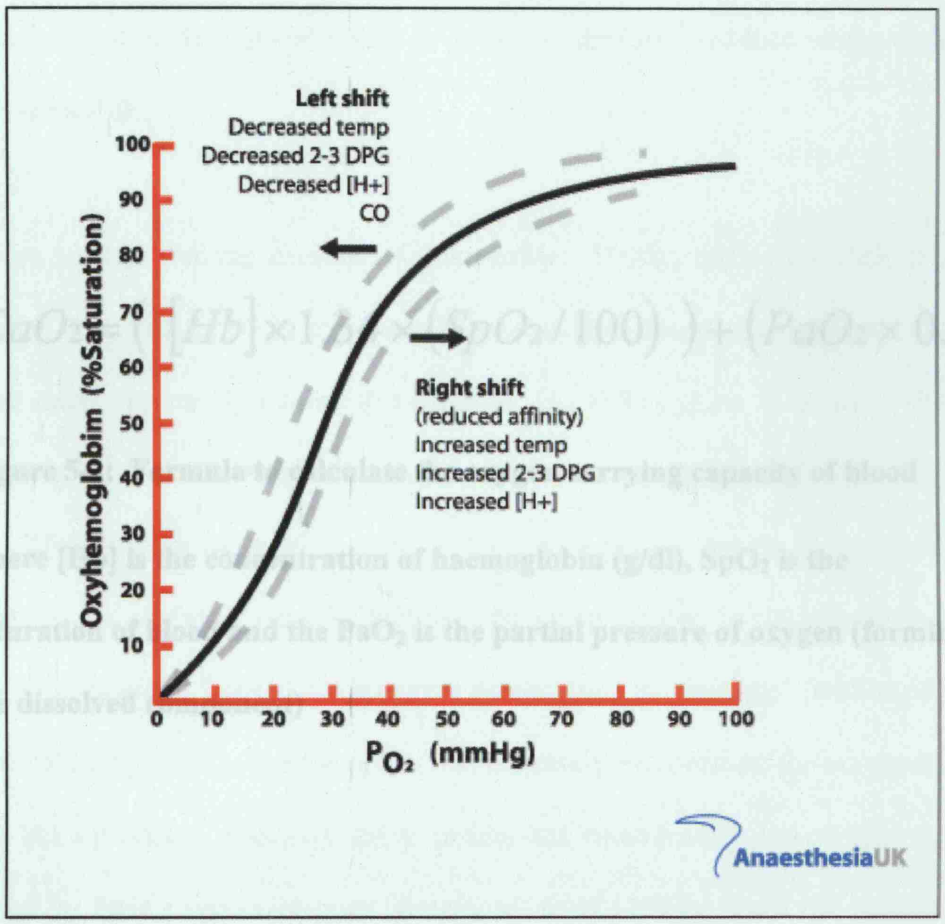

Figure 5-1: The oxygen dissociation curve

$$CaO_2 = \left([Hb] \times 1.34 \times (SpO_2 / 100) \right) + (PaO_2 \times 0.023)$$

Figure 5-2: Formula to calculate the oxygen carrying capacity of blood

where [Hb] is the concentration of haemoglobin (g/dl), SpO_2 is the saturation of blood and the PaO_2 is the partial pressure of oxygen (forming the dissolved component)

5.1.6 Withdrawal experiments

The withdrawal experiments whereby the probe was progressively withdrawn from deeper to superficial layers revealed a consistent PtO_2 profile; initially decreasing from the cortical values to a nadir at the CMJ and then rising slightly in the medulla.

There are two striking features of this profile. Firstly, the cortex PtO_2 is not higher than that found in the medulla. Secondly, results are generally lower than many commonly quoted (Nelimarkka, O., 1984), (Liss, P. *et al.*, 1997a), (Brezis, M. *et al.*, 1994a) but are within similar ranges to others (James, P.E. *et al.*, 1996), (Leichtweiss, H.P. *et al.*, 1969). An obvious concern is that regions close to the surface of the kidney may be contaminated by oxygen diffusing from the outside. I could not however demonstrate air 'leakage' (with a rise in cortical PtO_2), even when the probe was delicately balanced on the very cusp of the kidney edge. Although these results are considerably lower than those found by Brezis and colleagues (Brezis, M. *et al.*, 1994a), once the regions of interest had been defined, there was no need to *'move the probe until a good signal was obtained'* as was described in their paper. Furthermore, it should be noted that when Brezis moved the probe 'up to 3 mm' in order to find a good signal, it would be very easy indeed to move the probe to a completely different region and not be studying the cortex at all.

5.1.7 Anaesthesia

I have already suggested in my introductory chapter that the type of anaesthesia used may result in significant differences between models. However, I found no changes in either PtO_2 or intra-renal flows when maintenance of anaesthesia was switched to an intravenous technique. Changes have been studied in cardiac function comparing isoflurane against ketamine/inactin anaesthesia (Pena, J.R. and Wolska, B.M., 2005). The authors suggested that the additional sympathetic stimulation induced by ketamine may be cardiovascularly significant. Ketamine is known to be the most cardiovascularly stable of all general anaesthetic agents (Miller, R.D., 2004) but may not provide a stable environment as the animal may move and dislodge the probes. Certainly, higher initial blood pressures may imply lighter anaesthesia and risk awareness during experimentation, all of which will contribute to changes in sympathetic tract outflow and, therefore, changes in intra-renal blood flow.

In addition to cardiovascular changes, isoflurane has been found to pre-condition the myocardium (Cope, D.K. *et al.*, 1997) and protect it during ischaemic episodes (Haessler, R. *et al.*, 1994). It may be that our finding that oxygen consumption is reduced in the kidney may be enhanced by the anaesthetic used during the experiment. This certainly merits further study.

5.2 Tissue oxygen tension

In my model, paradoxical changes in PtO_2 were frequently noted between regions. Oxygen consumption was often reduced in the CMJ and unchanged in other regions. Only by matching changes in regional flow can we now appreciate that this may be due to a reduction in regional oxygen consumption.

The probes used in the present study are pre-calibrated. Maintained calibration was confirmed at the end of the experiment in a random number of probes. The ruthenium fluorescence technique is more accurate than the traditional Clark electrode technology at lower values of oxygen tension and is not prone to the effect of oxygen consumption by the probe itself. The fluorescence lifetime is longest at low pO_2 values, making these probes most sensitive in the physiological range of 0 - 60 mmHg. The probe also samples from a relatively large volume of tissue (0.7 – 1.0 mm^3) compared with many other probes, and may thus be less susceptible to small variations in probe position in proximity to blood vessels. Baumgartl *et al* (Baumgartl, H. *et al.*, 2002) used membranised, glass insulated pO_2 microelectrodes of 1-3 microns diameter to map oxygen gradients in the kidney and showed widespread variations within similar regions. By stepping through a kidney at 10 micron steps, they found that 90% of adjacent readings varied between -12 and +11 torr (-1.60 kPa to 1.47 kPa) from the previous, and that the variation could be as great as -35 to +49 torr (-4.67 kPa to 6.53 kPa). In the past, the assumption has been that reductions in oxygen consumption arise entirely from renally-derived cells. In particular, it is

known that vascular cells are highly metabolically active (Intaglietta, M. *et al.*, 1996). Nitric oxide (NO) is formed by the oxidation of L-arginine under the control of NO synthase and the expenditure of NADPH and was first isolated in the vascular endothelium (originally named EDRF – the endothelial-derived relaxant factor).

The Clark electrode consumes oxygen generating a current that is determined by the oxygen concentration gradient between the electrode metal surface and the medium. This oxygen gradient is located in the boundary layer near the electrode surface, thus any movement of the electrode (or medium such as pulsatile flow), or change of medium oxygen concentration, requires that a new stable boundary/diffusion layer be formed before an interpretable oxygen concentration measurement can be made. It is particularly difficult to establish a stable boundary layer at the tip of a microelectrode, which led Whalen *et al* (Whalen, W.J. *et al.*, 1967) to recess the metal surface from the glass micropipette tip, and to fill the tip with collodion, so that a motion free layer is always in contact with the metal. These electrodes have low drift and oxygen consumption (of the order of 10^{-6} μl/min) but still have a time constant of the order of 1 second making real time monitoring less reliable.

The location of the microelectrode tip defines the centre of the volume whose surface pO_2 is averaged by the electrode current; therefore, if the sampling volume includes a portion of an arteriole, the current generated will be higher. Therefore, the oxygen measurement will reflect, in part, the presence of this high oxygen concentration region, even though the oxygen tension at the very

tip of the electrode may be significantly lower. The volume of sampling is not specifically modelled in most analyses. By sampling from a wider area (such as performed by the OxyLite), the effects of significant changes because of the proximity of vessels is reduced. Schneiderman and Goldstick (Schneiderman, G. and Goldstick, T.K., 1978) reported the configuration of the oxygen field around polargraphic electrode tips with different ratios of electrode recession (l) to electrode diameter (d). They showed that the shape of field is strongly dependent upon the ratio l/d for shallow depths of recession (smaller than the electrode diameter) but a recess length-to-cathode diameter ratio of greater than 10 was found to give a negligible stirring artefact, a negligible measurement error, and a rapid response. Therefore, a precise interpretation of the data on tissue oxygen gradient measurement with microelectrodes cannot be made unless the l/d ratio is known.

It has been assumed until recently that transfer of oxygen from blood to tissue only occurred to a significant degree in the capillaries. The concept that capillaries are the sole suppliers of oxygen to the tissue continues to be taught and arose from work by Krogh and Erlangen in 1918, who described the "Krogh cylinder model" (Krogh, A., 1918). With the use of the capillary network of skeletal muscle as an example, this mathematical model describes how oxygen is delivered by a single capillary of a uniform array of capillaries to a surrounding tissue cylinder. At the time this model was developed there were no methods available to measure oxygen levels in the microcirculatory system. The model therefore assumed that all oxygen exchange takes place at the

capillary, with the PO_2 at the entrance being that in the large artery and the PO_2 at the exit being that in the large vein.

This model does not however predict tissue oxygenation (Popel, A.S., 1989). Experimental data have suggested that the large vessels themselves consume oxygen (Popel, A.S. *et al.*, 1989) and that studies into intra-capillary oxygen have suggested that the blood has already desaturated to almost 70% by the time it flows through the capillaries. Torres Filho and colleagues (Torres Filho, I. *et al.*, 1996) found that intraluminal pO_2 in 64.3μm Al arterioles of a hamster skin fold was 7.7 ± 1 kPa while A4 terminal arterioles had pO_2 values of 4.64 ± 0.9 kPa. This is already much lower than the expected arterial pO_2 of approximately 10 kPa. Furthermore, small venules do not exhibit any correlation between pO_2 and order or branching or diameter and have an average pO_2 of 3.9 ± 1.2 kPa.

Duling and Berne (Duling, B.R. and Berne, R.M., 1970) used Whalen-type polargraphic microelectrodes (2-6 μm tip diameter, (Whalen, W.J. *et al.*, 1967)) and estimated blood PO_2 by placing the microelectrode on the external wall of the arterioles of their hamster cheek pouch preparation. The PO_2 of arterioles of 60-100 μm diameter was 4.7 ± 0.5 kPa (67 ± 8% estimated HbO_2 saturation, assuming intraluminal and periarteriolar PO_2 are similar) and fell to 3.2 ± 0.4 kPa (44 ± 6% saturation) in terminal arterioles of 10-20 μm diameter, 2.9 ± 0.4 kPa (33 ± 6% saturation) in arterial capillaries, and 1.1 ± 0.3 kPa in the tissues. These experiments were similar when using a suffusion solution equilibrated at a PO_2 of 5.2 kPa or when animals breathed room air. When the hamster

breathed 95% oxygen, the PO_2 values increased to a greater degree in the proximal vessels, being 20.3 ± 1.9 kPa (100% saturation) in the 60-100 μm arterioles and 4.9 ± 1.2 kPa (73 ± 18% saturation) in arterial capillaries. In a subsequent study also using the hamster cheek pouch model, Duling (Duling, B.R., 1972) reported peri-arteriolar PO_2 values of 6.4 ± 0.3 kPa in 30-50 μm arterioles, 5.2 ± 0.3 kPa in 10-20 μm arterioles, 4.0 ± 0.4 kPa in 7-12 μm arterioles, and 2.4 ± 0.3 kPa in 4-6 μm arterioles.

Tsai and Intaglietta (Tsai, A.G. *et al.*, 1998) proposed that the vascular endothelium acts as a sink for oxygen, causing a large step-down from the higher oxygen concentrations found in blood to the low oxygen concentrations found in the tissues. This may explain, in part, the findings that PtO_2 is not as high as first reported by other authors (Brezis, M. *et al.*, 1994b), (Liss, P. *et al.*, 1997b).

Traditionally, the medulla is considered to be operating on 'the verge of hypoxia' (Heyman, S.N. *et al.*, 1997). However, I report much lower values of tissue pO_2 at the corticomedullary junction. This region also appeared to be the most resistant to the effects of blood withdrawal, both in terms of tissue pO_2 and microvascular flow, suggesting a relative intra-renal redistribution of blood flow away from the cortex and towards the deeper regions.

The logic that the medulla lives 'at the edge of anoxia' (Heyman, S.N. *et al.*, 1997) and leaves it vulnerable to any insult, is evolutionarily unsound. Varying pO_2 values have been found in the kidney. Indeed, the lowest published values

are found in an awake mouse model with little intervention (James, P.E. *et al.*, 1997). A family of hypoxia-inducible transcription factors (HIF) have been identified as mediators of transcriptional responses to hypoxia, which include the regulation of erythropoietin, metabolic adaptation, vascular tone, and neoangiogenesis. *In vitro*, the oxygen-regulated subunits HIF-1alpha and -2alpha are expressed in inverse relationship to oxygen tensions in every cell line investigated to date. The characteristics and functional significance of the HIF response *in vivo* are largely unknown. Studies using HIF as a marker of anoxia failed to show an increase in distribution in the medulla (Manotham, K. *et al.*, 2005). HIF gene expression has also been used to look at tissue oxygen gradients within the regions of the kidney. Rosenberger *et al* (Rosenberger, C. *et al.*, 2002) found that within a given region of the kidney, the distance a cell finds itself from a blood vessel determines whether or not it upregulates HIF expression in response to hypoxia, with those cells closest to the vascular bundles not being 'switched on'.

The wealth of data available to those who choose to investigate renal PtO_2 is overwhelming and frequently contradictory. In the 1990s Epstein's group published widely on renal PtO_2 under various conditions but came to some conclusions that are directly contradicted by those described here. Closer inspection of their conclusions reveals some interesting differences, both in experimental technique and in interpretation of results. Their work arose from data obtained in the 1980s in isolated kidney preparations which proposed that PtO_2 was higher in the cortex (Brezis, M. *et al.*, 1984a), (Brezis, M. *et al.*, 1984d). We suggest that in setting up an isolated kidney preparation, the

authors may have induced an ischaemia-reperfusion injury which would explain why the high cortical values are similar to those found in our experiments.

Their two major papers on this animal model (Brezis, M. *et al.*, 1994b), (Brezis, M. *et al.*, 1994a), formed the cornerstone of all subsequent *in vivo* work coming from the group. They did however use large numbers of animals to reduce the wide variation of results obtained. Baseline control readings differed between each paper by more than 10%. This may have been due to inadequate resuscitation with saline containing fluids. They openly explain that their probes, which were also very small and therefore highly specific, were moved *'2-3 mm until a good reading was obtained.'* This could mean that the depth of their cortical results could have ranged from 2-5 mm below the kidney surface and at levels that were unlikely to be measuring from the cortex.

5.3 Vulnerability of the corticomedullary junction

Much of the published literature has concentrated on the vulnerability of the medulla during various insults including radiocontrast (Liss, P. *et al.*, 1996), (Brezis, M. *et al.*, 1991). This has detracted from authors who have suggested that the juxtaglomerular apparatus, much of which is located in CMJ may be damaged, particularly in the hypertensive kidney (Adler, S. and Huang, H., 2002), (Roald, A.B. *et al.*, 2002), (Wilcox, C.S., 2002), (Wilcox, C.S., 2003).

Although the medulla is supplied by 'second-hand' blood, the high oxygen demand in the CMJ also makes an adequate oxygen supply important in this region. Much of the tubular function and juxtaglomerular apparatus are situated within this region and both are vital to normal renal function. Indeed, the term 'acute renal success' (Thurau, K. and Boylan, J.W., 1976) was coined in context to the tubuloglomerular interaction.

Decreased oxygen consumption in the cortex following exsanguination/resuscitation may point to the importance of the vasculature rather than renally derived cells. The pathophysiology of ischaemic acute renal failure (ARF) involves a complex interplay between renal haemodynamics, tubular and endothelial cell injury, and inflammatory processes (Molitoris, B.A. and Sutton, T.A., 2004). Following prolonged ischaemia in the rat (60 minutes), peritubular capillaries underwent permanent damage (Basile, D.P. *et al.*, 2001). The number of vessels in the outer stripe of the medulla also decreased and tubulointerstitial dysfunction occurred. Leukocyte activation following ischaemia causes an increase in reactive oxygen species (ROS) in the kidney (Willinger, C.C. *et al.*, 1992). ROS are known to inhibit mitochondrial function (Brealey, D. *et al.*, 2004), (Davies, N.A. *et al.*, 2003), and cause further blockage of the renal microvasculature (Linas, S.L. *et al.*, 1988). Similar responses may also be at play when decreases in intra-renal flow were noted during a septic insult; however, further study is desirable to fully elucidate mechanisms underlying sepsis-induced renal failure.

5.4 Future studies

This thesis has touched upon many mechanisms that affect renal oxygen consumption. It is hoped that this model may serve as a platform from which to study the effects of ischaemia/reperfusion, pre-conditioning, sepsis, drugs or any other physiological disturbance.

I believe that the physiological fragility of the rat under anaesthesia and its detection by rises in PtO_2 strengthen the model and reduce the possibility that the effects of surgical preparation are being detected rather than the intervention. Unfortunately, this fragility did not allow contemporaneous study of whole organ flows along side PtO_2 and intra-renal flow. The extra time needed and difficulty involved in this additional instrumentation, and possibly the extra surgical stress, caused irreversible tissue oxygen changes in pilot studies. Attempts were also made to collect urine from the renal pelvis by cannulating the ureter. Although urine was collected from the bladder, there was a delay in the appearance of urine for analysis of renal function. This did not allow contemporaneous measurement of renal function with the rapid changes in PtO_2. Furthermore, with the extra surgery involved with ureteric cannulation, there were similar rises in tissue oxygen. Linking changes in PtO_2 with changes in function would enhance this model. Given the problems outlined above, it may that a technique without extra surgery such as micro-puncture or micro-dialysis would enhance the results obtained.

Although it was not the intention of these studies to investigate the impact of the capsule on renal metabolism, my findings suggest alterations in oxygen consumption are brought about through its removal. Although I have speculated that this is probably due to the extra surgical stress induced by manipulation of the kidney, it may be that disruption of the sympathetic input to the kidney mediated through the capsule is important. I would therefore also like to investigate the effects of sympathetic agonists and antagonists on our model.

Whether with or without the capsule, the renal response to sympathetic agonists remains unclear and I feel that this model may contribute some useful data. 'Renal dose' dopamine continues to stimulate much research interest and use of the specific dopamine 1 receptor (DA_1) agonist, fenoldopam, (or similar) may allow the study of dopamine receptor mediation. Fenoldopam preferentially increases renal medullary blood flow (Singer, I. and Epstein, M., 1998) and provides the basis for theoretical protection against radiocontrast-induced acute renal failure. Interestingly, conflicting data exist regarding the effectiveness of fenoldopam to protect against radiocontrast-induced acute renal failure with the only blinded, randomised, trial (Stone, G.W. *et al.*, 2003) failing to find a benefit despite anecdotal evidence (Hunter, D.W. *et al.*, 2001), (Madyoon, H. *et al.*, 2001). The use of fenoldopam derives from theoretical evidence that the medulla is the source of renal failure (Heyman, S.N. *et al.*, 1997). My research suggests that the CMJ may have a more significant role to play and further study could dissect out the site of dysfunction.

There remains reluctance amongst some intensive care physicians to use norepinephrine when faced with a septic patient for fear of inducing intra-renal vasospasm and exacerbating renal failure. This is despite evidence (Bellomo, R. and Giantomasso, D.D., 2001) that norepinephrine is not harmful and may be beneficial when used in conjunction with the fluid-replete circulation. This model may contribute to dispel (or confirm) the theory that norepinephrine may be harmful to the kidney.

Finally, this model could facilitate further investigations into the pathophysiological mechanisms invoked during the various challenges. For example, specific nitric oxide synthase inhibitors could be used during an endotoxin infusion or during use of enalaprilat to investigate the role of NO during these responses.

I therefore present a model measuring renal tissue oxygen in the rat matched with intra-renal flows that change in a predicable manner when exposed to a variety of pharmacological and physiological challenges. I have uniquely demonstrated *in vivo* control of cellular respiration in this rat renal model. Like others, I found that the region containing the juxtamedullary apparatus, the corticomedullary junction, was the most affected by a circulatory insult. I also confirmed these changes by showing a decrease in oxygen consumption following sacrifice of a previously healthy animal. My results differ from many landmark studies frequently quoted in the literature, possibly relating to the methodological differences described above. This new model could serve as a base from which to perform further studies.

6 References

1. Adler S, Huang H (2002). Impaired regulation of renal oxygen consumption in spontaneously hypertensive rats. *J Am Soc Nephrol.***13:**1788-1794.

2. Adler S, Huang H, Loke KE et al (2001). Endothelial nitric oxide synthase plays an essential role in regulation of renal oxygen consumption by NO. *Am J Physiol Renal Physiol.***280:**F838-F843.

3. Agmon Y, Brezis M (1993). Effects of nonsteroidal anti-inflammatory drugs upon intrarenal blood flow: selective medullary hypoperfusion. *Exp Nephrol.***1:**357-363.

4. Agmon Y, Dinour D, Brezis M (1993). Disparate effects of adenosine A1- and A2-receptor agonists on intrarenal blood flow. *Am J Physiol.***265:**F802-F806.

5. Agmon Y, Peleg H, Greenfeld Z, Rosen S, Brezis M (1994). Nitric oxide and prostanoids protect the renal outer medulla from radiocontrast toxicity in the rat. *J Clin Invest.***94:**1069-1075.

6. Anwer MS, Clayton LM (1985). Role of extracellular Ca2+ in hepatic bile formation and taurocholate transport. *Am J Physiol.***249:**G711-G718.

7. Aperia AC (1969). The influence of arterial PO2 on renal tissue PO2. *Acta Physiol Scand.***75:**353-359.

8. Asher EF, Garrison RN, Ratcliffe DJ, Fry DE (1983). Endotoxin, cellular function, and nutrient blood flow. *Arch Surg.***118:**441-445.

9. Atkins JL, Lankford SP (1991). Changes in cytochrome oxidation in outer and inner stripes of outer medulla. *Am J Physiol.***261:**F849-F857.

10. Aukland K, Wolgast M (1968). Effect of hemorrhage and retransfusion on intrarenal distribution of blood flow in dogs. *J Clin Invest.***47:**488-501.

11. Babcock GT, Wikstrom M (1992). Oxygen activation and the conservation of energy in cell respiration. *Nature.***356:**301-309.

12. Bachmann S, Bosse HM, Mundel P (1995). Topography of nitric oxide synthesis by localizing constitutive NO synthases in mammalian kidney. *Am J Physiol.***268:**F885-F898.

13. Basile DP, Donohoe D, Roethe K, Osborn JL (2001). Renal ischemic injury results in permanent damage to peritubular capillaries and influences long-term function. *Am J Physiol Renal Physiol.***281:**F887-F899.

14. Baumgartl H, Zimelka W, Lubbers DW (2002). Evaluation of PO(2) profiles to describe the oxygen pressure field within the tissue. *Comp Biochem Physiol A Mol Integr Physiol.***132:**75-85.

15. Bellomo R, Chapman M, Finfer S, Hickling K, Myburgh J (2000). Low-dose dopamine in patients with early renal dysfunction: a placebo-controlled randomised trial. Australian and New Zealand Intensive Care Society (ANZICS) Clinical Trials Group. *Lancet.***356:**2139-2143.

16. Bellomo R, Giantomasso DD (2001). Noradrenaline and the kidney: friends or foes? *Crit Care.***5:**294-298.

17. Beltran B, Mathur A, Duchen MR, Erusalimsky JD, Moncada S (2000). The effect of nitric oxide on cell respiration: A key to understanding its role in cell survival or death. *Proc Natl Acad Sci U S A.***97:**14602-14607.

18. Blinks LR, Skow RK (1938). The Time Course of Photosynthesis as Shown by a Rapid Electrode Method for Oxygen. *Proc Nat Acad Sci.***24:**420-427.

19. Boekstegers P, Weidenhofer S, Kapsner T, Werdan K (1994). Skeletal muscle partial pressure of oxygen in patients with sepsis. *Crit Care Med.***22:**640-650.

20. Boveris A, D'Amico G, Lores-Arnaiz S, Costa LE (2003). Enalapril increases mitochondrial nitric oxide synthase activity in heart and liver. *Antioxid Redox Signal*.**5:**691-697.

21. Brealey D, Brand M, Hargreaves I et al (2002). Association between mitochondrial dysfunction and severity and outcome of septic shock. *Lancet*.**360:**219-223.

22. Brealey D, Karyampudi S, Jacques TS et al (2004). Mitochondrial dysfunction in a long-term rodent model of sepsis and organ failure. *Am J Physiol Regul Integr Comp Physiol*.**286:**R491-R497.

23. Brealey D, Singer M (1999). Mitochondrial dysfunction in sepsis. In: *Mitochondria and cell death.* Brown GC, Nicholls DG, Cooper CE (editors). London: Portland Press; pp. 149-166.

24. Breen D, Bihari D (1998). Acute renal failure as a part of multiple organ failure: the slippery slope of critical illness. *Kidney Int Suppl*.**66:**S25-S33.

25. Brezis M, Agmon Y, Epstein FH (1994a). Determinants of intrarenal oxygenation. I. Effects of diuretics. *Am J Physiol*.**267:**F1059-F1062.

26. Brezis M, Heyman SN, Dinour D, Epstein FH, Rosen S (1991). Role of nitric oxide in renal medullary oxygenation. Studies in isolated and intact rat kidneys. *J Clin Invest*.**88:**390-395.

27. Brezis M, Heyman SN, Epstein FH (1994b). Determinants of intrarenal oxygenation. II. Hemodynamic effects. *Am J Physiol.***267:**F1063-F1068.

28. Brezis M, Rosen S (1995). Hypoxia of the renal medulla--its implications for disease. *N Engl J Med.***332:**647-655.

29. Brezis M, Rosen S, Silva P, Epstein FH (1984a). Renal ischemia: a new perspective. *Kidney Int.***26:**375-383.

30. Brezis M, Rosen S, Silva P, Epstein FH (1984b). Selective anoxic injury to thick ascending limb: an anginal syndrome of the renal medulla? *Adv Exp Med Biol.***180:**239-249.

31. Brezis M, Rosen S, Silva P, Epstein FH (1984c). Selective vulnerability of the medullary thick ascending limb to anoxia in the isolated perfused rat kidney. *J Clin Invest.***73:**182-190.

32. Brezis M, Rosen S, Silva P, Epstein FH (1984d). Selective vulnerability of the medullary thick ascending limb to anoxia in the isolated perfused rat kidney. *J Clin Invest.***73:**182-190.

33. Brezis M, Rosen S, Silva P, Epstein FH (1984e). Transport activity modifies thick ascending limb damage in the isolated perfused kidney. *Kidney Int.***25:**65-72.

34. Brezis M, Shanley P, Silva P et al (1985). Disparate mechanisms for hypoxic cell injury in different nephron segments. Studies in the isolated perfused rat kidney. *J Clin Invest.***76:**1796-1806.

35. Brown GC (2000). Nitric oxide as a competitive inhibitor of oxygen consumption in the mitochondrial respiratory chain. *Acta Physiol Scand.***168:**667-674.

36. Brown GC (2001). Regulation of mitochondrial respiration by nitric oxide inhibition of cytochrome c oxidase. *Biochim Biophys Acta.***1504:**46-57.

37. Brown GC, Bolanos JP, Heales SJ, Clark JB (1995). Nitric oxide produced by activated astrocytes rapidly and reversibly inhibits cellular respiration. *Neurosci Lett.***193:**201-204.

38. Brown SD, Gutierrez G (1996). Does gastric tonometry work? Yes. *Crit Care Clin.***12:**569-585.

39. Brudvig GW, Stevens TH, Chan SI (1980). Reactions of nitric oxide with cytochrome c oxidase. *Biochemistry.***19:**5275-5285.

40. Brun C, MUNCK O (1957). Lesions of the kidney in acute renal failure following shock. *Lancet.***272:**603-607.

41. Butler PJ, Jones DR (1997). Physiology of diving of birds and mammals. *Physiol Rev.***77:**837-899.

42. Camacho MT, Totapally BR, Torbati D, Wolfsdorf J (2001). Pulmonary and extrapulmonary effects of increased colloid osmotic pressure during endotoxemia in rats. *Chest.***120:**1655-1662.

43. Carriere S, Daigneault B (1970). Effect of retransfusion after hemorrhagic hypotension on intrarenal distribution of blood flow in dogs. *J Clin Invest.***49:**2205-2217.

44. Clark LCJ, Lyons C (1962). Electrode systems for continuous monitoring in cardiovascular surgery. *Ann N Y Acad Sci.***102:**29-45.

45. Clementi E, Brown GC, Feelisch M, Moncada S (1998). Persistent inhibition of cell respiration by nitric oxide: crucial role of S-nitrosylation of mitochondrial complex I and protective action of glutathione. *Proc Natl Acad Sci U S A.***95:**7631-7636.

46. Cope DK, Impastato WK, Cohen MV, Downey JM (1997). Volatile anesthetics protect the ischemic rabbit myocardium from infarction. *Anesthesiology.***86:**699-709.

47. Cox BF, Brody MJ (1989). Mechanisms of respiration-induced changes in vasomotor control exerted by rostral ventrolateral medulla. *Am J Physiol.***257:**R626-R634.

48. Cronenwett JL, Lindenauer SM (1978). Distribution of intrarenal blood flow during bacterial sepsis. *J Surg Res.***24:**132-141.

49. Cunarro JA, Weiner MW (1978). Effects of ethacrynic acid and furosemide on respiration of isolated kidney tubules: the role of ion transport and the source of metabolic energy. *J Pharmacol Exp Ther.***206:**198-206.

50. Davies NA, Cooper CE, Stidwill R, Singer M (2003). Inhibition of mitochondrial respiration during early stage sepsis. *Adv Exp Med Biol.***530:**725-736.

51. Davis RW, Kanatous SB (1999). Convective oxygen transport and tissue oxygen consumption in Weddell seals during aerobic dives. *J Exp Biol.***202:**1091-1113.

52. De Hert SG, Turani F, Mathur S, Stowe DF (2005). Cardioprotection with volatile anesthetics: mechanisms and clinical implications. *Anesth Analg.***100:**1584-1593.

53. de Mendonca A, Vincent JL, Suter PM et al (2000). Acute renal failure in the ICU: risk factors and outcome evaluated by the SOFA score. *Intensive Care Med.***26:**915-921.

54. Dikshit K, Vyden JK, Forrester JS, Chatterjee K, Prakash R, Swan HJ (1973). Renal and extrarenal hemodynamic effects of furosemide in

congestive heart failure after acute myocardial infarction. *N Engl J Med.***288:**1087-1090.

55. Dobrowolski L, dzynska B, Sadowski J (2000). Differential effect of frusemide on renal medullary and cortical blood flow in the anaesthetised rat. *Exp Physiol.***85:**783-789.

56. Dorrington KL, Talbot NP (2004). Human pulmonary vascular responses to hypoxia and hypercapnia. *Pflugers Arch.***449:**1-15.

57. Dukacz SA, Kline RL (1999). Differing effects of enalapril and losartan on renal medullary blood flow and renal interstitial hydrostatic pressure in spontaneously hypertensive rats. *J Hypertens.***17:**1345-1352.

58. Duling BR (1972). Microvascular responses to alterations in oxygen tension. *Circ Res.***31:**481-489.

59. Duling BR, Berne RM (1970). Longitudinal gradients in periarteriolar oxygen tension. A possible mechanism for the participation of oxygen in local regulation of blood flow. *Circ Res.***27:**669-678.

60. Eknoyan G, Sawa H, Hyde S, III, Wood JM, Schwartz A, Suki W (1975). Effect of diuretics on oxidative phosphorylation of dog kidney mitochondria. *J Pharmacol Exp Ther.***194:**614-623.

61. Epstein FH, Prasad P (2000). Effects of furosemide on medullary oxygenation in younger and older subjects. *Kidney Int.***57:**2080-2083.

62. Esson ML, Schrier RW (2002). Diagnosis and treatment of acute tubular necrosis. *Ann Intern Med.***137:**744-752.

63. Evans RG, Eppel GA, Anderson WP, Denton KM (2004). Mechanisms underlying the differential control of blood flow in the renal medulla and cortex. *J Hypertens.***22:**1439-1451.

64. Fatt I (1964). An Ultramicro Oxygen Electrode. *J Appl Physiol.***19:**326-329.

65. Finckh ES, JEREMY D, WHYTE HM (1962). Structural renal damage and its relatin to clinical features in acute oliguric renal failure. *Q J Med.***31:**429-446.

66. Flemming B, Seeliger E, Wronski T, Steer K, Arenz N, Persson PB (2000). Oxygen and renal hemodynamics in the conscious rat. *J Am Soc Nephrol.***11:**18-24.

67. Freeman BA, Crapo JD (1981). Hyperoxia increases oxygen radical production in rat lungs and lung mitochondria. *J Biol Chem.***256:**10986-10992.

68. Galley HF (2000a). Can acute renal failure be prevented? *J R Coll Surg Edinb.***45:**44-50.

69. Galley HF (2000b). Renal-dose dopamine: will the message now get through? *Lancet.***356:**2112-2113.

70. Garrison RN, Ratcliffe DJ, Fry DE (1982). The effects of peritonitis on murine renal mitochondria. *Adv Shock Res.***7:**71-76.

71. Garvin JL, Hong NJ (1999). Nitric oxide inhibits sodium/hydrogen exchange activity in the thick ascending limb. *Am J Physiol.***277:**F377-F382.

72. Guerin C, Girard R, Selli JM, Ayzac L (2002). Intermittent versus continuous renal replacement therapy for acute renal failure in intensive care units: results from a multicenter prospective epidemiological survey. *Intensive Care Med.***28:**1411-1418.

73. Gunther H, Aumuller G, Kunke S, Vaupel P, Thews G (1974). [The oxygen supply of the kidney. I. Distribution of O2 partial pressures in the rat kidney under normal conditions (author's transl)]. *Res Exp Med (Berl).***163:**251-264.

74. Guppy M, Hill RD, Schneider RC et al (1986). Microcomputer-assisted metabolic studies of voluntary diving of Weddell seals. *The American Journal Of Physiology.***250:**R175-R187.

75. Gutierrez G, Brown SD (1995). Gastric tonometry: a new monitoring modality in the intensive care unit. *J Intensive Care Med.***10:**34-44.

76. Guyton AC, Hall JE (1998). Textbook of Medical Physiology. 10 edition. WB Saunders.

77. Haessler R, Kuzume K, Chien GL, Wolff RA, Davis RF, Van Winkle DM (1994). Anaesthetics alter the magnitude of infarct limitation by ischaemic preconditioning. *Cardiovasc Res.***28:**1574-1580.

78. Heyman SN, Brezis M, Greenfeld Z, Rosen S (1989). Protective role of furosemide and saline in radiocontrast-induced acute renal failure in the rat. *Am J Kidney Dis.***14:**377-385.

79. Heyman SN, Darmon D, Goldfarb M et al (2000a). Endotoxin-induced renal failure. i. A role for altered renal microcirculation. *Exp Nephrol.***8:**266-274.

80. Heyman SN, Fuchs S, Brezis M (1995). The role of medullary ischemia in acute renal failure. *New Horiz.***3:**597-607.

81. Heyman SN, Rosen S, Brezis M (1997). The renal medulla: life at the edge of anoxia. *Blood Purif.***15:**232-242.

82. Heyman SN, Rosen S, Darmon D et al (2000b). Endotoxin-induced renal failure. ii. A role for tubular hypoxic damage. *Exp Nephrol.***8:**275-282.

83. Heyman SN, Rosen S, Epstein FH, Spokes K, Brezis ML (1994). Loop diuretics reduce hypoxic damage to proximal tubules of the isolated perfused rat kidney. *Kidney Int.***45:**981-985.

84. Hochachka PW (1980). Living Without Oxygen. **Harvard Univ. Press, Cambridge.**

85. Hollenberg SM, Ahrens TS, Annane D et al (2004). Practice parameters for hemodynamic support of sepsis in adult patients: 2004 update. *Crit Care Med.***32:**1928-1948.

86. Holmes CL, Patel BM, Russell JA, Walley KR (2001). Physiology of vasopressin relevant to management of septic shock. *Chest.***120:**989-1002.

87. Holmes CL, Walley KR (2003). Bad medicine: low-dose dopamine in the ICU. *Chest.***123:**1266-1275.

88. Hotchkiss RS, Swanson PE, Freeman BD et al (1999). Apoptotic cell death in patients with sepsis, shock, and multiple organ dysfunction. *Crit Care Med.***27:**1230-1251.

89. Hunter DW, Chamsuddin A, Bjarnason H, Kowalik K (2001). Preventing contrast-induced nephropathy with fenoldopam. *Tech Vasc Interv Radiol.***4:**53-56.

90. Ichihara A, Navar LG (1999). Neuronal NOS contributes to biphasic autoregulatory response during enhanced TGF activity. *Am J Physiol.***277:**F113-F120.

91. Intaglietta M, Johnson PC, Winslow RM (1996). Microvascular and tissue oxygen distribution. *Cardiovasc Res.***32:**632-643.

92. Jakobsson A, Nilsson GE (1993). Prediction of sampling depth and photon pathlength in laser Doppler flowmetry. *Med Biol Eng Comput.***31:**301-307.

93. James PE, Bacic G, Grinberg OY et al (1996). Endotoxin-induced changes in intrarenal pO2, measured by in vivo electron paramagnetic resonance oximetry and magnetic resonance imaging. *Free Radic Biol Med.***21:**25-34.

94. James PE, Grinberg OY, Goda F, Panz T, O'Hara JA, Swartz HM (1997). Gloxy: an oxygen-sensitive coal for accurate measurement of low oxygen tensions in biological systems. *Magn Reson Med.***38:**48-58.

95. James PE, Jackson SK, Grinberg OY, Swartz HM (1995). The effects of endotoxin on oxygen consumption of various cell types in vitro: an EPR oximetry study. *Free Radic Biol Med.***18:**641-647.

96. Jones D, Bellomo R (2005). Renal-dose dopamine: from hypothesis to paradigm to dogma to myth and, finally, superstition? *J Intensive Care Med.***20:**199-211.

97. Kellum JA, Angus DC, Johnson JP et al (2002). Continuous versus intermittent renal replacement therapy: a meta-analysis. *Intensive Care Med.***28:**29-37.

98. Khan RZ, Badr KF (1999). Endotoxin and renal function: perspectives to the understanding of septic acute renal failure and toxic shock. *Nephrol Dial Transplant.***14:**814-818.

99. King CJ, Tytgat S, Delude RL, Fink MP (1999). Ileal mucosal oxygen consumption is decreased in endotoxemic rats but is restored toward normal by treatment with aminoguanidine. *Crit Care Med.***27:**2518-2524.

100. Koivisto A, Pittner J, Froelich M, Persson AE (1999). Oxygen-dependent inhibition of respiration in isolated renal tubules by nitric oxide. *Kidney Int.***55:**2368-2375.

101. Komune S, Huangfu M, Snow JB, Jr. (1985). A possible site of production of the negative endocochlear DC potential. *Hear Res.***18:**153-158.

102. Korkeila M, Ruokonen E, Takala J (2000). Costs of care, long-term prognosis and quality of life in patients requiring renal replacement therapy during intensive care. *Intensive Care Med.***26:**1824-1831.

103. Kotajima F, Meadows G, Morrell M, Corfield D (2005). Cerebral blood flow changes associated with fluctuations in alpha and theta rhythm during sleep onset in humans. *J Physiol.*

104. Krogh A (1918). The number and distribution of capillaries in muscle with the calculation of the pressure necessary for supplying the tissue. *J Physiol.***52:**409-515.

105. Kwan MR, Hunt TK (1973). Continuous tissue oxygen tension measurements during acute blood loss. *J Surg Res.***14:**420-425.

106. Leichtweiss HP, Lubbers DW, Weiss C, Baumgartl H, Reschke W (1969). The oxygen supply of the rat kidney: measurements of intrarenal pO2. *Pflugers Arch.***309:**328-349.

107. Levy EM, Viscoli CM, Horwitz RI (1996). The effect of acute renal failure on mortality. A cohort analysis. *JAMA.***275:**1489-1494.

108. Liano F, Pascual J (1996). Epidemiology of acute renal failure: a prospective, multicenter, community-based study. Madrid Acute Renal Failure Study Group. *Kidney Int.***50:**811-818.

109. Lien B, Norstein J, Salerud EG, Kvernebo K, Flatmark A (1992). Renal microvascular perfusion evaluated by single fibre laser Doppler flowmetry. *Int J Microcirc Clin Exp.***11:**307-317.

110. Linas SL, Shanley PF, Whittenburg D, Berger E, Repine JE (1988). Neutrophils accentuate ischemia-reperfusion injury in isolated perfused rat kidneys. *Am J Physiol.***255:**F728-F735.

111. Liss P (1997). Effects of contrast media on renal microcirculation and oxygen tension. An experimental study in the rat. *Acta Radiol Suppl.***409:**1-29.

112. Liss P, Nygren A, Erikson U, Ulfendahl HR (1998). Injection of low and iso-osmolar contrast medium decreases oxygen tension in the renal medulla. *Kidney Int.***53:**698-702.

113. Liss P, Nygren A, Hansell P (1999a). Hypoperfusion in the renal outer medulla after injection of contrast media in rats. *Acta Radiol.***40:**521-527.

114. Liss P, Nygren A, Olsson U, Ulfendahl HR, Erikson U (1996). Effects of contrast media and mannitol on renal medullary blood flow and red cell aggregation in the rat kidney. *Kidney Int.***49:**1268-1275.

115. Liss P, Nygren A, Revsbech NP, Ulfendahl HR (1997a). Intrarenal oxygen tension measured by a modified clark electrode at normal and

low blood pressure and after injection of x-ray contrast media. *Pflugers Arch.***434:**705-711.

116. Liss P, Nygren A, Revsbech NP, Ulfendahl HR (1997b). Measurements of oxygen tension in the rat kidney after contrast media using an oxygen microelectrode with a guard cathode. *Adv Exp Med Biol.***411:**569-576.

117. Liss P, Nygren A, Ulfendahl HR, Erikson U (1999b). Effect of furosemide or mannitol before injection of a non-ionic contrast medium on intrarenal oxygen tension. *Adv Exp Med Biol.***471:**353-359.

118. Lote CJ (2000). Principles of Renal Physiology. The Hague, Netherlands: Kluwer Academic Publishers.

119. Lubbers DW, Baumgartl H (1997). Heterogeneities and profiles of oxygen pressure in brain and kidney as examples of the pO2 distribution in the living tissue. *Kidney Int.***51:**372-380.

120. Madyoon H, Croushore L, Weaver D, Mathur V (2001). Use of fenoldopam to prevent radiocontrast nephropathy in high-risk patients. *Catheter Cardiovasc Interv.***53:**341-345.

121. Majid DS, Navar LG (2001). Nitric oxide in the control of renal hemodynamics and excretory function. *Am J Hypertens.***14:**74S-82S.

122. Manotham K, Tanaka T, Ohse T et al (2005). A biologic role of HIF-1 in the renal medulla. *Kidney Int.***67:**1428-1439.

123. Manuel MA, Weiner MW (1976). Effects of ethacrynic acid and furosemide on isolated rat kidney mitochondria: inhibition of electron transport in the region of phosphorylation site II. *J Pharmacol Exp Ther.***198:**209-221.

124. Marik PE (1993). Low-dose dopamine in critically ill oliguric patients: the influence of the renin-angiotensin system. *Heart Lung.***22:**171-175.

125. Marik PE (2004). Renal dose norepinephrine! *Chest.***126:**335-337.

126. Mattson DL, Lu S, Roman RJ, Cowley AW, Jr. (1993). Relationship between renal perfusion pressure and blood flow in different regions of the kidney. *Am J Physiol.***264:**R578-R583.

127. McNaught KS, Brown GC (1998). Nitric oxide causes glutamate release from brain synaptosomes. *J Neurochem.***70:**1541-1546.

128. Mela L (1981). Direct and indirect effects of endotoxin on mitochondrial function. *Prog Clin Biol Res.***62:**15-21.

129. Mela L, Miller LD (1983). Efficacy of glucocorticoids in preventing mitochondrial metabolic failure in endotoxemia. *Circ Shock.***10:**371-381.

130. Michel F, Duriez M, Levy BI, Boulanger CM (2004). Minimally invasive, in vivo exploration of mouse small artery reactivity. *J Cardiovasc Pharmacol.***43:**271-275.

131. Millar CG, Thiemermann C (1997). Intrarenal haemodynamics and renal dysfunction in endotoxaemia: effects of nitric oxide synthase inhibition. *Br J Pharmacol.***121:**1824-1830.

132. Miller RD (2004). Anesthesia. 6 edition. London: Churchill Livingstone.

133. Molitoris BA, Sutton TA (2004). Endothelial injury and dysfunction: role in the extension phase of acute renal failure. *Kidney Int.***66:**496-499.

134. Nauntofte B, Poulsen JH (1986). Effects of Ca2+ and furosemide on Cl-transport and O2 uptake in rat parotid acini. *Am J Physiol.***251:**C175-C185.

135. Nelimarkka O (1984). Renal oxygen and lactate metabolism in hemorrhagic shock. An experimental study. *Acta Chir Scand Suppl.***518:**1-44.

136. Nelimarkka O, Halkola L, Niinikoski J (1982). Distribution of renal cortical and Medullary tissue oxygenation in hemorrhagic shock. *Acta Chir Scand.***148:**213-219.

137. Nelimarkka O, Niinikoski J (1986). Renal venous oxygen tension as an indicator of tissue hypoxia in hemorrhagic shock. *Crit Care Med.***14:**128-131.

138. Nilsson AB, Friberg P (2000). Acute renal responses to angiotensin-converting enzyme inhibition in the neonatal pig. *Pediatr Nephrol.***14:**1071-1076.

139. Noble JS, MacKirdy FN, Donaldson SI, Howie JC (2001). Renal and respiratory failure in Scottish ICUs. *Anaesthesia.***56:**124-129.

140. Norman JT, Stidwill R, Singer M, Fine LG (2003). Angiotensin II blockade augments renal cortical microvascular pO2 indicating a novel, potentially renoprotective action. *Nephron Physiol.***94:**39-46.

141. Nuutinen LS, Tuononen S (1976). The effect of furosemide on renal blood flow and renal tissue oxygen tension in dogs. *Ann Chir Gynaecol.***65:**272-276.

142. O'Leary MJ, Bihari DJ (2001). Preventing renal failure in the critically ill. There are no magic bullets-just high quality intensive care. *BMJ.***322:**1437-1439.

143. Oberg PA (1990). Laser-Doppler flowmetry. *Crit Rev Biomed Eng.***18:**125-163.

144. Olsen TS, Olsen HS, Hansen HE (1985). Tubular ultrastructure in acute renal failure in man: epithelial necrosis and regeneration. *Virchows Arch A Pathol Anat Histopathol.***406:**75-89.

145. Orita Y, Fukuhara Y, Yanase M, Ando A, Okada N, Abe H (1983). Effect of furosemide on mitochondrial electron transport system and oxidative phosphorylation. *Arzneimittelforschung.***33:**1446-1450.

146. Ortiz PA, Garvin JL (2000). Autocrine effects of nitric oxide on HCO(3)(-) transport by rat thick ascending limb. *Kidney Int.***58:**2069-2074.

147. Ortiz PA, Garvin JL (2002). Role of nitric oxide in the regulation of nephron transport. *Am J Physiol Renal Physiol.***282:**F777-F784.

148. Ortiz PA, Hong NJ, Garvin JL (2001). NO decreases thick ascending limb chloride absorption by reducing Na(+)-K(+)-2Cl(-) cotransporter activity. *Am J Physiol Renal Physiol.***281:**F819-F825.

149. Park HP, Jeon YT, Hwang JW et al (2005). Isoflurane preconditioning protects motor neurons from spinal cord ischemia: Its dose-response effects and activation of mitochondrial adenosine triphosphate-dependent potassium channel. *Neurosci Lett.***387:**90-94.

150. Pena JR, Wolska BM (2005). Differential effects of isoflurane and ketamine/inactin anesthesia on cAMP and cardiac function in FVB/N

mice during basal state and beta-adrenergic stimulation. *Basic Res Cardiol.***100:**147-153.

151. Perkins RS, Dent G, Chung KF, Barnes PJ (1992). The effect of anion transport inhibitors and extracellular Cl- concentration on eosinophil respiratory burst activity. *Biochem Pharmacol.***43:**2480-2483.

152. Popel AS (1989). Theory of oxygen transport to tissue. *Crit Rev Biomed Eng.***17:**257-321.

153. Popel AS, Pittman RN, Ellsworth ML (1989). Rate of oxygen loss from arterioles is an order of magnitude higher than expected. *Am J Physiol.***256:**H921-H924.

154. Prasad PV, Edelman RR, Epstein FH (1996). Noninvasive evaluation of intrarenal oxygenation with BOLD MRI. *Circulation.***94:**3271-3275.

155. Priatna A, Epstein FH, Spokes K, Prasad PV (1999). Evaluation of changes in intrarenal oxygenation in rats using multiple gradient-recalled echo (mGRE) sequence. *J Magn Reson Imaging.***9:**842-846.

156. Rangel-Frausto MS, Pittet D, Costigan M, Hwang T, Davis CS, Wenzel RP (1995). The natural history of the systemic inflammatory response syndrome (SIRS). A prospective study. *JAMA.***273:**117-123.

157. Ravikant T, Lucas CE (1977). Renal blood flow distribution in septic hyperdynamic pigs. *J Surg Res.***22:**294-298.

158. Richman AV, Okulski EG, Balis JU (1981). New Concepts in the pathogenesis of acute tubular necrosis associated with sepsis. *Ann Clin Lab Sci.***11:**211-219.

159. Richter C, Gogvadze V, Schlapbach R, Schweizer M, Schlegel J (1994). Nitric oxide kills hepatocytes by mobilizing mitochondrial calcium. *Biochem Biophys Res Commun.***205:**1143-1150.

160. Roald AB, Ofstad J, Iversen BM (2002). Attenuated buffering of renal perfusion pressure variation in juxtamedullary cortex in SHR. *Am J Physiol Renal Physiol.***282:**F506-F511.

161. Robin ED (1977). Special report: dysoxia. Abnormal tissue oxygen utilization. *Arch Intern Med.***137:**905-910.

162. Roczniak A, Burns KD (1996). Nitric oxide stimulates guanylate cyclase and regulates sodium transport in rabbit proximal tubule. *Am J Physiol.***270:**F106-F115.

163. Rosen S, Epstein FH, Brezis M (1992). Determinants of intrarenal oxygenation: factors in acute renal failure. *Ren Fail.***14:**321-325.

164. Rosenberger C, Mandriota S, Jurgensen JS et al (2002). Expression of hypoxia-inducible factor-1alpha and -2alpha in hypoxic and ischemic rat kidneys. *J Am Soc Nephrol.***13:**1721-1732.

165. Rosser DM, Stidwill RP, Jacobson D, Singer M (1995). Oxygen tension in the bladder epithelium rises in both high and low cardiac output endotoxemic sepsis. *J Appl Physiol.***79:**1878-1882.

166. Rosser DM, Stidwill RP, Jacobson D, Singer M (1996). Cardiorespiratory and tissue oxygen dose response to rat endotoxemia. *Am J Physiol.***271:**H891-H895.

167. Rothe CF, Maass-Moreno R, Flanagan AD (1990). Effects of hypercapnia and hypoxia on the cardiovascular system: vascular capacitance and aortic chemoreceptors. *Am J Physiol.***259:**H932-H939.

168. Sandin R, Feuk U, Modig J (1990). Disturbances in renal cortical perfusion with reference to the microsphere technique. *Acta Anaesthesiol Scand.***34:**457-462.

169. Schiffl H, Lang SM, Fischer R (2002). Daily hemodialysis and the outcome of acute renal failure. *N Engl J Med.***346:**305-310.

170. Schneiderman G, Goldstick TK (1978). Oxygen electrode design criteria and performance characteristics: recessed cathode. *J Appl Physiol.***45:**145-154.

171. Schwartz D, Brasowski E, Raskin Y et al (2001). The outcome of non-selective vs selective nitric oxide synthase inhibition in lipopolysaccharide treated rats. *J Nephrol.***14:**110-114.

172. Seeliger E, Persson PB, Boemke W, Mollenhauer G, Nafz B, Reinhardt HW (2001). Low-dose nitric oxide inhibition produces a negative sodium balance in conscious dogs. *J Am Soc Nephrol.***12:**1128-1136.

173. Sela S, Shasha SM, Mashiach E, Haj M, Kristal B, Shkolnik T (1993). Effect of oxygen tension on activity of antioxidant enzymes and on renal function of the postischemic reperfused rat kidney. *Nephron.***63:**199-206.

174. Severinghaus JW, Astrup PB (1986). History of blood gas analysis. V. Oxygen measurement. *J Clin Monit.***2:**174-189.

175. Sharpe MA, Cooper CE (1998). Interaction of peroxynitrite with mitochondrial cytochrome oxidase. Catalytic production of nitric oxide and irreversible inhibition of enzyme activity. *J Biol Chem.***273:**30961-30972.

176. Singer I, Epstein M (1998). Potential of dopamine A-1 agonists in the management of acute renal failure. *Am J Kidney Dis.***31:**743-755.

177. Singer M, De S, V, Vitale D, Jeffcoate W (2004). Multiorgan failure is an adaptive, endocrine-mediated, metabolic response to overwhelming systemic inflammation. *Lancet.***364:**545-548.

178. Singer M, Millar C, Stidwill R, Unwin R (1996). Bladder epithelial oxygen tension--a new means of monitoring regional perfusion? Preliminary study in a model of exsanguination/fluid repletion. *Intensive Care Med.***22:**324-328.

179. Smits GJ, Roman RJ, Lombard JH (1986). Evaluation of laser-Doppler flowmetry as a measure of tissue blood flow. *J Appl Physiol.***61:**666-672.

180. Soller BR, Heard SO, Cingo NA et al (2001). Application of fiberoptic sensors for the study of hepatic dysoxia in swine hemorrhagic shock. *Crit Care Med.***29:**1438-1444.

181. Stein JH, Boonjarern S, Mauk RC, Ferris TF (1973). Mechanism of the redistribution of renal cortical blood flow during hemorrhagic hypotension in the dog. *J Clin Invest.***52:**39-47.

182. Stern MD, Lappe DL, Bowen PD et al (1977). Continuous measurement of tissue blood flow by laser-Doppler spectroscopy. *Am J Physiol.***232:**H441-H448.

183. Stidwill RP, Rosser DM, Singer M (1998). Cardiorespiratory, tissue oxygen and hepatic NADH responses to graded hypoxia. *Intensive Care Med.***24:**1209-1216.

184. Stone GW, McCullough PA, Tumlin JA et al (2003). Fenoldopam mesylate for the prevention of contrast-induced nephropathy: a randomized controlled trial. *JAMA*.**290:**2284-2291.

185. Strick DM, Fiksen-Olsen MJ, Lockhart JC, Roman RJ, Romero JC (1994). Direct measurement of renal medullary blood flow in the dog. *Am J Physiol*.**267:**R253-R259.

186. Suehiro K, Shimizu J, Yi GH et al (2001). Selective renal vasodilation and active renal artery perfusion improve renal function in dogs with acute heart failure. *J Pharmacol Exp Ther*.**298:**1154-1160.

187. Swedberg K, Held P, Kjekshus J, Rasmussen K, Ryden L, Wedel H (1992). Effects of the early administration of enalapril on mortality in patients with acute myocardial infarction. Results of the Cooperative New Scandinavian Enalapril Survival Study II (CONSENSUS II). *N Engl J Med*.**327:**678-684.

188. Sweet SJ, Glenney CU, Fitzgibbons JP, Friedmann P, Teres D (1981). Synergistic effect of acute renal failure and respiratory failure in the surgical intensive care unit. *Am J Surg*.**141:**492-496.

189. Szabo G, Posch E, Rosivall L, Fazekas A, Harsing L (1977). The effect of haemorrhage on renal blood flow and intrarenal flow distribution. *Injury*.**9:**146-150.

190. Takahashi GH, Goldstick TK (1966). Oxygen consumption rate of tissue measured by a micropolarographic method. *J Gen Physiol.***50:**317-335.

191. Task Force of the American College of Critical Care Medicine SoCCM (1999). Practice parameters for hemodynamic support of sepsis in adult patients in sepsis. *Crit Care Med.***27:**639-660.

192. Thadhani R, Pascual M, Bonventre JV (1996). Acute renal failure. *N Engl J Med.***334:**1448-1460.

193. Thurau K, Boylan JW (1976). Acute renal success. The unexpected logic of oliguria in acute renal failure. *Am J Med.***61:**308-315.

194. Torres Filho I, Kerger H, Intaglietta M (1996). pO2 measurements in arteriolar networks. *Microvasc Res.***51:**202-212.

195. Tsai AG, Friesenecker B, Mazzoni MC et al (1998). Microvascular and tissue oxygen gradients in the rat mesentery. *Proc Natl Acad Sci U S A.***95:**6590-6595.

196. Turrens JF, Freeman BA, Crapo JD (1982). Hyperoxia increases H2O2 release by lung mitochondria and microsomes. *Arch Biochem Biophys.***217:**411-421.

197. Wagner PD (1991). Central and peripheral aspects of oxygen transport and adaptations with exercise. *Sports Med.***11:**133-142.

198. Wallach S, Charbon GA, Beijer HJ, Struyvenberg A (1982). Furosemide vasodilates the canine gastrointestinal tract. *J Clin Pharmacol.***22:**348-358.

199. Whalen WJ, Riley J, Nair P (1967). A microelectrode for measuring intracellular PO2. *J Appl Physiol.***23:**798-801.

200. Whitworth JA, Lawrence JR, (Eds) (1994). Textbook of renal disease. 2nd Edition edition. Edinburgh: Churchill Livingstone.

201. Wilcox CS (2002). Reactive oxygen species: roles in blood pressure and kidney function. *Curr Hypertens Rep.***4:**160-166.

202. Wilcox CS (2003). Redox regulation of the afferent arteriole and tubuloglomerular feedback. *Acta Physiol Scand.***179:**217-223.

203. Willinger CC, Schramek H, Pfaller K, Pfaller W (1992). Tissue distribution of neutrophils in postischemic acute renal failure. *Virchows Arch B Cell Pathol Incl Mol Pathol.***62:**237-243.

204. Wilson SR, Hirsch NP, Appleby I (2005). Management of subarachnoid haemorrhage in a non-neurosurgical centre. *Anaesthesia.***60:**470-485.

205. Wray GM, Millar CG, Hinds CJ, Thiemermann C (1998). Selective inhibition of the activity of inducible nitric oxide synthase prevents the

circulatory failure, but not the organ injury/dysfunction, caused by endotoxin. *Shock.***9:**329-335.

206. Zheng S, Zuo Z (2005). Isoflurane preconditioning decreases glutamate receptor overactivation-induced Purkinje neuronal injury in rat cerebellar slices. *Brain Res.*

207. Zou AP, Cowley AW, Jr. (2003). Reactive oxygen species and molecular regulation of renal oxygenation. *Acta Physiol Scand.***179:**233-241.

208. Zwemer CF, Shoemaker JL, Jr., Hazard SW, III, Davis RE, Bartoletti AG, Phillips CL (2000). Hyperoxic reperfusion exacerbates postischemic renal dysfunction. *Surgery.***128:**815-821.